ON THE BEHAVIOR OF SELF-OSCILLATORY SYSTEMS WITH EXTERNAL FORCE(Dissertation_全文)

AUTHOR(S):

Akamatsu, Norio

ON THE BEHAVIOR OF SELF-OSCILLATORY SYSTEMS WITH EXTERNAL FORCE

NORIO AKAMATSU

ON THE BEHAVIOR OF SELF-OSCILLATORY SYSTEMS WITH EXTERNAL FORCE

Norio Akamatsu

Department of Electrical Engineering

Tokushima University, Tokushima

1973

CONTENTS

NOTATION

B amplitude of the external force

ν frequency of the external force

μ damping coefficient of the system

c_1 coefficient of linear restoring term

c_3 coefficient of nonlinear restoring term

ω_0 natural frequency of the self-oscillation

Δ maximum finite invariant set

M set of central points

C invariant closed curve

m_1, m_2 characteristic multipliers

ρ rotation number correlated with the invariant closed curve

S^n completely stable n-periodic point

U^n completely unstable n-periodic point

D^n directly unstable n-periodic point

I^n inversely unstable n-periodic point

In the phase-plane portraits, we shall use the symbols ${}^jS_i^n$, ${}^jU_i^n$, ${}^jD_i^n$ and ${}^jI_i^n$ for fixed points (n = 1) and periodic points (n = 2, 3, ...). The symbol ${}^jS_i^n$ denotes a completely stable n-periodic point which belongs to the jth periodic group, if there exist plural groups, and

$$T({}^jS_i^n) = {}^jS_{i+1}^n \qquad 0 \leq i \leq n-1$$
$$T^n({}^jS_i^n) = {}^jS_i^n$$

Similar notation applies also to unstable periodic points U, D and I.

INTRODUCTION

Strictly speaking, most phenomena in physical systems may be described, more or less, by nonlinear equations. In this monograph, as an example of nonlinear systems, we shall study the forced self-oscillatory circuit containing a negative resistance, such as an Esaki-diode. One of the most attractive features of negative resistance may be the existence of a wide variety of complicated new phenomena, such as several types of nonperiodic oscillations. Though such a circuit is very simple, it has a generality and many applications to the theory of plasma physics and micro-wave circuits. The author has a slight impression that a fund of knowledge of negative resistances could and would not be used in practice if physicists and circuit designers were more familiar with nonlinear phenomena.

However, the differential equations which describe a real system are inherently nonlinear, so that it is very difficult in general to solve them by the analytical methods. Hence we are obliged to obtain the approximate solutions, comparing with experimental results. For this purpose, considerable studies were made and many important results were already reported by using the perturbation method, the averaging method and the method of harmonic balance and so on [1,2].* But, by using only these means, it might be impossible to deal with not only the problems concerning nonperiodic oscillations but also the global aspects for periodic oscillations in the phase plane.

---

*Numerals in brackets indicate references on page 81 to 83.

It may be effective to apply the transformation theory to ordinary differential equations which are arised in many physical systems. This theory was first studied by H. Poincaré [3], and greatly developed by G. D. Birkhoff [4] and etc., in the field of celestial mechanics, especially the problem of three bodies.

Therefore, the aim of this paper is not to treat the nonlinear differential equations quantitatively, but rather to focus our attention on the qualitative feature of phenomena. The qualitative investigation makes quantitative investigation also substantially easier or, more precisely, makes it easier to solve the quantitative problems which arised in the real systems. And by applying the qualitative investigation to the nonlinear differential equations, we can obtain topologically the global aspects in the phase plane.

This monograph is composed of the six chapters.

Chapter 1 is concerned with the derivation of the fundamental differential equation from the forced self-oscillatory circuit which contains a negative resistance. We shall devote to study, as precisely as possible, the solutions of this equation in later chapters.

The method of analysis is briefly described in Chap. 2. We apply the transformation theory to the second-order nonlinear differential equations, making use of the periodicity of their external force. Such mapping procedure is found to be usefull to search various types of solutions and to reveal their global aspects in the phase plane. In this theory a steady-state response in the

system is topologically represented by a set of central points in the phase plane. A periodic solution correlates to a fixed point of the mapping and an almost periodic solution to an invariant closed curve on which successive images continue to move.

In the following three chapters, we shall numerically deal with the fundamental equation and represent the various types of phase-portraits by using the mapping concepts based upon the transformation theory of ordinary differential equations.

The phenomena occurring in the above-mentioned system are inherently different, according to the presence, or absence, of a nonlinear restoring term in the fundamental equation. Then in Chap. 3, in order to survey the representative phase-portraits of van der Pol's equation with an external force, we shall expressly investigate the system whose restoring force is only composed of a linear function and damping coefficient is not small, $\mu = 1$.

It might be too difficult to investigate in detail the transition of phase-portraits occurring in the system with linear restoring force. However, nonperiodic oscillations, which result apart from the entrained region must be caused by the complicated periodic oscillations. Therefore, in Chap. 4 for the preparation to explain the reasons of occurring such nonperiodic oscillations, we represent the precise transitions of phase-portraits for the harmonic oscillations and the subharmonic oscillations of orders 1/2, 1/3 and 3/5 appeared in the system with nonlinear restoring force. Moreover, the effect of the system parameters on the configurations

of the higher-harmonic oscillations are discussed.

If the system parameters are set outside the region of frequency entrainment, there result nonperiodic oscillations in the system. In Chap. 5, two types of nonperiodic oscillations will be studied. That is, an almost periodic oscillation whose successive images move on a simple invariant closed curve under iterations of the mapping and a nonperiodic oscillation whose successive images do not move on a simple invariant closed curve but are dispersed in a certain area which correlated with a set of central points. Such nonperiodic oscillation is occassionally occurred in a system with nonlinear restoring force. The mapping procedure based on the transformation theory of differential equation is found to be effective to study such complicated nonperiodic oscillations, and the approximate estimation is powerless against them. According to the structure of phase-portraits, such nonperiodic oscillations are classified into three types. We shall represent the set of central points and the invariant curves passing through the unstable fixed points in each case. The reason for the occurrence of such nonperiodic oscillations is also considered. Judging from the deformation of phase-portraits in the entrained region, such nonperiodic oscillations are greatly concerned with doubly asymptotic points and successive multiplication of fixed points.

Chapter 1 Differential Equation Describing Forced Self-Oscillatory Systems

The schematic diagram illustrated in Fig. 1.1(a) shows a self-oscillatory circuit under the impression of a sinusoidal voltage $E \cos \omega t$. A pair of Esaki-diodes is a suitable example of the negative resistance element N in this circuit.

Figure 1.1 may represent not only the most fundamental oscillatory circuit containing a negative resistance, but also the equivalent circuit for a tunnel diode in the high-frequency range [6]. That is, the capacitance of p-n junction is represented by C, and the series inductance and the resistance of two lead lines by L and R respectively.

It may be necessary to analyze closely the fundamental circuit of the tunnel diode, such as shown in Fig. 1.1, for many practical applications of its high-speed operation. Thus, this monograph is devoted to study the various phenomena occurred in the forced self-oscillatory system.

Following the notations in Fig. 1.1, the equations for this circuit are written as

$$\begin{aligned} L \frac{d i}{d t} + R i + v &= E \cos \omega t \\ i_1 = C \frac{d v}{d t} \quad , \quad i &= i_1 + i_2 \end{aligned} \tag{1.1}$$

The nonlinear characteristic of the negative resistance N is shown in Fig. 1.1(b) and may be expressed by

$$i_2 = f(v) \tag{1.2}$$

Eliminating the current i_1, i_2 and i, we obtain the following equation with respect to the voltage v;

$$L\,C\,\frac{d^2 v}{d\,t^2} + \left(R\,C + L\,\frac{d\,f(v)}{d\,v} \right) \frac{d\,v}{d\,t} + v + R\,f(v) = E\cos\omega t \tag{1.3}$$

The nonlinear function f(v) is generally represented by the polynomial of v, but for the sake of simplicity it is assumed to be

$$i_2 = f(v) = S\,v\left(-1 + \frac{v^2}{V_S^2} \right) \tag{1.4}$$

where S and V_S are positive constants determined by the voltage-current characteristic of N. By virture of Eq. (1.4), Eq. (1.3) leads to

$$\frac{d^2 x}{d\,\tau^2} - \mu\left(1 - x^2 \right) \frac{d\,x}{d\,\tau} + c_1 x + c_3 x^3 = B\cos\nu\tau \tag{1.5}$$

where

$$x = \frac{v}{V_S}\sqrt{\frac{3\,L\,S}{L\,S - R\,C}}\,, \qquad \tau = \frac{t}{\sqrt{L\,C}}$$

$$B = \frac{E}{V_S}\sqrt{\frac{3\,L\,S}{L\,S - R\,C}}\,, \qquad \mu = \frac{L\,S - R\,C}{\sqrt{L\,C}} \qquad \nu = \omega\sqrt{L\,C}$$

$$c_1 = 1 - R\,S\,, \qquad c_3 = \frac{R\left(L\,S - R\,C \right)}{3\,L}$$

To put it briefly, it can be conjectured that the solution of Eq. (1.5) exhibits the properties of van der Pol's equation for the small external force. The large external force may suppress the

effect of the negative damping, so that the behavior of solutions is similar to the one appearing in Duffing's equation.

In the following, we shall treat Eq. (1.5) as a fundamental equation and investigate the global aspects of its solutions in the phase plane.

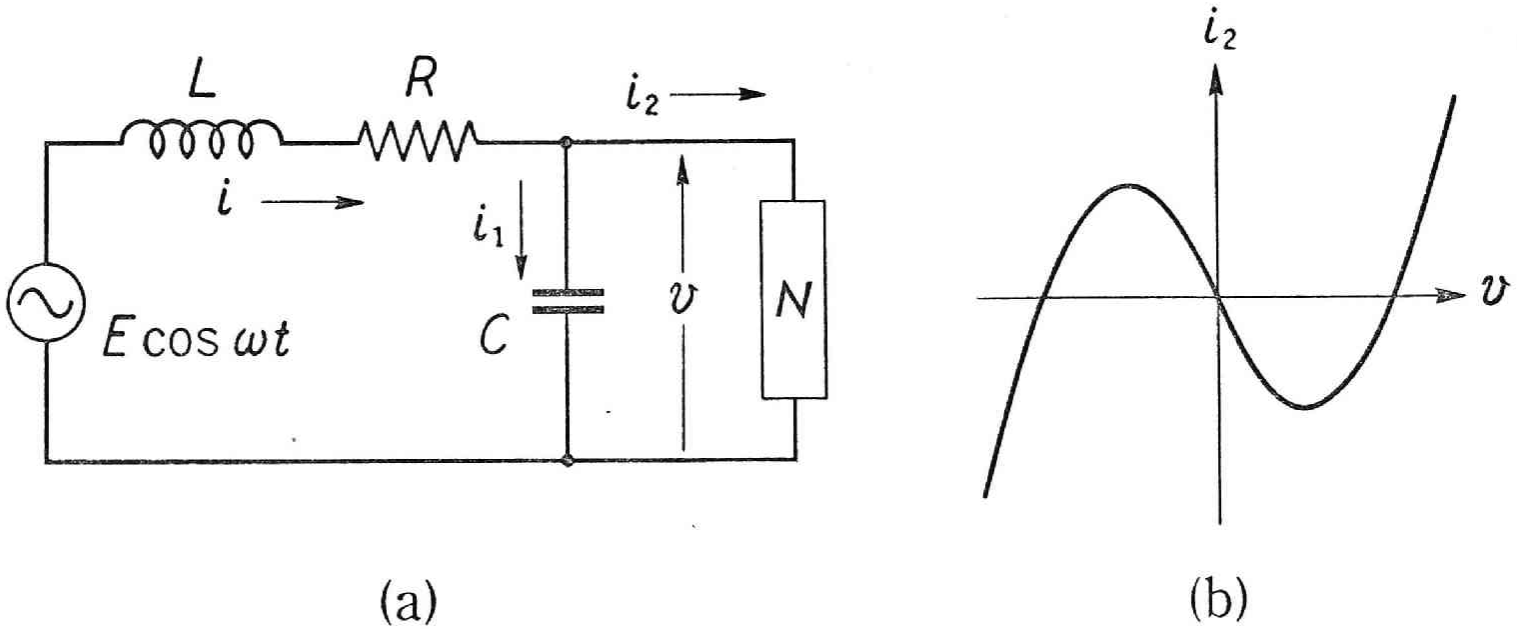

Fig. 1.1 (a) Negative-resistance oscillator with external force.

(b) Nonlinear characteristic of the negative-resistance element N.

Chapter 2 Transformation Theory of Differential Equations

2.1 Introduction

It may be difficult to apply generally the quadrature to nonlinear differential equations. However, the topological treatment for ordinary differential equations which has been made and developed mainly by H. Poincaré and G. D. Birkhoff is effective to study their solutions qualitatively. By applying the mapping theory based on the transformation theory of ordinary differential equations to the fundamental equation, we shall be able to consider the complicated phenomena, especially nonperiodic oscillations, in nonlinear systems.

In this chapter, we shall describe briefly about the method of analysis which is necessary to explain the behavior of the solutions in the fundamental equation. Specially, we shall introduce the notion; 'set of central points', with the intention of representing the steady states of nonperiodic oscillations. The further details of this theory were discussed in the references [4, 7, 8, 9].

2.2 Transformation Theory [7, 9]

By setting $\frac{dx}{dt} = y$, we rewright Eq. (1.5) in the following system

$$\begin{aligned} \frac{dx}{dt} &= y \equiv X(x,y,t) \\ \frac{dy}{dt} &= \mu(1-x^2)y - c_1 x - c_3 x^3 + B\cos\nu t \equiv Y(x,y,t) \end{aligned} \tag{2.1}$$

where $X(x,y,t)$ and $Y(x,y,t)$ are periodic function in t with period L.

Let us consider the solution $[\, x(x_0,y_0,t)\ ,\ y(x_0,y_0,t)\ ]$ of Eqs. (2.1) which starts from point (x_0,y_0) in the xy-phase plane at $t = 0$. Since X and Y are of period L, we now concentrate our attention upon point $P_n(x_n,y_n)$, whose coordinates are

$$x_n = x(x_0,y_0,nL)\ ,\quad y_n = y(x_0,y_0,nL)$$
$$(\quad n = 0,\ \pm 1,\ \pm 2,\ \ldots\quad)$$

For any integer i, we call the point transformation $P_i \longrightarrow P_{i+1}$ the mapping T, and define it as $P_{i+1} = TP_i$. Successively we can express the iterations of this mapping by $P_{i+2} = T(TP_i) = T^2P_i$, and so on. Similarly we describe the inverse mapping as $P_i = T^{-1}P_{i+1} = T^{-2}P_{i+2} = \cdots$. The above-defined mapping is known as a one-to-one continuous transformation of the xy-plane into itself [7].

A point in the xy-plane which is invariant under the mapping T is called a fixed point. Thus if P_0 is a fixed point, then $TP_0 = P_1 = P_0$. Let n be the smallest positive integer for which $T^nP = P_n = P_0$. Then P_0 will visit periodically n distinct points. Therefore, they are called n-periodic points.

The solution of Eqs. (2.1) which lies on a fixed point at $t = 0$ corresponds to the harmonic oscillation with period L. The solutions correlated with the n-periodic points are the subharmonic oscillations of order 1/n.

2.3 Maximum Finite Invariant Set and Set of Central Points

According to N. Levinson [7], if there exist an $R > 0$ and an integer $N > 0$ such that any solutions $x(t)$, $y(t)$ of Eqs. (2.1) satisfy the condition $x^2 + y^2 < R^2$ at a certain time t_0 and remain in this circle of radius R for all $t > t_0 + N \cdot L$, then such a system is called a dissipative system for large displacements, or of class D. As might be expected from energy considerations, most systems which arise in practice are in class D. For every system (2.1) of class D the existence of a maximum finite invariant set Δ in the xy-phase plane has been proved.* Even if we prescribe the initial values at any point apart from the set Δ, the successive images tend to Δ after the repeated applications of the mapping T. However, in the set Δ there occasionally exist some points whose successive images never return to the neighborhood of the initial points under the repeated applications of the mapping T. Following the mathematical method of G. D. Birkhoff [4,5], we shall try to exclude such points from the set Δ.**

We now confine our attention to the set Δ and discuss briefly about a 'set of central points'.

---

*The further details concerning the set Δ have been given by N. Levinson [7].

**The more precise discussions have been made by G. D. Birkhoff [4,5] and V. V. Nemytskii and V. V. Stepanov [11].

We consider the following sequence obtained by iterating the mappings T and T^{-1} to any region σ_0 in the set Δ .

$$\cdots , \sigma_{-2} , \sigma_{-1} , \sigma_0 , \sigma_1 , \sigma_2 , \cdots$$

where

$$\sigma_n = T^n \sigma_0 \qquad (n = \pm 1, \pm 2, \ldots)$$

In the case where the region σ_0 has no intersection to all σ_n, i.e., $\sigma_0 \bigcap \sigma_n = \phi$ (an empty set), we define σ_0 as a 'wandering region', and whose point is called a 'wandering point'. By collecting all the wandering regions, we obtain a set W_1. So, any point in the set W_1 can not return to its own vicinity by indefinite iterations of the mappings T and T^{-1}, so that the set W_1 is not related with the stationary states. Excluding the set W_1 from Δ , we write $M_1 = \Delta - W_1$, which is called a 'non-wandering set'.

Now we shall confine our attention to the set M_1 instead of Δ and continue the same operation as before. By applying the mapping T^n ($n = \pm 1, \pm 2, \ldots$) to the region σ_0 which is contained in the set M_1, we obtain the following sequence,

$$\cdots , \sigma_{-2} , \sigma_{-1} , \sigma_0 , \sigma_1 , \sigma_2 , \cdots$$

where

$$\sigma_n = T^n \sigma_0 \qquad (n = \pm 1, \pm 2, \ldots)$$

Thus we call the region σ_0 whose images σ_n do not intersect the original region σ_0 at all a 'wandering region with respect to M_1'. The set W_2 is constituted by all the wandering regions with respect to M_1. So, subtracting it from the set M_1, we make up the set M_2

($= M_1 - W_2$), which is a non-wandering set with respect to M_1.

Continuing this process, we obtain a chain of the set M_n included one within the other;

$$M_1 \supset M_2 \supset \cdots \supset M_n \supset \cdots$$

If for some number k we obtain $M_k = M_{k+1}$, then $M = M_k = M_{k+1} = \cdots$ and the set M is the required set of central points. If each set M_{k+1} is a proper subset of M_k, then we define

$$M = \bigcap_{k=1}^{\infty} M_k$$

The set M is evidently invariant under the mapping T.

In the following, we shall concentrate our attention on the set of central points M particularly in the case where the non-periodic oscillation results.

2.4 Fixed Points, Periodic Points and Related Properties

As mentioned in the preceding, the stationary solutions of differential equations are represented by the set of central points. The set of central points is divided into the subset of periodic solutions and the subset of nonperiodic ones. Here, we shall consider the stability of the periodic solution.

In order to sustain the periodic solution in the stable state, it is necessary that the fixed point correlated with it should be stable with respect to small variations. The stability of the fixed point may be determined by investigating the movements of any point which is located in its vicinity under the mapping T by means of the transformation theory. That is, in the case where all

points in the vicinity of the fixed point converge asymptotically under iterations of the mapping T to it, this fixed point is stable.

Let any point Q_0 ($x_0 + u_0$, $y_0 + v_0$) existing in the vicinity of the fixed point P_0 (x_0 , y_0) be transformed into Q_1 ($x_0 + u_1$, $y_0 + v_1$) by the mapping T. Then the following relations result;

$$\begin{aligned} x_0 + u_1 &= x (x_0 + u_0 , y_0 + v_0 , L) \\ y_0 + v_1 &= y (x_0 + u_0 , y_0 + v_0 , L) \end{aligned} \tag{2.2}$$

It means $u_1 = v_1 = 0$ when $u_0 = v_0 = 0$ that P_0 is a fixed point under the mapping T. Therefore, for small quantities of u_0 and v_0 , u_1 and v_1 can be expanded into power series in u_0 and v_0 , i.e.,

$$\begin{aligned} u_1 &= a\, u_0 + b\, v_0 + \cdots \\ v_1 &= c\, u_0 + d\, v_0 + \cdots \end{aligned} \tag{2.3}$$

where

$$a = \frac{\partial x(x_0 , y_0 , L)}{\partial x_0} \quad , \quad b = \frac{\partial x(x_0 , y_0 , L)}{\partial y_0}$$

$$c = \frac{\partial y(x_0 , y_0 , L)}{\partial x_0} \quad , \quad d = \frac{\partial y(x_0 , y_0 , L)}{\partial y_0}$$

The terms not explicitly given in the right sides of Eqs. (2.3) are of degree higher than the first in u_0 and v_0 . Equations (2.3) express the transformation (u_0 , v_0) $\longrightarrow$ (u_1 , v_1) in the neighborhood of the fixed point P_0 , and this transformation is characterized by the roots m_1 and m_2 of the characteristic equation

$$\begin{vmatrix} a - m & b \\ c & d - m \end{vmatrix} = 0 \qquad (2.4)$$

The fixed point P_0 is called simple if both $|m_1|$ and $|m_2|$ are different from unity. Simple fixed points are classified as follows [7] ;

Completely stable if	$\|m_1\| < 1 \ , \ \|m_2\| < 1$
Completely unstable if	$\|m_1\| > 1 \ , \ \|m_2\| > 1$
Directly unstable if	$0 < m_1 < 1 < m_2$
Inversely unstable if	$m_1 < -1 < m_2 < 0$

The same classification is also applied to the periodic points.

This is a completely stable fixed point P_0 such that if P be any point in the neighborhood of P_0 then $T^nP \longrightarrow P_0$ as $n \longrightarrow \infty$; that is, successive images TP, T^2P, etc., of the point P tend to the fixed point P_0. By definition, this fixed point corresponds to the stable solution of Eqs. (2.1), and the other fixed point corresponds to the unstable solution of Eqs. (2.1). In the completely unstable case, images move away from the fixed point under the repeated applications of the mapping T.

This is a directly or inversely unstable fixed point P_0 through which there passes two invariant curves under the mapping T. Points on the one invariant curve approach P_0 under iterations of the mapping T, while points on the other invariant curve approach P_0 under iterations of the inverse mapping T^{-1} . In this case the loci of successive images are analogous to that of the integral curves in

the neighborhood of a saddle point in the theory of singular points.

N. Levinson [7] and J. L. Massera [8] discussed the number of fixed points and periodic points in the set of central points.

From now on, we shall use the following notations;

S(n) : the total number of completely stable n-periodic points
U(n) : the total number of completely unstable n-periodic points
D(n) : the total number of directly unstable n-periodic points
I(n) : the total number of inversely unstable n-periodic points

Thus we obtain the relations;

$$\begin{aligned} &\text{For } n = 1, && S(1) + U(1) + I(1) = D(1) + 1 \\ &\text{For } n = 2, 4, 6, \ldots, && S(n) + U(n) + I(n) = D(n) + 2\cdot I(n/2) \\ &\text{For } n = 3, 5, 7, \ldots, && S(n) + U(n) + I(n) = D(n) \end{aligned} \tag{2.5}$$

2.5 Invariant Closed Curves and Almost Periodic Solutions

We shall study the case in which the maximum finite invariant set Δ is not of zero area and its boundary is constructed by a simple closed curve. If a closed curve is invariant under the mapping, it is called an invariant closed curve.

Let us denote the simple invariant closed curve by C. The solutions of Eqs. (2.1) emanating from C when $t = 0$ form a surface in the xyt-space. As the curve C is invariant under the mapping T, the portion of this surface lying between $t = 0$ and $t = L$ can be mapped on a torus. Therefore the solutions of Eqs. (2.1) starting from C can be written as $x = f(\theta, t)$ and $y = g(\theta, t)$, where f

and g are of period 1 in θ and period L in t. In fact, f and g can be so chosen that, for any fixed $t = t_1$, θ is proportional to arc length along the curve $x = f(\theta, t_1)$, $y = g(\theta, t_1)$.

Then the discussion on these solutions of Eqs. (2.1) is reduced to investigate the following differential equation on a torus;

$$\frac{d\theta}{dt} = h(\theta, t) \qquad (2.6)$$

where h is a periodic function with period 1 in θ and L in t.

The differential equation on a torus has been studied by H. Poincaré [12], A. Denjoy [13] and P. Bohl [14]. Here we shall briefly describe their results concerning the transformation of C into itself [15].

Related to the solution curves of Eq. (2.6), there corresponds a rotation number ρ, which is the average advance of θ for the lapse of L in t.

If ρ is rational and of the form p/q, where p and q have no common factors, Eqs. (2.1) have periodic solutions with period qL correlated with q-periodic points on C.

In the case where ρ is irrational, the character of the solution of Eq. (2.6) may be inherently classified into the following possibilities;

(a) the mapping T is the ergodic or transitive case

(b) the mapping T is the singular or intransitive case

In the case (a), the derived set of the sequence $\{P_i\}$ ($P_i = T^i P_o$, $i = \pm 1, \pm 2, \ldots$; P_o is an arbitrary point on C) may coincide with

C itself. Then the solution of Eq. (2.6) is given by

$$\theta(t) = \rho\frac{t}{L} + c + \phi\left(\frac{t}{L}, \rho\frac{t}{L} + c\right) \qquad (2.7)$$

where $\phi(u, v)$ is both periodic in u and v of period 1, and c is an arbitrary constant [13, 14]. Therefore Eqs. (2.1) have almost periodic solutions.

In the case (b), the above-mentioned derived set of the sequence $\{P_i\}$ is nowhere dense on C. Then the corresponding solutions of Eqs. (2.1) are extremely complicated. Until now, their precise properties are not well-known.

2.6 Doubly Asymptotic Points

In this section, we shall consider the properties of invariant branches introduced by H. Poincaré [3] and investigated deeply by G. D. Birkhoff [16, 17, 18].

Let P_0 be a directly or inversely unstable fixed point.* There abut at point P_0 two α-branches and two ω-branches which are invariant under the mapping. All points on the α-branch converge toward P_0 on the indefinite iterations of the inverse mapping T^{-1}, and on the ω-branch converge toward P_0 on the iterations of T. From the uniqueness of solutions of Eqs. (2.1), it is readily shown that no α- (or ω-) branch can intersect to another α- (or ω-) branch. However the α-branch may occasionally intersect to the ω-branch one another, and the intersecting points in such a case are

---

*Similar duscussions will be made for a periodic point.

called doubly asymptotic points.

A doubly asymptotic point is called homoclinic in the case where the α- and ω-branches on which it lies issue from the same point or from two points belonging to the same periodic point group. A homoclinic point of the former type is called simple. A doubly asymptotic point is called heteroclinic if the α- and ω-branches on which it lies issue from two periodic points, each of them belonging to the different set of periodic points.

The following theorems concerning the homoclinic point have been proved by G. D. Birkhoff [16].

(a) An arbitrary small neighborhood of a homoclinic point contains an infinite number of homoclinic points.

(b) An arbitrary small neighborhood of a homoclinic point contains an infinite number of periodic points.

Chapter 3 Self-Oscillatory Systems with Linear Restoring Force

3.1 Introduction

If we generally deal with a system containing nonlinear restoring force, the behavior of the solution is too complicated to discuss its details in the first stage. Therefore, the qualitative study divide itself into two parts, according to the presence, or absence of a nonlinear restoring term in Eq. (1.5). Our attention will be, hence, given to the two extreme cases, (a) when there is no nonlinear restoring term, i.e., $c_3 = 0$ in Eq. (1.5), (b) when the restoring term is composed only of a nonlinear function, i.e., $c_1 = 0$ in Eq. (1.5).

In order to survey the pure influence of the negative damping and avoid the complexity arising from the nonlinear restoring force, we first discuss the particular case where R = 0 in Fig. 1.1, i.e., $c_1 = 1$ and $c_3 = 0$ in Eq. (1.5), so that*

$$\frac{d^2x}{dt^2} - \mu(1 - x^2)\frac{dx}{dt} + x = B \cos \nu t \qquad (3.1)$$

When μ is comparatively small in Eq. (3.1), many close investigations have been made by van der Pol [19], M. L. Cartwright [2], C. Hayashi [1,20] and so on. Following their results, the periodic oscillations would occur in the regions of frequency entrainment, and nonperiodic

---

*A vacuum-tube oscillator with an alternating voltage in the grid circuit is also governed by Eq. (3.1) [19].

oscillations outside the entrained region. However, for the large value of μ in Eq. (3.1), the behavior of the system is not known.

For the present, we shall set the parameter $\mu = 1$ in Eq. (3.1) so as to focus our attention on the effect of the negative damping, and represent the phase-portraits of van der Pol's equation with a forcing term.

3.2 Regions of Frequency Entrainment and Iso-ρ Curves

The regions of frequency entrainment for $\mu = 1$ in Eq. (3.1) are shown in Fig. 3.1. As the damping coefficient μ is not small, the various types of oscillations, especially the harmonic and the subharmonic of order 1/3, are entrained in a wide range. There also occur slightly the 1/2-harmonic and the third-harmonic entrainments in the neighborhood of $\nu = 2$ and $\nu = 1/3$ respectively.

In the case where at least one completely unstable fixed point exists in the phase plane, it is surrounded by the invariant closed curve. As mentioned in Sec. 2.5, the rotation number ρ characterize the behavior of the solutions emanating from the points on the invariant closed curve. The number ρ has been computed, and the iso-ρ curves are plotted in Fig. 3.1. When ρ takes an irrational value, the corresponding solution of Eq. (3.1) is almost periodic function. On the other hand, if ρ is rational, Eq. (3.1) has periodic solutions. However, in this figure the regions of the subharmonic oscillations of higher orders can scarcely be recognized. In proportion as the parameter μ is increased, these entrainments appear in small portions. In Sec. 3.4, we shall study the system with

large nonlinearity, $\mu = 10$.

3.3 Phase-Plane Analysis of the System with Linear Restoring Force [20]

We shall show several representative types of the phase-plane portraits when the system parameters are prescribed in each region of Fig. 3.1.

(a) Harmonic Oscillations

Let the external force in Eq. (3.1) be taken off, then the self-excited oscillation whose natural frequency ω_0 is equal to 0.939... sustains. Under the impression of an external force whose frequency ν is not far from ω_0, a harmonic entrainment occurs.

As a typical example of the harmonic oscillations, the system parameters are chosen at point a in Fig. 3.1, then

$$\frac{d^2x}{dt^2} - (1 - x^2)\frac{dx}{dt} + x = 0.5 \cos t \qquad (3.2)$$

As shown in Fig. 3.2, we obtain three fixed points S^1, D^1 and U^1 which correspond to the harmonic solutions of Eq. (3.2). The set of central points is constituted by them. The locations of these points and their properties are listed in Table 3.1. In this figure, we have also shown the invariant curves passing through the directly unstable fixed point.

Contiguous to the directly unstable fixed point D^1 there exist four invariant curves under the mapping T, i.e., two α-branches (drawn in thick lines) and two ω-branches (drawn in thin lines).

All points on the α-branches move along them and ultimately converge to the completely stable fixed point S^1 under the indefinite iterations of the mapping T. Therefore, the invariant closed curve which surrounds the maximum finite invariant set Δ is constituted by both α-branches. On the other hand, any point on the ω-branches may approach to the completely unstable fixed point U^1 or tend to infinity under the inverse mapping T^{-1}.

Now, we consider the case in which the invariant closed curve encircles the completely unstable fixed point U^1 and the points S^1 and D^1 divide it into two α-branches as shown in Fig. 3.2. For convenience, these α-branches are classified into two different groups according to their directions of the successive images under the iterations of the mapping T. The α-branch along which the successive images move clockwise is called an α_1-branch. On the other hand, points on an α_2-branch are mapped counterclockwise under the repeated applications of the mapping T. Terefore, the oscillation corresponding to the α_1-branch (or α_2-branch) has a higher (or lower) frequency than that of the directly unstable fixed point which is synchronized with the external force.

We shall also use this definition when many points S and D appear on the invariant closed curve, and show the deformation of phase-plane portraits by explaining the behavior of the α_1-branches and α_2-branches.

(b) Almost Periodic Oscillations

We proceed to investigate the loci of fixed points on the invariant closed curve, as the frequency ν of the external force varies while the amplitude B is kept constant (B = 0.5).

First, if we increase the frequency ν from the value of Fig. 3.2, i.e., ν = 1.0, the α_1-branch is shortened and the α_2-one is elongated. So the points S^1 and D^1 approach each other, and ultimately both coalesce if the system parameters are chosen at the rightward boundary of the harmonic entrainment. A further increase in ν results in the disappearance of these coalesced points S^1 and D^1. As an example of this case, we choose the system parameters at point b (B = 0.5, ν = 1.1) in Fig. 3.1, and show its phase-portrait in Fig. 3.3. Since the α_1-branch has disappeared and the α_2-branch has solely left, the successive images of any point on the invariant closed curve keep on moving counterclockwise under iterations of the mapping T, as shown its direction by the arrows in this figure. The corresponding properties of the unstable point U^1 in Fig. 3.3 is given in Table 3.2. The rotation number correlated with the invariant closed curve is computed to be ρ = 0.9285.... Therefore, the invariant closed curve in the rightward region of the harmonic entrainment has a rotation number less than unity as illustrated in Fig. 3.1.

Contrary to the above-mentioned argument, if we decrease the frequency ν from the value of Fig. 3.2, the α_1-branch is elongated

and the α_2-branch is shortened. Consequently, in the leftward region of the harmonic entrainment there only rests the α_1-branch. Here the invariant closed curve has a rotation number greater than unity, so we can obtain the higher-harmonic oscillations.

Summing up the transition between the entrained oscillation and the almost periodic oscillation, we can conclude that if the frequency ν is decreased (or increased), the α_1- (or α_2-) branch is elongated and the α_2- (or α_1-) branch is shortened. Still more, this fact remains independently of the nonlinear restoring term in Eq. (1.5).

(c) Subharmonic Oscillations of Order 1/2

We can obtain the subharmonic oscillations of order 1/2, when the rotation number ρ is equal to 0.5 (at $\nu = 2.0$). Owing to the symmetrical nonlinear characteristic of the system [1], the region of the 1/2-harmonic entrainment is narrow as shown in Fig. 3.1. In proportion to the decrease of μ, this region will become extremely small.

As an example of such a case, we choose the system parameters at point c ($B = 2.0$, $\nu = 1.9$) in Fig. 3.1. In this case, we obtain eight fixed points under the mapping T^2. Their locations and the invariant curves of the mapping T^2 are shown in Fig. 3.4. The details of fixed and periodic points are given in Table 3.3. We can also discuss the transition of invariant curves in the region of the 1/2-harmonic entrainment as the previous case. However, we can obtain the wide region of the 1/2-harmonic entrainment in the

system with nonlinear restoring force. A close study on the 1/2-harmonic oscillations will be accomplished in Sec. 4.4.

(d) Subharmonic Oscillations of Order 1/3

We now discuss three types of representative phase-plane portraits in the region of the 1/3-harmonic entrainment.

At point d (B = 5.0, ν = 2.8) in Fig. 3.1, there occur the 1/3-harmonic oscillations whose phase-portrait is shown in Fig. 3.5. The details of fixed and periodic points are given in Table 3.4.

In this figure, all the α-branches of points D^3, drawn in heavy lines, constitute the boundary of the maximum finite invariant set Δ. However the set of central points M is composed of all points S^3, D^3 and U^1. Since the 3-periodic points exist on the invariant closed curve, this phase-portrait is refered to as a representative one in van der Pol's equation. In the following, we shall confine our attention to the differences relating to the set of central points and the maximum finite invariant set in the region of the 1/3-harmonic entrainment.

If the system parameters are set in the area common to the harmonic and 1/3-harmonic entrainments, such as at point e (B = 14.5, ν = 3.3) in Fig. 3.1, we obtain the phase-portrait as shown in Fig. 3.6. The locations of fixed and periodic points and their properties are listed in Table 3.5. In this case the set of central points consists of all points S^3, D^3 and S^1. From this figure,

it is evident that the ω-branches of points D^3 (drawn in thick lines) separate the whole plane into two domains, in one of which the harmonic oscillation, correlated to point S^1, results with the lapse of time, while in the other the 1/3-harmonic oscillations. The α-branches of points D^3 in addition to the set of central points M correspond to the maximum finite invariant set Δ. So the set Δ, evidently, has no area. Then, we can image that the effect of the negative damping may be equivalently depressed by the large external force. The similar phase-portraits can also be seen in a system without negative damping, so the structure of Fig. 3.6 is not proper to the one in van der Pol's equation.*

With decreasing B, while ν is kept constant ($\nu = 3.3$), the completely stable fixed point S^1 in Fig. 3.6 turns into the completely unstable one U^1. Though not shown explicitly in Fig. 3.1, there appears an almost periodic oscillation which is described by the invariant closed curve around the point U^1 in the phase plane, if the system parameters are chosen just below the boundary of the harmonic entrainment. As an example of this case, we set the system parameters at point f ($B = 14.2$, $\nu = 3.3$) in Fig. 3.1, and show its phase-portrait in Fig. 3.7. The details of fixed and periodic points are given in Table 3.6. The rotation number which characterizes the invariant closed curve (drawn in heavy lines) is

---

* For instance, we can see the same pattern as the one appeared in Duffing's equation [1, 9].

ρ = 0.3103.... The slight alternation in B from the value of Fig. 3.6 has scarcely influenced to the configuration with regard to the invariant set under the mapping T^3. In this case the set of central points is constituted by the invariant closed curve in addition to all points S^3, D^3 and U^1.

The transitions of phase-portraits in the region of the 1/3-harmonic oscillations will be closely investigated in Sec. 4.4.

3.4 Self-Oscillatory Systems with Large Nonlinearity

In Fig. 3.1, we have seen the regions of main entrainment at the frequencies 1/3, 1/2, 1 and 3 times the driving frequency ν in the case where μ = 1 in Eq. (3.1). Generally speaking, there must be occurred periodic oscillations in a forced self-oscillatory system, if its rotation number ρ is rational.

With increasing the damping coefficient μ in Eq. (3.1), that is, we can obtain the strongly nonlinear system, then many regions of frequency entrainment in higher orders which were scarcely recognized in a weakly nonlinear system appear in the system with linear restoring force. Therefore, in this section we shall consider the system with large nonlinear damping, i.e., μ = 10 in Eq. (3.1).

A differential equation containing the large positive and negative damping have a solution which is far from the sinusoidal wave, i.e., the relaxation type. Since its higher-harmonic components are not small, it is hard to obtain precisely the solution of Eq. (3.1) in this case.

Therefore, we rewright Eq. (3.1) such as

$$\frac{d^2z}{dt^2} - \mu(1 - z^2)\frac{dz}{dt} + z = B\cos\nu t \tag{3.2}$$

This is integrated to give

$$\frac{dz}{dt} - \mu(1 - \frac{1}{3}z^2)z + \int z\,dt + c = \frac{B}{\nu}\sin\nu t \tag{3.3}$$

where c is an integral constant. Furthermore, we introduce new variables defined by

$$\begin{aligned} x &= \int z\,dt + c \\ F &= B/\nu \end{aligned} \tag{3.4}$$

Then Eq. (3.3) may be changed as

$$\frac{d^2x}{dt^2} - \mu[1 - \frac{1}{3}(\frac{dx}{dt})^2]\frac{dx}{dt} + x = F\sin\nu t \tag{3.5}$$

Since x(t) of Eq. (3.5) is obtained by integrating z(t) of Eq. (3.2) (see Eq. (3.4)), x(t) is such slowly varing function of t that it may be rather easily realized to simulate Eq. (3.5) by using an analog-computer.

Thus, as an example of large nonlinear systems we put $\mu = 10$ in Eq. (3.5), and consider the following system;

$$\begin{aligned} \frac{dx}{dt} &= y \\ \frac{dy}{dt} &= 10\,[1 - \frac{1}{3}y^2]\,y - x + F\sin\nu t \end{aligned} \tag{3.6}$$

In Fig. 3.8 we have represented the regions of principal frequency entrainments obtained by using an analog-computer. The numbers marked in this figure, such as 1, 1/2, 1/3, ···, exhibit the orders of the subharmonic oscillations.

We can notice that each entrained region, especially of the odd harmonic oscillations, in Fig. 3.8 is far greater than the previous one in the case where $\mu = 1.0$, as shown in Fig. 3.1. Therefore, in the areas common to the different frequencies, two types of oscillations are obtained, if we vary the initial conditions.

As an example of such oscillations, we consider the case where the system parameters are given by $F = 4.6$, $\nu = 2.0$ in Eq. (3.6), and write

$$\frac{dx}{dt} = y$$

$$\frac{dy}{dt} = 10\left[1 - \frac{1}{3}y^2\right]y - x + 4.6 \sin 2t \qquad (3.7)$$

Since the external force is located in the area common to the region of the 1/3- and 1/5-harmonic entrainments, there appear completely stable 3-periodic points (indicated by 1, 2 and 3) and 5-periodic points (indicated by 4, 5, 6, 7 and 8) as shown in Fig. 3.9. The trajectories of the stable solutions are drawn in heavy lines and the domains of attraction leading to the 1/3- and 1/5-harmonic responses are also drawn in fine lines.

However, as the damping coefficient in Eq. (3.6) is too large

($\mu = 10$) to determine the positions of the unstable periodic points, we can not fully discuss the properties of the invariant curves, perhaps very complicated, passing through the directly and inversely unstable periodic points, such as in the preceding section.

By the way, the large nonlinearity in Eq. (3.6) may bring about the fact that many other regions of frequency entrainment are densely aggregated. In order to know their features closely, we expand the neighborhood of the 1/2-harmonic entrainment which is indicated by dashed lines in Fig. 3.8 and show the entrained regions of ultra-subharmonic oscillations, such as 3/4, 5/7, $\cdots$, in Fig. 3.10.* It may be conjectured that there also occur many other frequency entrainments which have not shown in this figure. However their regions are too small and narrow to represent their details clearly. Although the theoretical analysis for them has not yet been accomplished for the sake of too large nonlinear damping, the ultra-subharmonic oscillations in the system with nonlinear restoring force will be considered in Sec. 4.4

*These ultra-subharmonic oscillations may be hardly recognized when μ is small. However, they are often obtained in a forced self-oscillatory system with nonlinear restoring force.

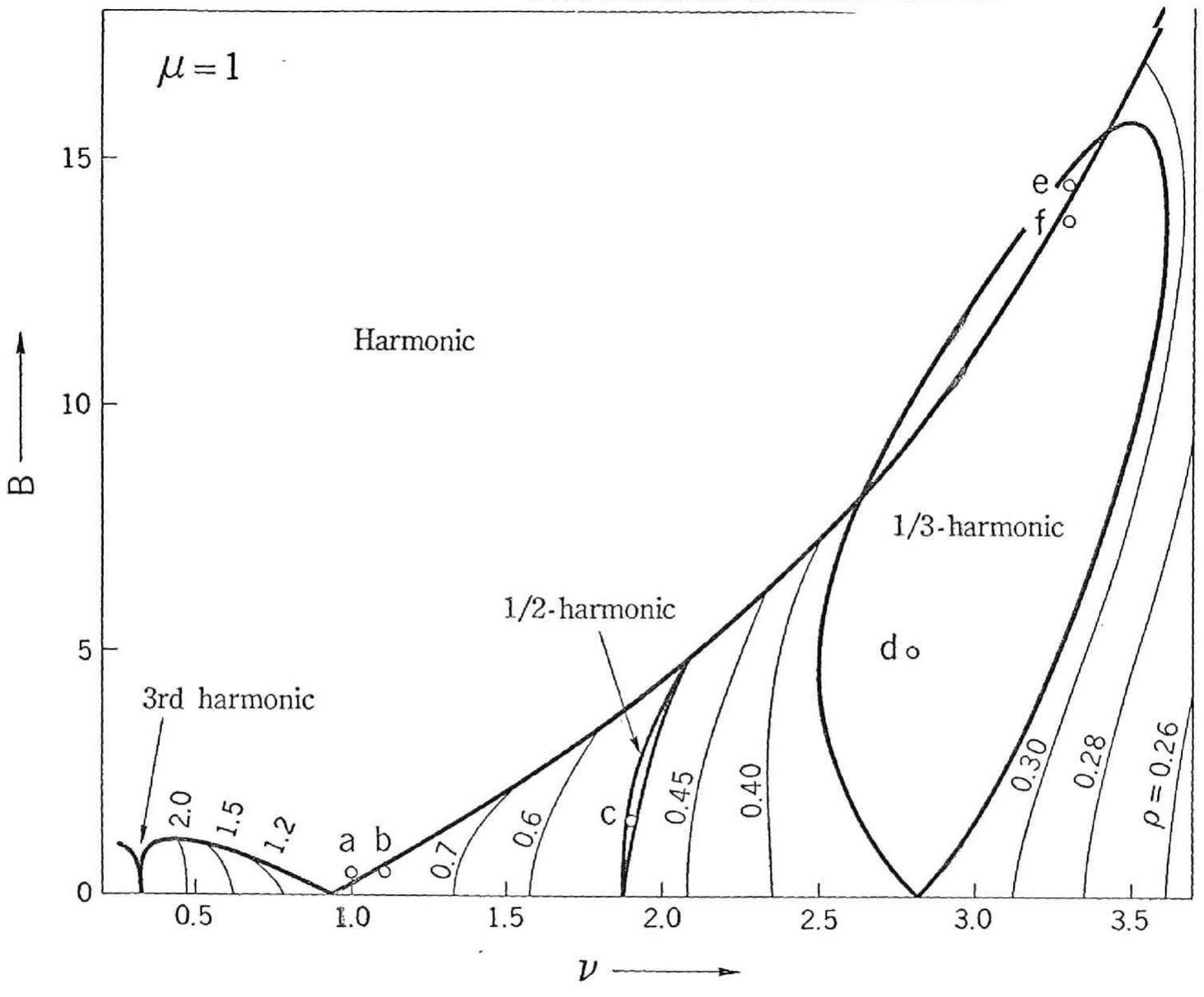

Fig. 3.1 Regions of frequency entrainment and iso-ρ curves.

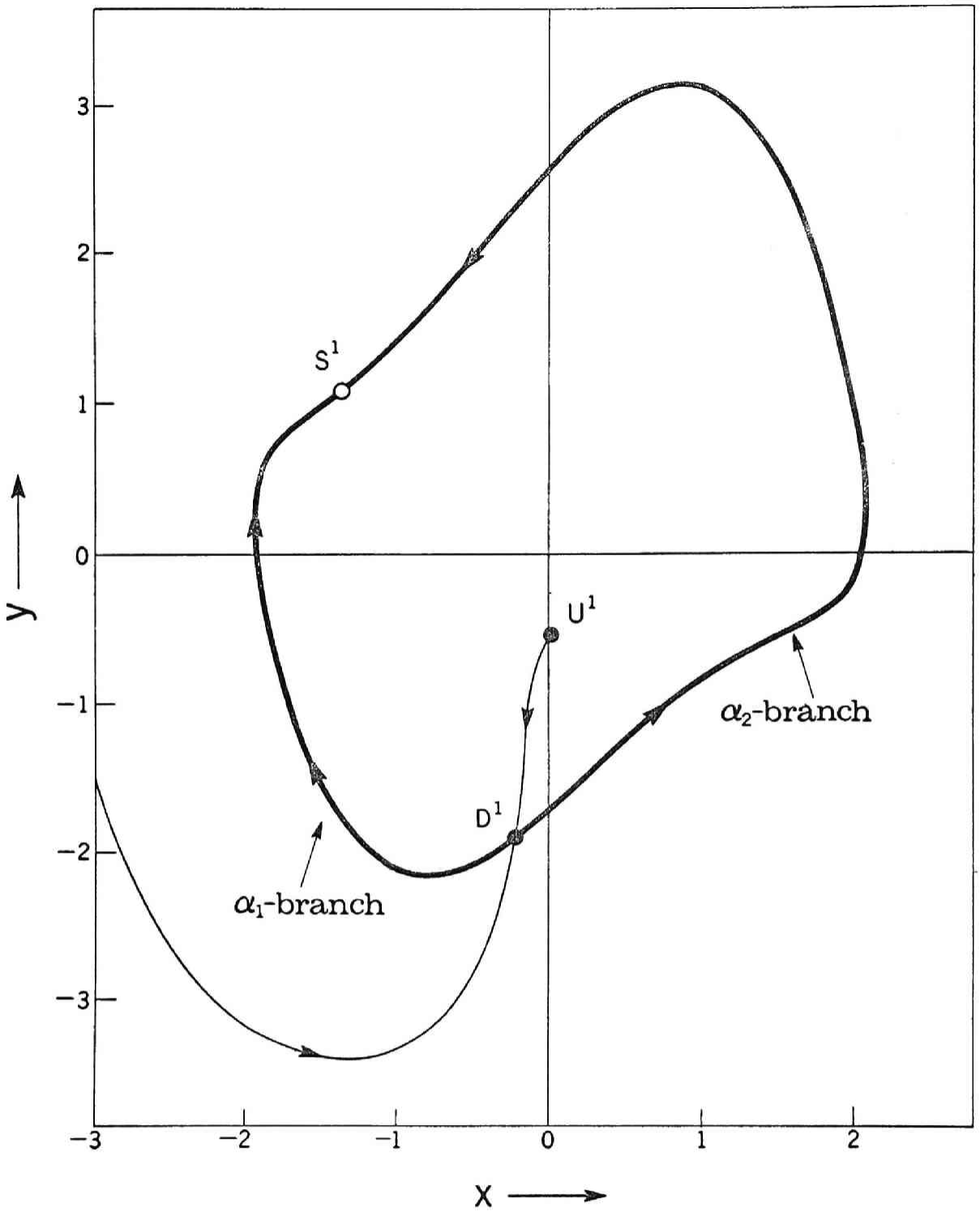

Fig. 3.2 Fixed points and invariant curves of the mapping for Eq. (3.1).
(a) B = 0.5, ν = 1.0

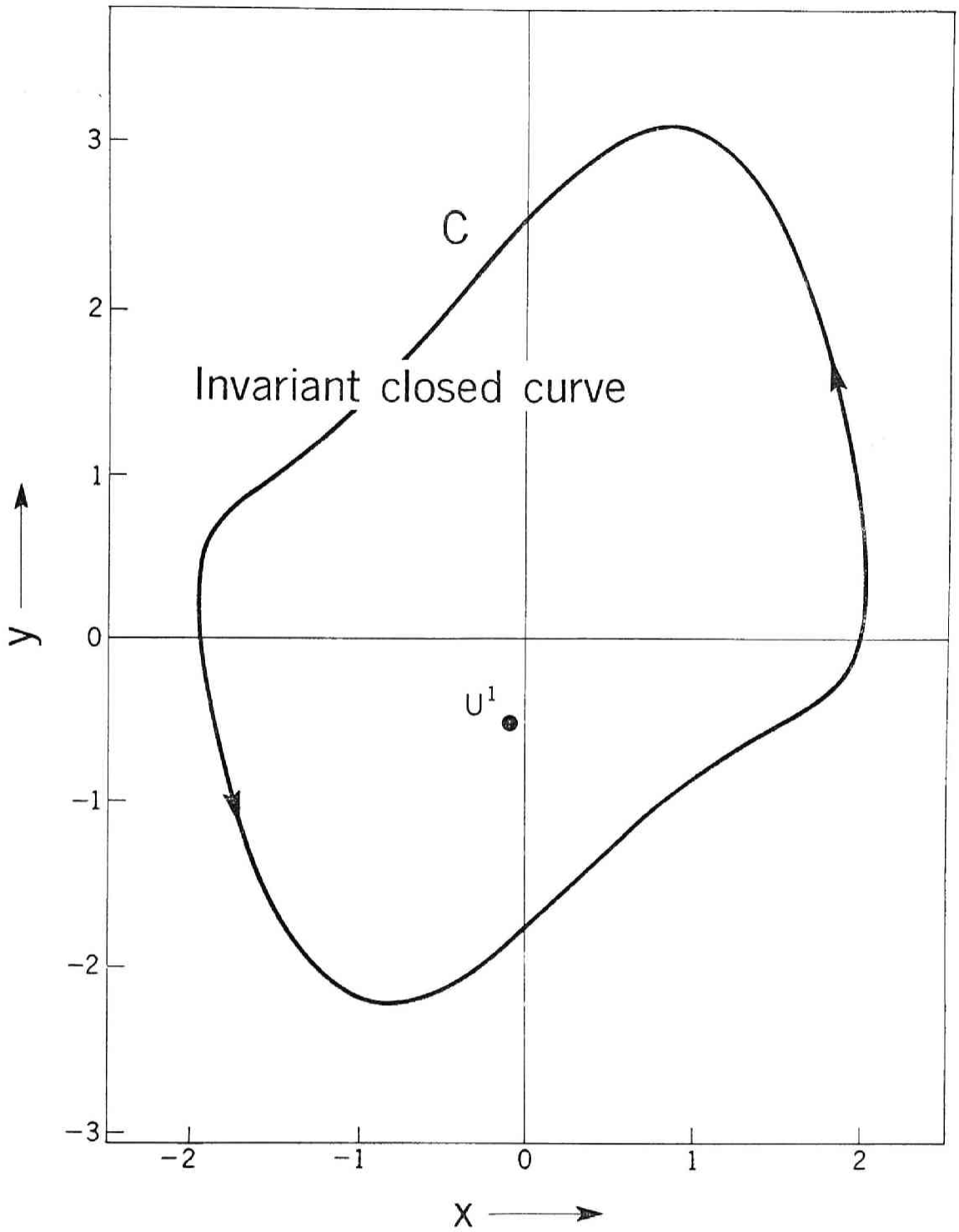

Fig. 3.3 Fixed points and invariant closed curve of the mapping for Eq. (3.1).
(b) B = 0.5, ν = 1.1

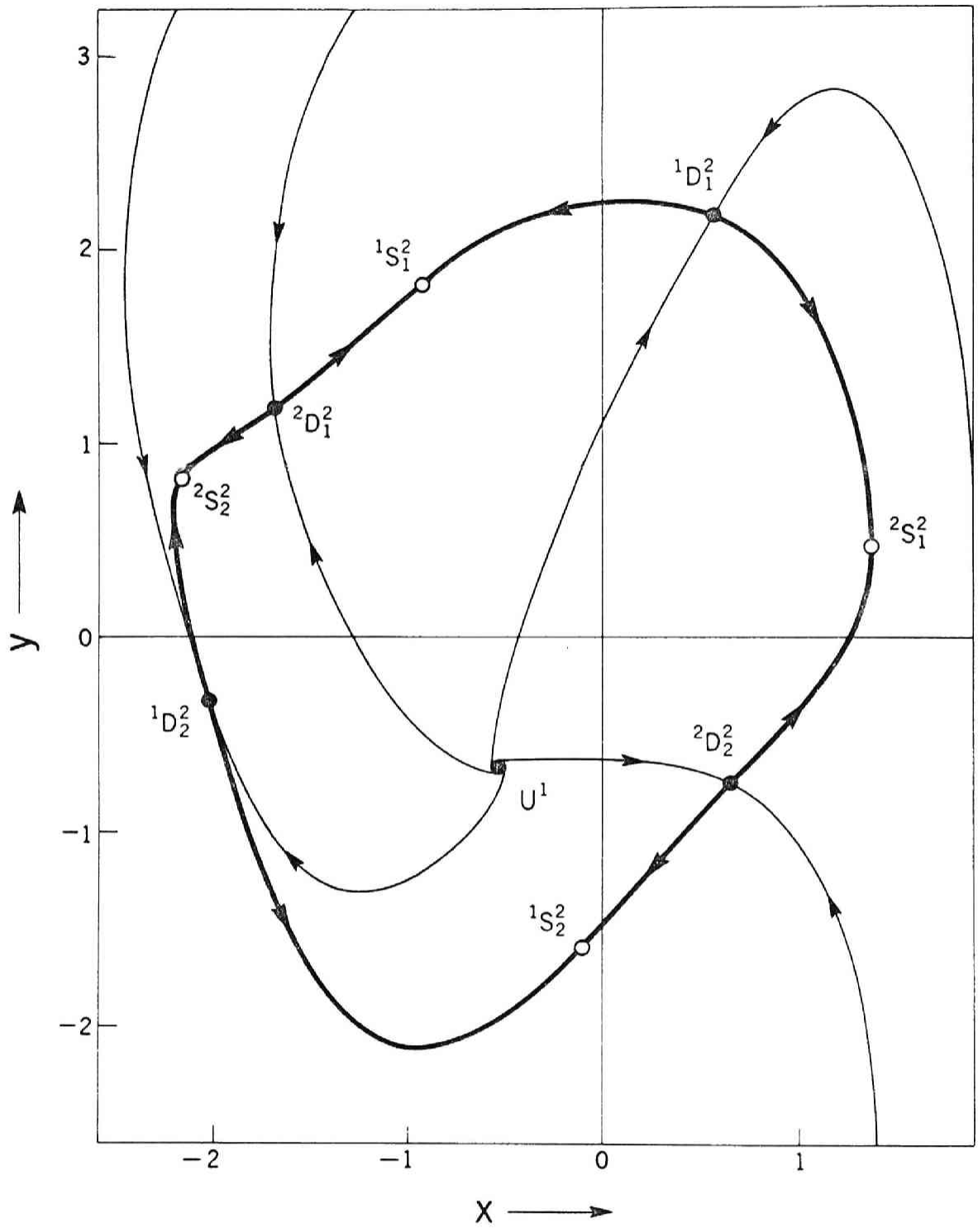

Fig. 3.4 Fixed points and invariant curves of the mapping for Eq. (3.1).

(c) B = 2.0, ν = 1.9

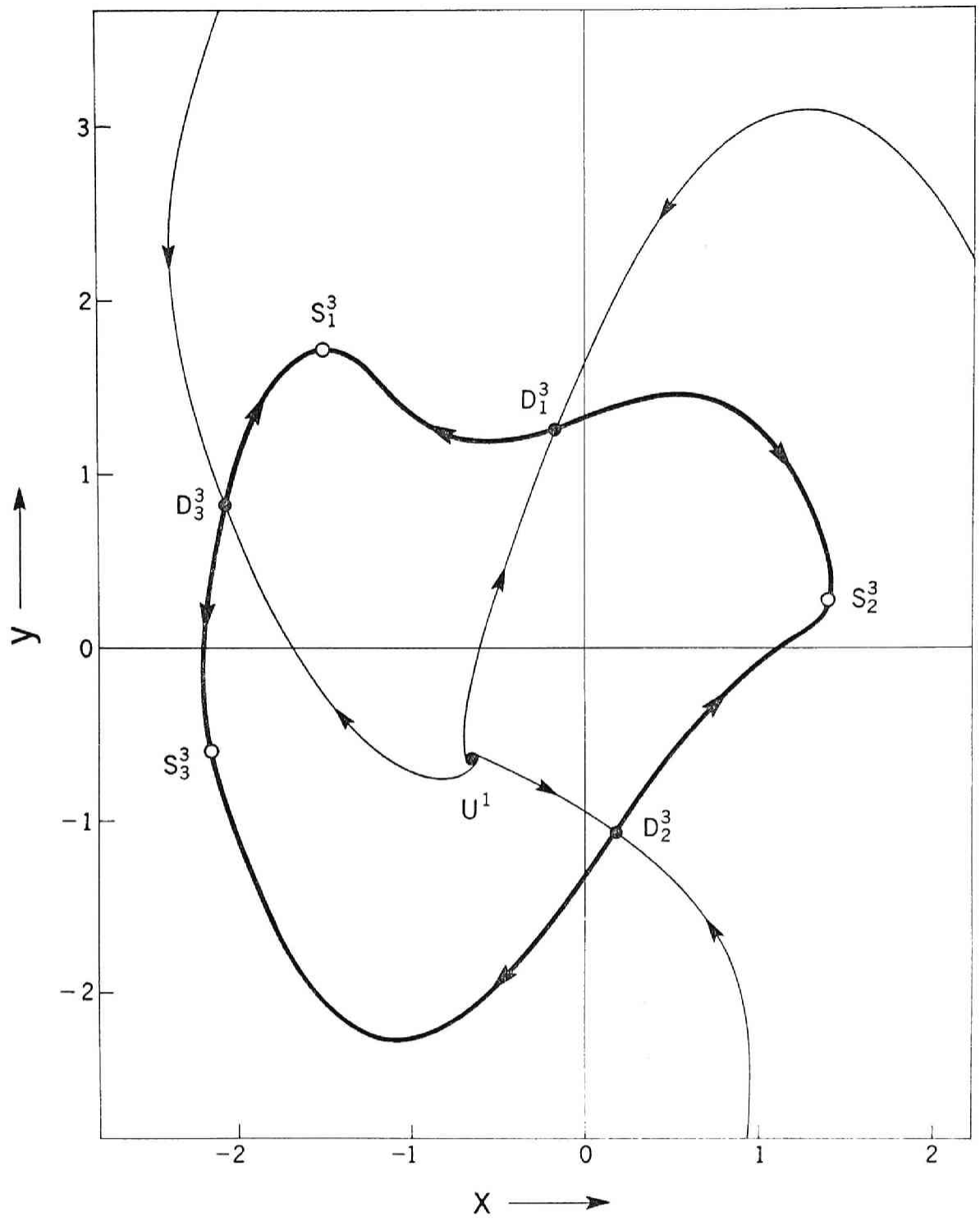

Fig. 3.5 Fixed points and invariant curves of the mapping for Eq. (3.1).

(d) B = 5.0, ν = 2.8

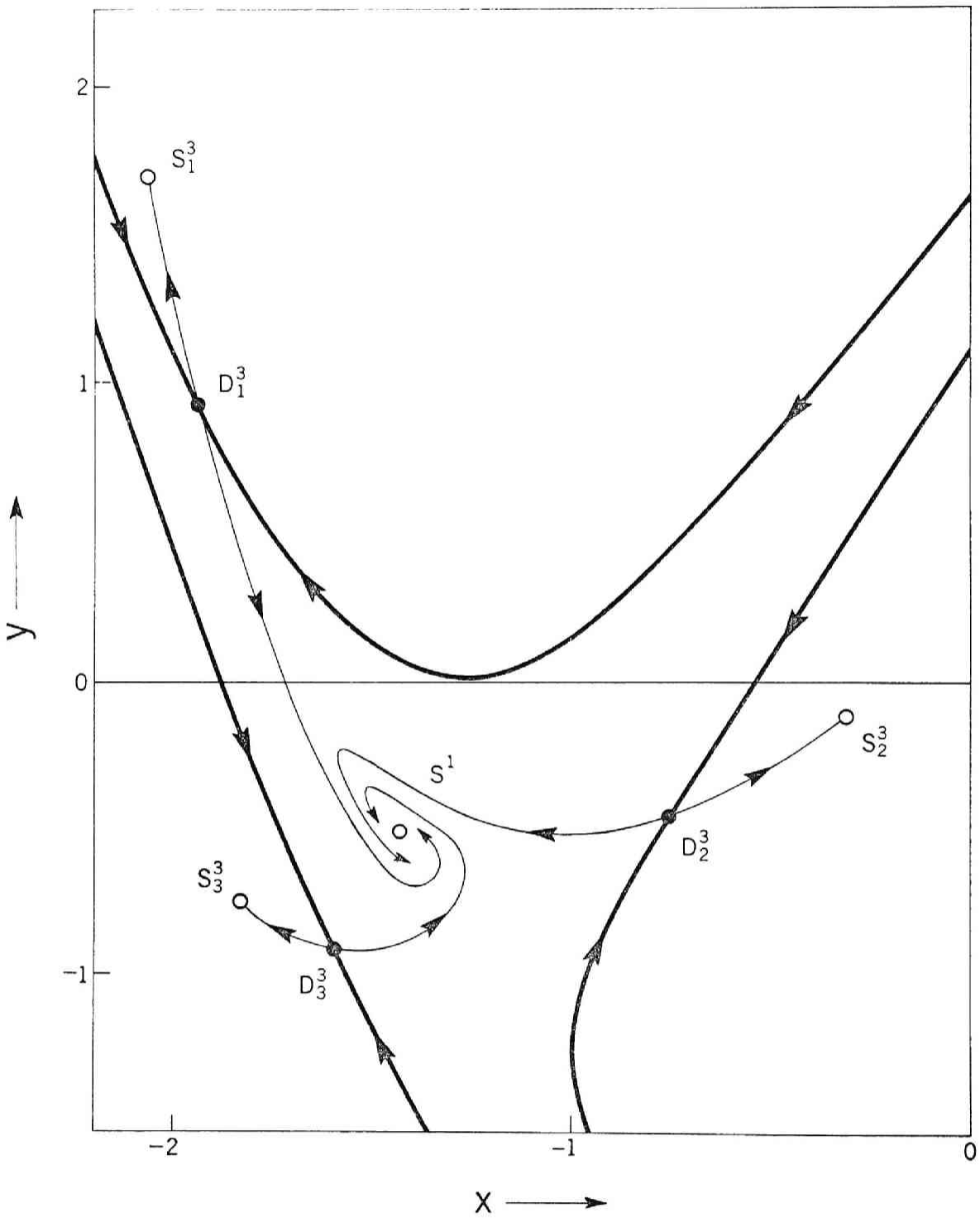

Fig. 3.6 Fixed points and invariant curves of the mapping for Eq. (3.1).
(e) B = 14.5, ν = 3.3

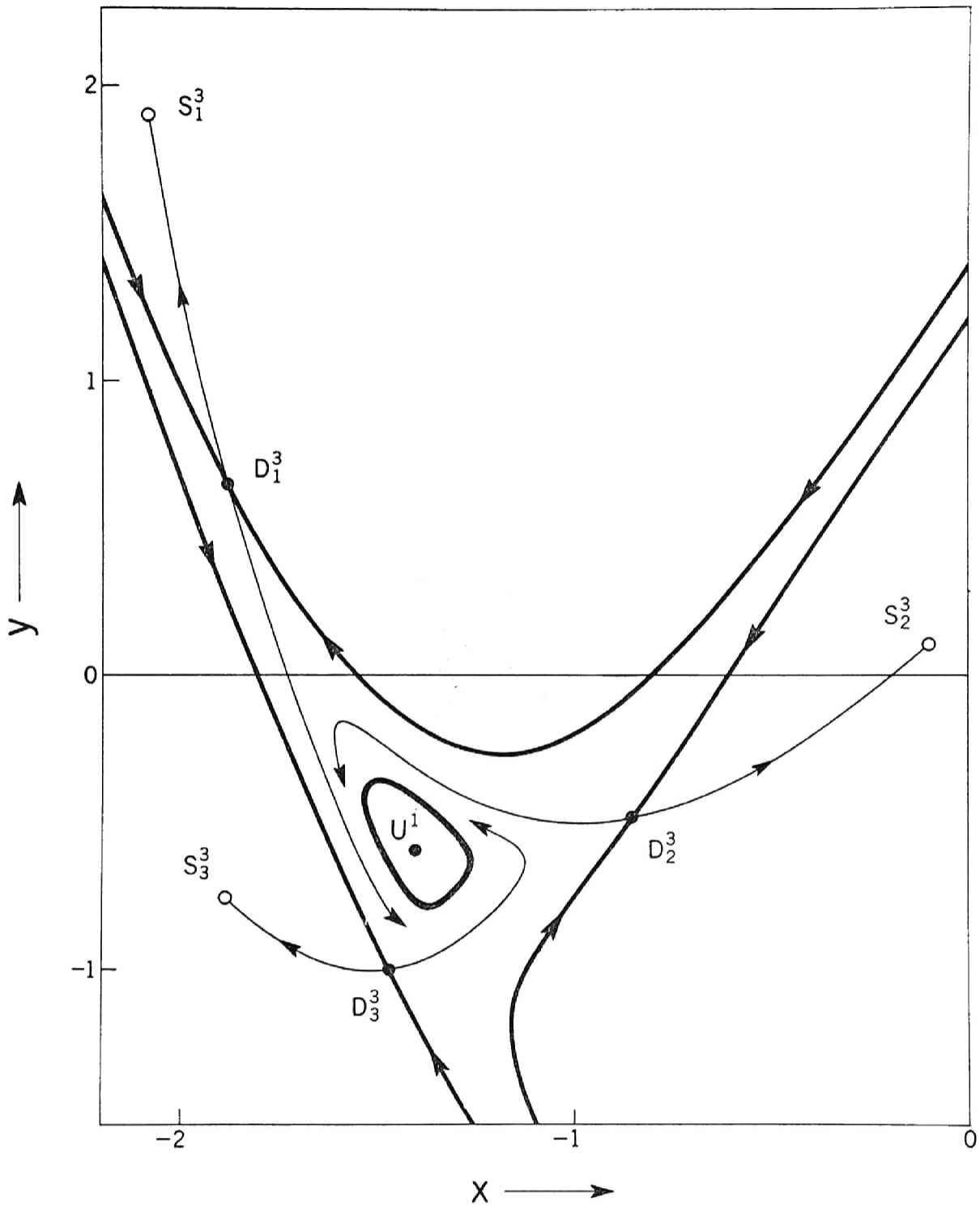

Fig. 3.7 Fixed points and invariant curves of the mapping for Eq. (3.1).
(f) B = 14.2, ν = 3.3

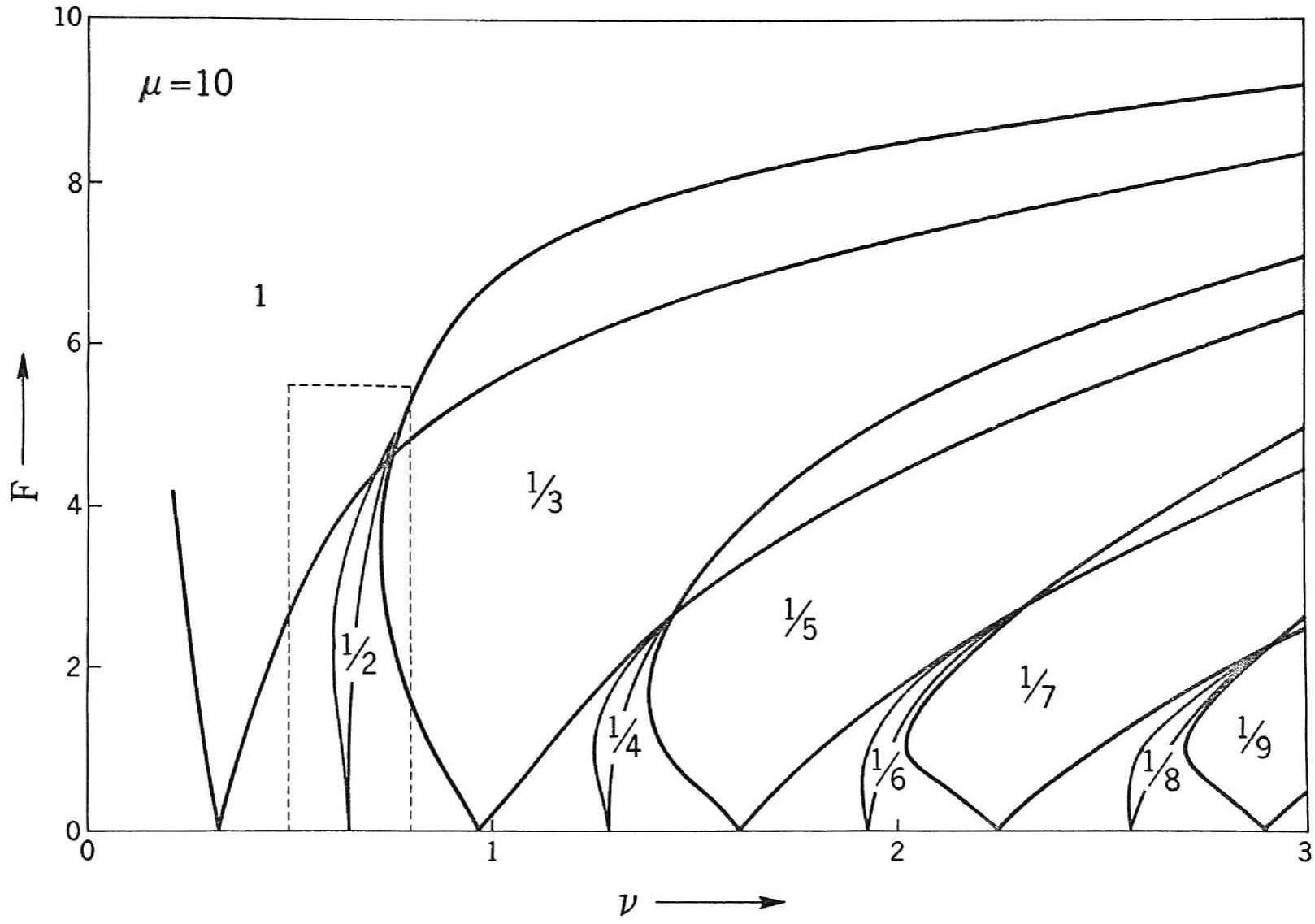

Fig. 3.8 Regions of frequency entrainment for Eq. (3.5).

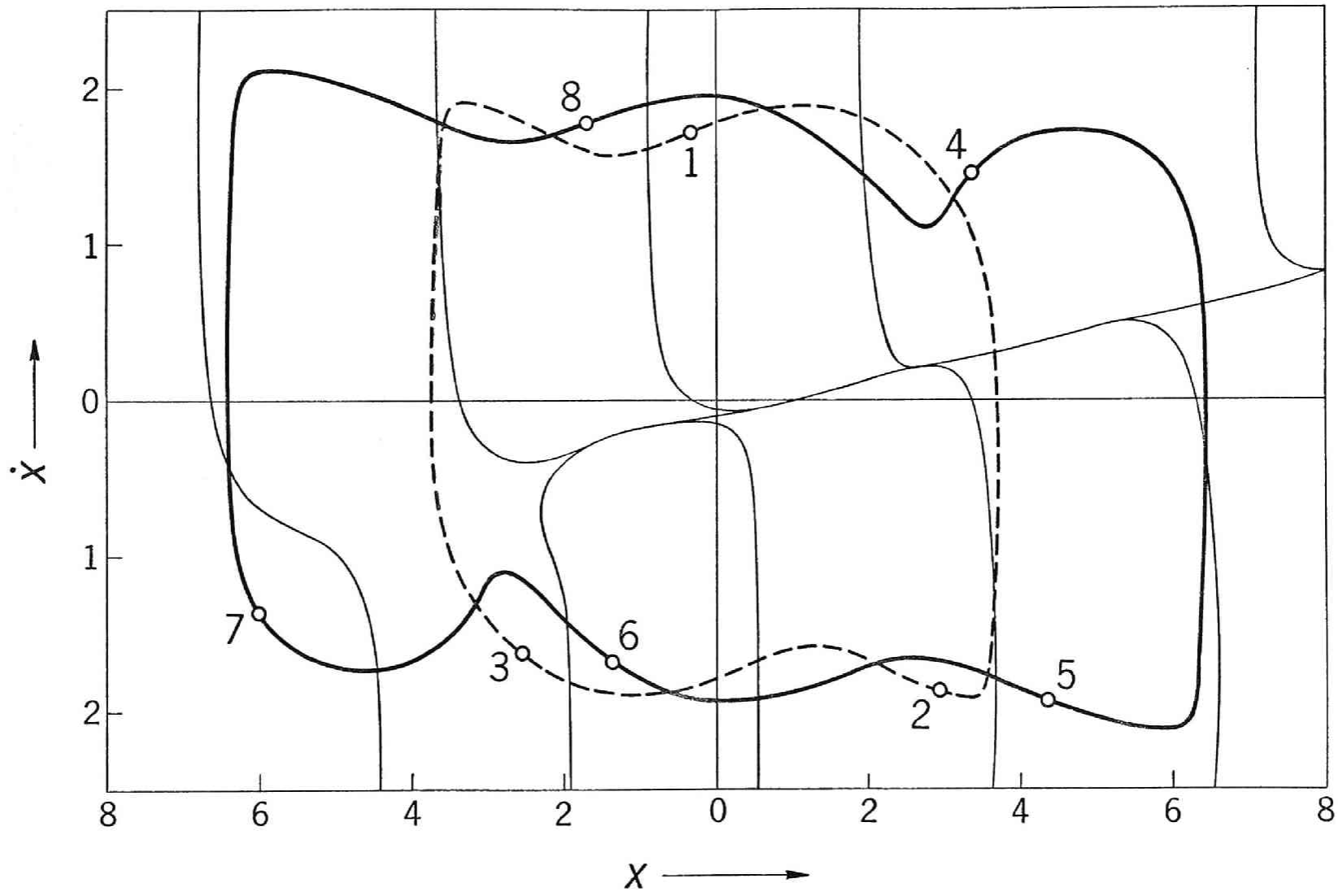

Fig 3.9 Regions of initial conditions leading to the 1/3- and 1/5-harmonic responses, and the trajectories correlated with the stable fixed points for Eq. (3.5). ($F = 4.6$, $\nu = 2.0$)

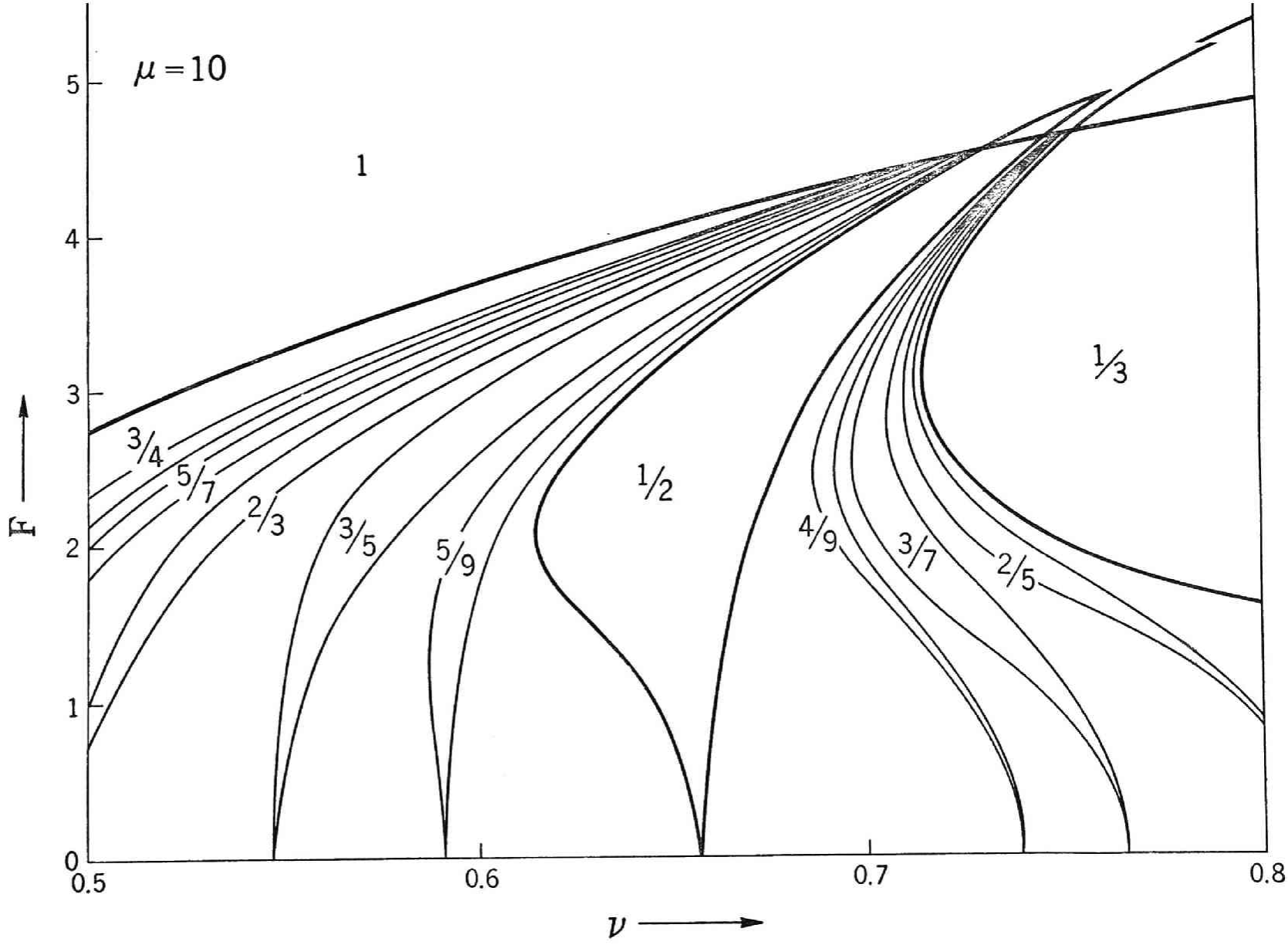

Fig. 3.10 Entrained regions of ultra-subharmonic oscillations for Eq. (3.5).

Table 3.1 Fixed Points and Related Properties in Fig. 3.2 (B = 0.5, ν = 1.0)

Fixed point	x	y	m_1 , m_2	|m|
S^1	-1.351	1.098	0.000 , 0.477	
D^1	-0.220	-1.895	0.028 , 2.457	
U^1	0.004	-0.535	12.498 $\pm$ 7.649i	14.653

Table 3.2 Fixed Points and Related Properties in Fig. 3.3 (B = 0.5, ν = 1.1)

Fixed point	x	y	m_1 , m_2	|m|
U^1	-0.091	-0.511	5.126 $\pm$ 11.571i	12.656

Table 3.3 Fixed Points and Related Properties in Fig. 3.4 (B = 2.0, ν = 1.9)

Fixed point	x	y	m_1 , m_2	|m|
$^1S_1^2$	-0.932	1.816	0.002 , 0.777	
$^1S_2^2$	-0.107	-1.584	0.002 , 0.777	
$^2S_1^2$	1.371	0.464	0.002 , 0.777	
$^2S_2^2$	-2.170	0.819	0.002 , 0.777	
$^1D_1^2$	0.564	2.166	0.004 , 1.311	
$^1D_2^2$	-2.028	-0.325	0.004 , 1.311	
$^2D_1^2$	-1.701	1.174	0.004 , 1.311	
$^2D_2^2$	0.650	-0.738	0.004 , 1.311	
U^1	-0.541	-0.673	-3.699 $\pm$ 0.383i	3.719

Table 3.4 Fixed Points and Related Properties in Fig. 3.5 (B = 5.0, ν = 2.8)

Fixed point	x	y	m_1 , m_2	|m|
S_1^3	-1.493	1.717	0.002 , 0.021	
S_2^3	1.396	0.259	0.002 , 0.021	
S_3^3	-2.144	-0.597	0.002 , 0.021	
D_1^3	-0.170	1.260	0.012 , 11.476	
D_2^3	0.180	-1.063	0.012 , 11.476	
D_3^3	-2.065	0.821	0.012 , 11.476	
U^1	-0.650	-0.641	$-1.138 \pm 2.062i$	2.355

Table 3.5 Fixed Points and Related Properties in Fig. 3.6 (B = 14.5, ν = 3.3)

Fixed point	x	y	m_1 , m_2	|m|
S_1^3	-2.062	1.676	0.035 , 0.669	
S_2^3	-0.328	-0.132	0.035 , 0.669	
S_3^3	-1.825	-0.768	0.035 , 0.669	
D_1^3	-1.938	0.916	0.143 , 1.318	
D_2^3	-0.756	-0.462	0.143 , 1.318	
D_3^3	-1.595	-0.917	0.143 , 1.318	
S^1	-1.436	-0.515	$-0.326 \pm 0.904i$	0.961

Table 3.6 Fixed Points and Related Properties in Fig. 3.7 (B = 14.2, ν = 3.3)

Fixed point	x	y	m_1 , m_2	|m|
S_1^3	-2.080	1.898	0.022 , 0.424	
S_2^3	-0.106	0.101	0.022 , 0.424	
S_3^3	-1.885	-0.754	0.022 , 0.424	
D_1^3	-1.875	0.623	0.232 , 1.593	
D_2^3	-0.856	-0.487	0.232 , 1.593	
D_3^3	-1.471	-1.002	0.232 , 1.593	
U^1	-1.404	-0.550	$-0.339 \pm 0.943i$	1.002

Chapter 4 Self-Oscillatory Systems with Nonlinear Restoring Force

4.1 Introduction

In the preceding chapter, we have investigated the forced self-oscillatory systems with linear restoring force and shown several typical phase-plane portraits of van der Pol's equation. But under the circumstance that $c_3 = 0$ in Eq. (1.5), a slight alternation of the system parameters B and ν brought about the rapid transition of the invariant set in the phase plane. That is, the maximum finite invariant set Δ had a certain area for small B, and it had no area for large B. Such transition of phase-portraits occurred in the extremely narrow range of the system parameters. Therefore it may be impossible to investigate the changes of phase-portraits closely. However, with increasing the coefficient c_3 of the nonlinear restoring term in Eq. (1.5), the regions of frequency entrainment is expanded, although the parameter μ is kept in a small value.

In order to consider as finely as possible the influence of the nonlinear restoring force upon the behavior of the solutions and investigate the above-mentioned transitions, we shall deal with, for the time being, the following equation, the system parameters being $\mu = 0.2$, $c_1 = 0$ and $c_3 = 1$ in Eq. (1.5);

$$\frac{d^2x}{dt^2} - 0.2\,(1 - x^2)\,\frac{dx}{dt} + x^3 = B\cos\nu t \qquad (4.1)$$

In this chapter we show various types of phase-portraits in the

regions of frequency entrainment, and describe their changes when the system parameters are varied. In this case we confine our attention to the behavior of α- and ω-branches, in particular so as to discuss the reason why the nonperiodic oscillations* whose successive images of the mapping are dispersed in the phase plane arise outside the region of frequency entrainment.

4.2 Regions of Frequency Entrainment

The regions of frequency entrainment in Eq. (4.1), obtained by using an analog-computer, are illustrated in Fig. 4.1.** In this figure, we can see the regions of entrainment at the frequencies 1, 1/2 and 1/3 times the driving frequency ν.

When the external force is taken off from Eq. (4.1), i.e., $B = 0$, there appears a self-excited oscillation whose natural frequency ω_0 is equal to 1.621.... Therefore, we can obtain the harmonic oscillations in the neighborhood of the natural frequency ω_0 as shown in Fig. 4.1. The 1/2-harmonic entrainment and the 1/3-harmonic one also appear at $\nu \cong 2\omega_0$ and $\nu \cong 3\omega_0$ respectively. By virture of a symmetrical nonlinearity of the system, the regions

---

*The discussion on such nonperiodic oscillations will be given later in Chap. 5.

**The reason that the boundary of this region bends abruptly at $\nu = 4.8$ will be explained in Sec. 4.3, relating to the occurrence of two different types of the harmonic oscillation.

of odd harmonic entrainments are extremely large, so the harmonic entrainments of different orders have the overlapped region for comparatively large B. So the regions of the 1/2-harmonic and 1/3-harmonic entrainments are drawn by changing the direction of the hatched lines in Fig. 4.1.

Under certain combinations of the system parameters, there appear many other frequency entrainments in Eq. (4.1). Here, we call them ultra-subharmonic oscillations. But their entrained regions are so small that they have been omitted in Fig. 4.1.*

4.3 Harmonic Oscillations [21]

The region of harmonic entrainment in Fig. 4.1 is expanded as shown in Fig. 4.2, in order to concentrate our attention to the change of its phase-portrait. Above the broadest line in this figure, there appears at least one completely stable fixed point, correlated with a stable periodic solution of Eq. (4.1), in the phase plane.

Since many types of phase-portraits appear in the region of harmonic entrainment, they are classified as shown in Fig. 4.2 according to the difference of their own configurations.

To begin with, we shall show a representative phase-portrait of the harmonic oscillation. In the case where B = 0 in Eq. (4.1),

---

*As an example of such ultra-subharmonic oscillations, we shall show the region of the 3/5-harmonic entrainment in Fig. 4.21.

the damping is negative for the small value of x, so that a self-oscillation whose natural frequency ω_0 is equal to 1.621... results. Then under the impression of the small external force, while $\nu \cong \omega_0$, one may expect the occurrence of harmonic entrainment. For such a case, we have chosen the system parameters at point a (B = 0.2, ν = 1.6) in Fig. 4.2 and shown its phase-portrait, which is the typical one in van der Pol's equation, in Fig. 4.3. The details of fixed points are given in Table 4.1. In the portion represented by point a of Fig. 4.2, there results the same structure of the phase-portrait as the one in Fig. 4.3.

Comparing this figure with Fig. 3.2, we must point out a remarkable difference between two figures concerning the movement near the completely stable fixed point S^1, though both have same constructions in topology. In fact, the characteristic multipliers of point S^1 in Fig. 3.2 were m_1= 0.000 and m_2= 0.477*, so that the stable point S^1 was a nodal type. On the other hand, in Fig. 4.3 both α-branches starting from point D^1 converge spirally to point S^1, because the value of m_1 and m_2 of point S^1 are 0.581 ± 0.490i.** These features near the stable point S^1 will play an important role later on, when the system parameters are varied.

Next, we shall investigate the transitions of phase-portraits in the region of harmonic entrainment, by using the notion;

---

* These were given in Table 3.1.

** These were given in Table 4.1.

" an α_1-branch and an α_2-branch ", which has been already introduced in Sec. 3.3.

With increasing the driving frequency ν from this state, the frequency of the oscillation corresponding to the invariant closed curve is apt to decrease conversely. Then the α_2-branch contiguous to point D^1 is gradually lengthened. Since this α_2-branch proceeds spirally to point S^1, it makes its way into the maximum finite invariant set Δ still more. Ultimately, this α_2-branch intersects the ω-branch of point D^1 mutually, so there may appear an infinite number of homoclinic points near the intersections. These phenomena occur in the shaded domain ▨ of Fig. 4.2. As an example of such homoclinic types, we choose the system parameters at point c ($B = 8.5$, $\nu = 3.0$) in Fig. 4.2, and show its phase-portrait in Fig. 4.4. The details of these fixed points are given in Table 4.2. In this figure the α- and ω-branches intersect one another, so infinitely many homoclinic points may appear. This phase-portrait is similar to the one obtained in Duffing's equation [9]. However, in Duffing's equation there appear the completely stable fixed point S^1 which corresponds to the nonresonant state in the ferroresonance phenomenon instead of the unstable point U^1 of Fig. 4.4.

Furthermore, we shall consider the case where the amplitude B is increased or decreased from this case, while ν is kept constant ($\nu = 3.0$). In both cases, the α-branch can not intersect to the ω-branch, then the domains where each α-branch stays are perfectly separated by two ω-branches as shown in Fig. 4.5. The

system parameters of this figure have been chosen at point b ($B = 5.8$, $\nu = 3.0$) in Fig. 4.2. The locations of fixed points and their properties are given in Table 4.3. Since one of the α-branches can find no stable point where it should finally converge, its successive images meander repeatedly and wander complicatedly around point U^1 under the influence of doubly asymptotic points. Conversely speaking, such meanderings foreshadow the appearance of homoclinic points.

If we decrease the amplitude B from this state, the distance between point S^1 and point D^1 is shortened, so ultimately they coalesce at the boundary (drawn in the broadest line) of harmonic entrainment in Fig. 4.2. Then in the outside of this region, both points do not exist any longer. As a result, in the phase plane there remains only one set of random points correlated with the nonperiodic oscillation, whose details will be mentioned in the following chapter.

If the system parameters are prescribed below the dashed line in Fig. 4.2, there exists at least one completely unstable fixed point whose characteristic multiplier $|m|$ is greater than unity, for instance $|m| = 1.102$ at point c. According as the amplitude B is increased, $|m|$ is gradually decreased. Then $|m|$ becomes to be less than unity in the region above the dashed line, so that the completely unstable fixed point turns into the stable one. Therefore, in the shaded region ▤ of Fig. 4.2, two completely stable fixed points $^1S^1$ and $^2S^1$ appear in the phase plane as shown in Fig. 4.6. For this feature, we have chosen the system parameters

at point d (B = 11.0, ν = 3.0) in Fig. 4.2. The details of fixed points are listed in Table 4.4. This phase-portrait is topologically similar to the one occurring in Duffing's equation [9]. And in this case, the maximum finite invariant set Δ has no area, because there exists no completely unstable fixed point in the phase plane.

A further increase in B yields the coalescence of points $^2S^1$ and D^1 on the upper boundary of the region ▤ in Fig. 4.2. As a result of the disappearance of points $^2S^1$ and D^1, only one completely stable fixed point $^1S^1$ remains in the phase plane.

Summarizing the above argument, the broadest line in Fig. 4.2 corresponds to the border line for the existence of point $^1S^1$, and the dashed line for the existence of point $^2S^1$. As these two lines interchange their own locations each other at $\nu \cong 4.8$, that is, the broadest line in Fig. 4.2 lies above the dashed one for the greater ν than 4.8, the boundary of harmonic entrainment bends here abruptly as shown in Fig. 4.1.

4.4 Subharmonic Oscillations

In the preceding section, we have investigated the various phase-portraits of harmonic oscillations occurring in the self-oscillatory system with nonlinear restoring force. From the foregoing study on the system with linear restoring force in Chap. 3, it may be conjectured that the presence of the nonlinear restoring term is more desirable for the occurrence of subharmonic oscillations in spite of the small damping coefficient.

It may be worth while investigating the various types of phase-

portraits in the region of the subharmonic entrainments. So, in the present section we shall deal with the main subharmonic oscillations of orders 1/2 and 1/3 and the ultra-subharmonic ones in the self-oscillatory system with nonlinear restoring force under the condition that the damping coefficient μ is comparatively small.

(a) Subharmonic Oscillations of Order 1/2

In spite of the small damping coefficient μ in Eq. (4.1), there occurs the 1/2-harmonic entrainment in a comparatively wide range. The region of the 1/2-harmonic entrainment shown in Fig. 4.1 is divided into five portions, according to the difference of structures among their own phase-portraits. Let us call each domain by Type I, Type II, ..., Type V of the 1/2-harmonic oscillations as marked by Roman numerals in Fig. 4.7. Especially, in the domains II and IV there appear different types of heteroclinic points, so that these parts have been indicated by changing the directions of the hatched lines.

We shall proceed to show the representative phase-portraits in each domain, and investigate closely the mutual transitions of invariant sets, when the system parameters B and ν are varied, because they have been hardly recognized in a system with linear restoring force. For this purpose, the notion; " an α_1-branch and an α_2-branch ", will be found to be effective to explain the transition of phase-portraits.

(1) Type I

Under the circumstance that the driving frequency ν in Eq. (4.1) is nearly equal to $2\omega_0$ (= 3.242...), while the amplitude B is comparatively small, there occur the 1/2-harmonic oscillations whose phase-portrait is named 'Type I' as indicated in Fig. 4.7.

As an example of Type I, we shall consider the case where the system parameters are chosen at point a (B = 2.0, ν = 3.2) in Fig. 4.7. And its phase-portrait is illustrated in Fig. 4.8. The fixed and periodic points and their related properties are listed in Table 4.5.

The configuration of this phase-portrait is similar to the one occurring in the system with linear restoring force (see Fig. 3.4). In this figure there appear two pairs of points S^2 and D^2 on the invariant closed curve. The structure of the maximum finite invariant set Δ which is encircled by the above-mentioned curve may be complicated by changing the impressed external force.

In order to survey the modifications of this phase-portrait, we shall confine our attention to the branches connected to point ${}^1D_1^2$ in Fig. 4.8, as a special example, but the branches of the other directly unstable points behave similarly.

(2) Type II

With decreasing the frequency ν from the state of Fig. 4.8, the frequency of the oscillation correlated with the invariant closed curve increases, then the α_1-branch of point ${}^1D_1^2$ grows gradually.

Now, this α_1-branch is winding around the point ${}^1S_1^2$ and spirally converging to it, as shown in Fig. 4.8. Consequently, a further decrease in ν may bring about the possibility that the α_1-branch of point ${}^1D_1^2$ intersects the one of the ω-branches of point ${}^2D_2^2$ one another. In fact, if we set the system parameters at point b (B = 2.5, ν = 3.0) in the domain II indicated by hatched lines ▨ in Fig. 4.7, there appear the homoclinic and the heteroclinic structures of invariant curves as shown in Fig. 4.9. The details of fixed and periodic points are listed in Table 4.6. Making a comparison between Fig. 4.8 and Fig. 4.9, one notices that they have the same configuration except only one difference that all α_1-branches of points D^2 intersect the ω-branches of points D^2, then an infinite number of doubly asymptotic points appear in Fig. 4.9. In this figure, the maximum finite invariant set Δ is too complicated to investigate it closely.

(3) Type III

We shall further decrease the frequency ν from the value of Type II.

The lower frequency of the external force becomes, the more own growth the α_1-branch of point ${}^1D_1^2$ promotes. Ultimately, such α_1-branch disjoints its intersections with the ω-branch of point ${}^2D_2^2$, and goes outward apart from all the ω-branches.

As a representative example of this case, we choose the point c (B = 2.0, ν = 2.9) which belongs to Type III as shown in

Fig. 4.7, and illustrate its phase-portrait in Fig. 4.10. The details of fixed and periodic points are listed in Table 4.7. The α_1-branches passing through points D^2 do not intersect to the ω-branche of points D^2, and converges to the other stable periodic points (for instance, to the 5-periodic points corresponding to the 3/5-harmonic oscillations*). In order to avoid complexity, we have not shown these periodic points and their invariant curves in this figure.

On the other hand, the α_2-branches of points D^2 which converge monotonously to the stable points S^2 as shown in Fig. 4.10 is gradually shortened by virtue of the lower frequency of the external force. Consequently, if we make further decrease in ν, there result the coalescences of points D^2 and S^2 on the leftward boundary of the 1/2-harmonic entrainment. Then the coalesced points disappear outside the region of the 1/2-harmonic entrainment.

(4) Type IV

Next, we shall consider the transitions of phase-portraits in the case where the frequency ν is increased from the state of Type I.

With increasing ν, the frequency of the oscillation corresponding to the invariant closed curve decreases contrary to the

---

*These oscillations will be studied as the ultra-subharmonic oscillations in the last of this section. And the regions of the ultra-subharmonic entrainment overlap with the one of the 1/2-harmonic entrainment.

preceding case. Therefore, the α_2-branch connected to point ${}^1D_1^2$ in Fig. 4.8 is prolonged, on the other hand, the α_1-branch is gradually shortened. In the result, there may appear an infinite number of the intersections between the α_2-branch contiguous to point ${}^1D_1^2$ and the one of the ω-branches to point ${}^2D_1^2$ in the hatched region ▨ marked by Type IV in Fig. 4.7.

As a typical example of this case, we choose the system parameters at point d (B = 4.0, ν = 3.3) in Fig. 4.7 and show its phase-portrait in Fig. 4.11. The details of fixed and periodic points are listed in Table 4.8. The α_1-branches of points D^2 converge to the stable points S^2 without intersecting the ω-branch, although they are meandering around the stable points S^2.

(5) Type V

With further increasing the frequency ν from the value of Type IV, the α_2-branch of point ${}^1D_1^2$ becomes to make its head for the invariant set with the lower frequency. That is to say, it leaves gradually from the stable point ${}^2S_1^2$, and ultimately breakes off all intersections with the ω-branch of point ${}^2D_1^2$ and proceeds only to the stable points S^3 which locate near the origin. Such a case is called Type V whose region is indicated in Fig. 4.7.

As a representative example of this case, we choose the system parameters at point e (B = 7.0, ν = 4.0) in Fig. 4.7, and show its phase-portrait in Fig. 4.12. The details of fixed and periodic points are given in Table 4.9. In this figure there also appear

3-periodic points S^3 and D^3, so that the invariant curves for the mapping T^2 are drawn in solid lines, on the other hand, those for the mapping T^3 in dashed lines. The α_2-branch of point ${}^1D_1^2$ does not intersect to the ω-branches of points D^2, but to the ones of points D^3, visiting all the stable points S^3. However, the α_1-branches of points D^2 converge monotonously to the stable points S^2 whose frequency of oscillation is greater than the points S^3.

If we set the frequency ν still more largely, the α_1-branches of points D^2 are extremely shortened. Then points D^2 and S^2 concur each other, if the system parameters are set on the rightward boundary of frequency entrainment, and the coalesced points disappear outside the region of the 1/2-harmonic entrainment.

(b) Subharmonic Oscillations of Order 1/3

As observed in Fig. 4.1, the subharmonic oscillations of order 1/3 have occurred in a wide region. Then we can expect the 1/3-harmonic oscillations to yield the more varieties of phase-portraits than the 1/2-harmonic ones, because the nonlinear character of the system is symmetrical. For convenience' sake, we divide the region of the 1/3-harmonic oscillation into seven portions according to the structure of their invariant sets. They are named as Type I, Type II, ..., Type VII of the 1/3-harmonic oscillations, whose regions are illustrated in Fig. 4.13. We attract our attention to study the transition of phase-portraits, when the system parameters are varied in the region of the 1/3-harmonic entrainment.

(1) Type I

Since a self-excited oscillation whose frequency ω_0 is equal to 1.621... results when B = 0 in Eq. (4.1), the subharmonic oscillations of order 1/3 result, provided that the driving frequency ν is given in the neighborhood of $3\omega_0$ (= 4.863...). Such 1/3-harmonic oscillations appear in the region indicated by Type I in Fig. 4.13.

As an example for this case, the phase-portrait whose system parameters are chosen at point a (B = 2.0, ν = 5.0) in Fig. 4.13 is shown in Fig. 4.14. The corresponding details of fixed and periodic points in this figure are listed in Table 4.10. The invariant closed curve is composed of all the α-branches (drawn in thick-line curves) which abut at points D^3 as before (see Fig. 3.5). The domain encircled by the invariant closed curve may be the maximum finite invariant set Δ . Although its area is evidently not equal to zero, Δ will be to have no area, when the system parameters are varied. Therefore, we intend to investigate the relationship between the typical phase-portraits of van der Pol's equation, in which Δ has non-zero area, and the ones of Duffing's equation, whose Δ has zero area.

For a simpler description in discussing the transition of phase-portraits, we shall pay specially our attention to the point D_1^3 in Fig. 4.14. However, the similar explanations will be made with respect to the other points D_2^3 and D_3^3.

(2) Type II

We decrease the driving frequency ν from the value of Type I, reminding of the notion; 'an α_1-branch and an α_2-branch'. The α_1-branch (drawn in heavy line) of point D_1^3 in Fig. 4.14 converges to point S_1^3 spirally, so it grows gradually around here, because the frequency of the oscillation correlated to the invariant closed curve is increased. As mentioned in Sec. 4.4(a), an infinite number of homoclinic points will be caused by the intersections between the α_1-branch of point D^3 and the ω-branch (drawn in fine line) of point D^3. Such phenomena occur in the region named Type II, which is indicated by the shaded portion ▨ in Fig. 4.13.

By way of such an example, we have chosen the system parameters at point b (B = 5.0, ν = 4.0) in Fig. 4.13 and shown its phase-portrait in Fig. 4.15. The details of fixed and periodic points are given in Table 4.11. The α_2-branch (drawn in heavy line) of point D_1^3 converges to point S_3^3 having no intersection with the ω-branches of points D^3.

Next, two cases, either the amplitude B is increased or decreased from this type, will be investigated.

(3) Type III

First, we shall increase the amplitude B from the value of Type II, while ν is kept constant (ν = 4.0), besides the α_1-branch of point D_1^3 its α_2-branch intersects its own ω-branch as shown in Fig. 4.16, whose system parameters are chosen at point

c (B = 8.0, ν = 4.0) in Fig. 4.13. The details of fixed and periodic points in this figure are listed in Table 4.12. This case is called Type III whose domain is indicated in Fig. 4.13. Thus, one of the ω-branches connected to the point D_1^3 in Fig. 4.16 tends simply to point U^1 under iterations of the inverse mapping T^{-1}. But the other ω-branch of point D_1^3 intersects not only the α_1-branches of points D^3 but also the α_2-branches mutually. Figure 4.16 has the same construction as Fig. 4.15 except only one difference that the α_2-branch of point D_1^3 intersects also the ω-ones in Fig. 4.16. With further increasing the amplitude B, all the stable points S^3 change into the completely unstable 3-periodic points U^3, outside the region of the 1/3-harmonic entrainment.

(4) Type IV

Now, we decrease the amplitude B from the value of Fig. 4.15 (Type II), while ν = 4.0, the α_1-branch of point D_1^3 is apt to go away from point S_1^3. Finally this α_1-branch can not intersect the ω-branch of point D_2^3. Thus the phase-portrait of Type II changes into the one of Type IV, which occurs in the region indicated in Fig. 4.13. As an example of this case, we choose the system parameters at point d (B = 3.0, ν = 4.0) in Fig. 4.13, and show its phase-portrait in Fig. 4.17. The corresponding properties of fixed and periodic points are listed in Table 4.13. Although the α_2-branch of point D_1^3 converges monotonously to point S_3^3, the α_1-branch proceeds to the completely stable periodic points which

are located in the outside and correspond to the ultra-subharmonic oscillations.* In Fig. 4.17 we can notice that the boundaries of the domains of attraction leading to the 1/3-harmonic responses have only one point U^1 as an original source. This fact is a remarkable feature of van der Pol's equation.

(5) Type V

With decreasing the frequency ν from the state of Fig. 4.17, while B = 3.0, the completely stable periodic points S^3 will turn into the completely unstable ones U^3 outside the entrained region. Therefore, it become difficult for images on the α_2-branch of point D_1^3 to reach rapidly the point S_3^3 under iterations of the mapping, when ν is lessened. In the midst of this change, the α_2-branch of point D_1^3 intersects its own ω-branch as shown in Fig. 4.18. To obtain this figure, we have set the system parameters at point e (B = 3.0, ν = 3.6) in Fig. 4.13 and the details of fixed and periodic points are listed in Table 4.14. Such a case occurs in the domain indicated by Type V in Fig. 4.13. It is the sole difference between Fig. 4.17 and Fig. 4.18 whether the α_2-branches and ω-ones of points D^3 make an infinite number of intersections or not. Since the characteristic multiplier |m| of point S^3 is

---

*In this case (Fig. 4.17) there occur the 4/9-harmonic oscillations. However we do not show these ultra-subharmonic responses, because they appear in the extremely narrow region.

equal to 0.953... as listed in Table 4.14, the further decrease of the frequency ν may lead the stable points S^3 to the completely unstable ones U^3 outside the region of the 1/3-harmonic entrainment.

(6) Type VI

Next, we shall consider the case where the frequency ν is increased.

According to the increase of ν from the quantity of Type I (see Fig. 4.14), the frequency of the oscillation corresponding to the invariant closed curve is decreased, so that the α_2-branch of point D_1^3, converging spirally to point S_3^3 in Fig. 4.14, moves gradually away from S_3^3. Then the distance between the α_2-branch of point D_1^3 and the ω-branch of point D_3^3 is diminished. Ultimately both branches intersect twistingly one another as shown in Fig. 4.19, whose system parameters are chosen at point f (B = 12, ν = 6) in Fig. 4.13. The details of fixed and periodic points in this figure are given in Table 4.15. This case is called Type VI which is depicted by hatched lines ▨ in Fig. 4.13. In the meanwhile, the α_1-branches of points D^3 converge monotonously to points S^3 without crossing the other branches.

It may be always necessary for the modification of phase-portraits from van der Pol's type to Duffing's type that the exchange in locations of the α-branches and the ω-ones is caused by the intersections of both branches. Consequently, we can image that there may also occur the above-mentioned intersections in

a forced self-oscillatory system with linear restoring force. However the parameter range in which the doubly asymptotic points appear is so narrow that we can not set the system parameters in it.

(7) Type VII

With further increasing ν from the value of Fig. 4.19, the α_2-branch of point D_1^3 goes apart from the stable point S_3^3 still further. Finally the α_2-branch of point D_1^3 proceeds to the inner where the invariant closed curve appears, having no intersections with the ω-branches. This case is called Type VII whose region is illustrated in Fig. 4.13. As an example of such a case, we have chosen the system parameters at point g (B = 60, ν = 7) in Fig. 4.13 and shown its phase-portrait in Fig. 4.20. The details of fixed and periodic points are listed in Table 4.16.

Comparing this figure with Fig. 4.14, we can see that the positions of the α_2-branches of points D^3 and the ω-branches of points D^3 exchange each other, and all the α_2-branches of points D^3 converge to the invariant closed curve (drawn in thick-line curve) around the point U^1. The construction of this phase-portrait is topologically similar to the one appearing in the system with linear restoring force (see Fig. 3.7).

As yet, the maximum finite invariant set Δ is composed of the whole α-branches of points D^3 in addition to the domain encircled by the invariant closed curve.

A further increase in B will bring about a shrinkage of the

invariant closed curve into one point S^1 correlated with the stable harmonic solution, then the area of the set Δ tends to zero. Such a phase-portrait is analogous to the one occurring in the forced self-oscillatory system with linear restoring force (see Fig. 3.6) and also in Duffing's equation [1].

(c) Ultra-Subharmonic Oscillations

As mentioned in Sec. 3.4, there appeared many subharmonic oscillations of higher orders, named as ultra-subharmonic oscillations [22], in a forced self-oscillatory system with large damping ($\mu = 10$) and linear restoring force. However, owing to the excessively large damping μ, we could scarcely discuss their structures in the phase plane. Here, we choose μ as a comparatively small value, i.e., $\mu = 0.2$, and investigate the ultra-subharmonic oscillations in the system with nonlinear restoring force.

As a typical example of these ultra-subharmonic oscillations, we represent the regions of the 2/3-harmonic and the 3/5-harmonic entrainments in Fig. 4.21. There also result many other frequency entrainments which are too narrow to show them in this figure. We specially refer to the region of the 3/5-harmonic entrainment which is indicated by the shaded area ▨ in Fig. 4.21.

We have fixed the system parameters B and ν at point a ($B = 2.0$, $\nu = 2.7$) and shown its phase-portrait in Fig. 4.22. The locations of fixed and periodic points and their related properties are given in Table 4.17. The wave-form passing through points S^5 is found

to be

$$x_0(t) = 0.310 \sin(1/5\ \nu t + \theta_1) + 1.724 \sin(3/5\ \nu t + \theta_3) + 0.507 \sin(5/5\ \nu t + \theta_5) + 0.062 \sin(7/5\ \nu t + \theta_7) + \ldots$$

where $\nu = 2.7$

Since the 3/5-harmonic component is dominant in this Fourier-series expansion of $x_0(t)$, it is called the 3/5-harmonic oscillation.

In Fig. 4.22, all the α-branches, drawn in heavy lines, of points D^5 are converging to points S^5, having no intersections with other branches. Therefore this feature is the same case as Type I of the 1/2-harmonic and the 1/3-harmonic oscillations, then it is regarded as a representative phase-portrait in van der Pol's equation.

On account of the appearance of doubly asymptotic points, the same complicated changes from this phase-portrait as the 1/2- and the 1/3-harmonic oscillations may be conjectured. Then in the exterior of entrained regions, such a complexity of the ultra-subharmonic oscillations may bring about an advent of nonperiodic oscillations whose sequential points under infinite iterations of the mapping are complicatedly dispersed in the phase plane. However, we shall here refrain from entering further considerations. The details of such nonperiodic oscillations will be concretely mentioned in Chap. 5.

4.5 Higher-Harmonic Oscillations

Under the circumstance that the driving frequency is impressed

to be less than the natural frequency of a self-oscillatory system, there result higher-harmonic oscillations. The higher-harmonic oscillation is entrained in the narrow region of the system parameters, when the restoring force of Eq. (1.5) is expressed by linear function. Therefore we can not fully investigate their details.* As the nonlinear restoring force in the system brings about the enlarged region of frequency entrainment, we study the higher-harmonic oscillations in Eq. (4.1) by using a procedure analogous to that of the previous section. We shall show the various types of phase-portraits in the region of the higher-harmonic entrainment, in order to study the relationship between the higher-harmonic oscillation and the complicated nonperiodic oscillation.

(a) Regions of Higher-Harmonic Entrainment

The regions of the higher-harmonic entrainment in Eq. (4.1) obtained by using computer facilities are shown in Fig. 4.23. In this figure we see that the entrained region of harmonic oscillations containing higher-harmonic components may be divided into two domains indicated by changing the direction of the hatched lines, according to the configurations of phase-portraits. The differences among these domains will be mentioned by representing the phase-portraits later on. After all, the harmonic oscillations result in

---

*The region of the third-harmonic entrainment in the system with linear restoring force has been shown in Fig. 3.1.

the region surrounded by the heavy-line curves in Fig. 4.23.

We can also recognize the second-harmonic ($\nu \simeq \omega_0/2$) and third-harmonic ($\nu \simeq \omega_0/3$) entrainments in this figure. Moreover, as an example of the subharmonic oscillations containing higher-harmonic components, the regions of the 5/3-harmonic entrainment, overlapped to the harmonic entrainment, and the 2/2-one, in the left side of the harmonic entrainment, are indicated by the hatched lines ▨ and ▨ respectively.

(b) Harmonic Oscillations Containing Higher-Harmonics

If the system parameters B and ν are located in the unshaded area of the fundamental harmonic entrainment in Fig. 4.23, we can obtain a simple phase-portrait where only one completely stable fixed point exists.

However, with decreasing the frequency ν, while B is kept constant (B = 2.4), there appear a pair of the completely stable fixed points $^1S^1$ and $^2S^1$ in the hatched area ▨ of Fig. 4.23. As a typical example of this case, we choose the system parameters at point a (B = 2.4, ν = 0.95) in Fig. 4.23, and show its phase-portrait in Fig. 4.24. The details of fixed points are listed in Table 4.18.

The periodic solution correlated with the directly unstable fixed point $^1D^1$ consists of the odd harmonic components only, such as

$$x_0(t) = 0.064 \sin \nu t + 1.610 \cos \nu t - 0.044 \sin 3\nu t$$

$$+ 0.271 \cos 3\nu t - 0.016 \sin 5\nu t + 0.032 \cos 5\nu t + \ldots$$

where $\nu = 0.95$

On the other hand, the periodic solutions corresponding to points $^1S^1$ and $^2S^1$ are found to be

$$x_1(t) = -x_2(t + \pi/\nu)$$
$$= -0.063 + 0.148 \sin \nu t + 1.331 \cos \nu t + 0.882 \sin 2\nu t - 0.020 \cos 2\nu t + 0.008 \sin 3\nu t - 0.011 \cos 3\nu t + 0.122 \sin 4\nu t + 0.014 \cos 4\nu t + \ldots$$

where $\nu = 0.95$

Though the fixed points in this case have the same constitution as the one in Fig. 4.6, it may be different that the solutions of stable points contain also the even harmonics in addition to the fundamental and odd harmonics.

With further decreasing the frequency ν, while B is kept constant ($B = 2.4$), the system parameters enter into the cross-hatched area ▦ in Fig. 4.23. In this domain, we obtain four kinds of harmonic oscillations, so four completely stable fixed points $^1S^1$, $^2S^1$, $^3S^1$ and $^4S^1$ appear in the phase plane. For a slight alternation in ν, such as from 0.912 to 0.900, we can recognize three different types of phase-portraits according to the behaviors of invariant curves in the phase plane, although the same fixed points still exist.

First, we have chosen the system parameters at point b

(B = 2.4, ν = 0.912) in Fig. 4.23, and shown its phase-portrait in Fig. 4.25. The details of fixed points in this case are listed in Table 4.19. The configuration regarding points $^1D^1$, $^1S^1$ and $^2S^1$ in Fig. 4.25 is the same as the one in Fig. 4.24. Besides them there also appear two pairs of fixed points ($^3S^1$, $^2D^1$) and ($^4S^1$, $^3D^1$) as shown in Fig. 4.25. The domains of attraction containing four stable points in their interiors are bordered by all ω-branches (drawn in heavy lines) passing through points $^1D^1$, $^2D^1$ and $^3D^1$.

In Fig. 4.25, both α-branches of point $^1D^1$ are meandering near point $^2D^1$ or point $^3D^1$, and they may approach gradually to the ω-branch of point $^2D^1$ or that of point $^3D^1$ in proportion to the decrease of ν. Then we obtain the second case in which the system parameters are set up at point c (B = 2.4, ν = 0.908) in Fig. 4.23, and show its phase-portrait in Fig. 4.26. The locations of fixed points and their properties are listed in Table 4.20. In this figure, the one of the α-branches emanating from point $^1D^1$ intersects to the ω-branch of point $^2D^1$, similarly the other α-branch of point $^1D^1$ to the ω-branch of point $^3D^1$.

With further decreasing the frequency ν from this state, while B = 2.4, each α-branch of point $^1D^1$ goes away from point $^1S^1$ or point $^2S^1$ gradually. And finally they do not intersect the ω-branch of point $^2D^1$ or $^3D^1$. As an example of this case, we choose the system parameters at point d (B = 2.4, ν = 0.90) in Fig. 4.23, and show its phase-portrait in Fig. 4.27. The details of fixed

points are given in Table 4.21. The α-branches (drawn in fine lines) of point $^1D^1$ converge to point $^3S^1$ or point $^4S^1$ without intersecting to the ω-branches.

Now, we shall further decrease the frequency ν, while B is kept 2.4, then the distance between points $^1S^1$ and $^2D^1$ in addition to the one between points $^2S^1$ and $^3D^1$ may be diminished. Consequently, such two pairs of points may respectively coalesce one another and disappear at the same time from the phase plane.

As a result, there remain stable points $^3S^1$ and $^4S^1$ as shown in Fig. 4.28, whose system parameters are chosen at point e (B = 2.4, ν = 0.85) in Fig. 4.23. The locations of fixed points and their properties are listed in Table 4.22. In this figure, one of the α-branches regarding point $^1D^1$ converges to point $^3S^1$ and the other to point $^4S^1$ without intersecting to the other ω-branches. The area where the completely stable points $^3S^1$ and $^4S^1$ exist is indicated by the hatched lines ▨ in Fig. 4.23. The periodic solutions correlated with points $^3S^1$ and $^4S^1$ are found to be

$$x_3(t) = -x_4(t + \pi/\nu)$$
$$= -0.368 + 0.094 \sin \nu t + 1.442 \cos \nu t + 0.165 \sin 2\nu t + 0.745 \cos 2\nu t - 0.041 \sin 3\nu t + 0.151 \cos 3\nu t + 0.000 \sin 4\nu t + 0.139 \cos 4\nu t + \ldots$$

where $\nu = 0.85$

They contain even harmonics in addition to the fundamental and

odd harmonics like the solutions corresponding to points $^1S^1$ and $^2S^1$ in Fig. 4.24. By comparison of this figure with Fig. 4.24, it may be seen that the whirling directions in the neighborhood of points $^1S^1$ and $^2S^1$ are different from those near points $^3S^1$ and $^4S^1$ respectively.

(c) Subharmonic Oscillations Containing Higher-Harmonics

We shall deal with the subharmonic oscillations whose higher-harmonic components are predominant in the self-oscillatory system with nonlinear restoring force. The subharmonic oscillations of orders 2/2 and 5/3 will be studied, with special attention directed to the occurrence of nonperiodic oscillations whose successive images are dispersed in the phase plane.

(1) Subharmonic Oscillations of Order 2/2

Here, we investigate the case where the frequency ν is still further decreased from the state of Fig. 4.28. In the hatched region ▨ of Fig. 4.23, the completely stable fixed points $^3S^1$ and $^4S^1$ in Fig. 4.28 have turned into the inversely unstable ones $^1I^1$ and $^2I^1$ respectively, then two pairs of stable 2-periodic points ($^1S_1^2$, $^1S_2^2$) and ($^2S_1^2$, $^2S_2^2$) appear in the phase plane. Their locations and invariant curves are illustrated in Fig. 4.29. In this figure, the system parameters have been set up at point f ($B = 3.2$, $\nu = 0.84$) in Fig. 4.23. The details of fixed and periodic points are listed in Table 4.23. The branches (drawn in full lines) passing through point D^1 are invariant curves

under the mapping T, on the other hand, the ones (drawn in dashed lines) passing through points ${}^1I^1$ and ${}^2I^1$ are invariant under the mapping T^2. Since both α-branches of point D^1 cross to all the ω-branches of point ${}^1I^1$ or ${}^2I^1$, converging to the whole α-branches of point ${}^1I^1$ or ${}^2I^1$, these intersections are called as heteroclinic points.

With further decreasing the frequency ν from this state, the stable periodic points S^2 in Fig. 4.29 will be changed into the inversely unstable ones I^2. Then the stable 4-periodic points S^4 correlated with the 4/4-harmonic oscillations may appear, but such a figure is not shown here. And in the next state, there appear points S^8, and so on.

From this inductive inference, we can image that such multiplications of periodic points will be proceeded successively as the frequency ν is decreased [9]. Therefore this phenomenon may bring about the occurrence of nonperiodic oscillations* whose successive images of the mapping T are dispersed in the phase plane.

(2) Subharmonic Oscillations of Order 5/3

For the second example of subharmonic oscillations occurring in the higher-harmonic range, we shall mention about the 5/3-harmonic oscillations, which may be concerned with the generation of nonperiodic oscillations.

---

*The details of such oscillations will be mentioned in Chap. 5.

In the portion indicated by the hatched lines ▨ in Fig. 4.23, we have obtained three pairs of periodic points S^3 and D^3 correlated with the 5/3-harmonic oscillations in the phase plane. The phase-portrait whose system parameters are prescribed at point g (B = 1.5, ν = 1.0) in Fig. 4.23 is shown in Fig. 4.30. The details of fixed and periodic points are listed in Table 4.24.

The periodic solution correlated with the stable point S_1^3 is found to be

$$x_0(t) = 0.282 \sin(1/3\ \nu t + \theta_1) + 1.000 \sin(3/3\ \nu t + \theta_3) + 1.091 \sin(5/3\ \nu t + \theta_5) + 0.178 \sin(7/3\ \nu t + \theta_7) + \ldots$$

where $\nu = 1.0$

The 5/3-harmonic component is dominantly appeared in this Fourier-series expansion, so that we call it subharmonic oscillation of order 5/3.

Since the system parameters are set in the area common to the harmonic and the 5/3-harmonic entrainments, we can see the stable points S_1^3, S_2^3, S_3^3 and S^1 in the phase plane. And the domains of attraction for these points are constructed by all the ω-branches (drawn in heavy lines) passing through points D^3.

If we decrease B and ν from this case and settle the system parameters just below the boundary of the harmonic and 5/3-harmonic entrainments, for example, point 1 (B = 1.2, ν = 0.95)* in

---

* We shall show the phase-portrait of point 1 in Fig. 5.6.

Fig. 4.23, the stable points S^1 and S^3 turned into the unstable ones U^1 and U^3 respectively. Then in this state, there exist no stable points in the phase plane. Moreover the α- and ω-branches of points D^3 intersect each other, so that the movement of successive images under the repeated applications of the mapping is greatly disturbed. Consequently, there results nonperiodic oscillation whose successive images do not move along a simple invariant closed curve but are dispersed in the phase plane. The details of such nonperiodic oscillations will be considered in the following chapter.

(d) Principal Higher-Harmonic Oscillations

As considered in Sec. 3.1, it is difficult to investigate the details of higher-harmonic oscillations in a system whose restoring force is only consisted of the linear function, because the regions of their frequency entrainments are very narrow. However, the higher-harmonic oscillations are widely entrained in a system with nonlinear restoring force. When the driving frequency is set in the neighborhood of integral submultiples of the natural frequency, i.e., $\nu \simeq \omega_0/n$ ($n = 2, 3, \ldots$), we obtain principal higher-harmonic oscillations. Here, we represent their phase-portraits, in order to investigate the transitions between the higher-harmonic oscillation and the nonperiodic one whose successive images of the mapping are dispersed in the phase plane.

(1) Second-Harmonic Oscillations

First, let us consider the second-harmonic oscillations, whose frequency entrainment occurs slightly near $\nu = \omega_0/2$ as shown in Fig. 4.23. As an example of such oscillations, we choose the system parameters at point h (B = 1.16, ν = 0.75) in Fig. 4.23 and show its phase-portrait in Fig. 4.31. The locations of fixed points and their related properties are listed in Table 4.25. The periodic solutions correlated with points $^1S^1$ and $^2S^1$ are found to be

$$x_1(t) = - x_2(t + \pi/\nu)$$
$$= - 0.055 - 0.031 \sin \nu t + 0.162 \cos \nu t$$
$$- 0.011 \sin 2\nu t + 1.582 \cos 2\nu t - 0.091 \sin 3\nu t$$
$$+ 0.299 \cos 3\nu t + \cdots$$

where $\nu = 0.75$

As expected, the second-harmonic components predominate in this Fourier-series expansion.

The maximum finite invariant set Δ in Fig. 4.31 is surrounded with all α-branches starting from points $^2D^1$ and $^3D^1$. In the interior of Δ there appear the completely unstable fixed points $^1U^1$ and $^2U^1$ which are connected each other by the ω-branches of point $^1D^1$. The one of the ω-branches of points $^2D^1$ (and $^3D^1$) intersects the α-branches of point $^1D^1$ and tends to points $^1U^1$ and $^2U^1$ under iterations of the inverse mapping T^{-1}.

Secondly, we consider the case where the system parameters are given by B = 1.3 and ν = 0.74. Since these parameters are located at point i in Fig. 4.23, one may expect the harmonic oscillations

and the second-harmonic oscillations in the steady state. Figure 4.32 shows the phase-portrait in this case. The locations of the fixed points and their related properties are listed in Table 4.26. The fixed points $^1S^1$, $^2S^1$, $^2D^1$ and $^3D^1$ appear on the invariant closed curve like the previous case (see Fig. 4.31) and correspond to the second-harmonic oscillations. Besides them there exist two pairs of the fixed points ($^3S^1$,$^4D^1$) and ($^4S^1$,$^5D^1$). The periodic solutions $x_3(t)$ and $x_4(t)$ correlated with the stable points $^3S^1$ and $^4S^1$ respectively are given by

$$\begin{aligned} x_3(t) &= -\, x_4(t + \pi/\nu) \\ &= 0.318 - 0.054 \sin \nu t + 1.104 \cos \nu t \\ &\quad + 0.111 \sin 2\nu t - 0.835 \cos 2\nu t - 0.048 \sin 3\nu t \\ &\quad + 0.070 \cos 3\nu t + \ldots \end{aligned}$$

where $\nu = 0.74$

These contain the even harmonics in addition to the odd harmonics, especially the second-harmonics. One of the α-branches of point $^1D^1$ intersects not only the ω-branch of point $^3D^1$ but also the ω-branch of point $^4D^1$, and similarly the other α-branch intersects both ω-branches of point $^2D^1$ and point $^5D^1$. This fact brings about a complexity of the phase-portrait.

(2) Third-Harmonic Oscillations

A self-excited oscillation whose natural frequency ω_0 is equal to 1.621... sustains when B = 0 in Eq. (4.1), so the region of the third-harmonic entrainment can be seen in the forced self-oscillatory

system (4.1) under the condition that ν is nearly equal to $\omega_0/3$ (= 0.540...), as shown in Fig. 4.23.

We shall proceed to investigate the third-harmonic oscillations which are closely related to the nonperiodic oscillations.

Let us choose the system parameters at point j (B = 2.0, ν = 0.55) in Fig. 4.23, and show its phase-portrait in Fig. 4.33. The details of fixed points are given in Table 4.27. In this figure, one of the α-branches of point D^1 converges spirally to the completely stable fixed point S^1 corresponding to the third-harmonic oscillation.

The periodic solutions, $x_s(t)$ and $x_d(t)$, correlated with points S^1 and D^1 respectively are given by

$$x_s(t) = 1.358 \sin (\nu t + \theta_1) + 0.871 \sin (3\nu t + \theta_3) + 0.130 \sin (5\nu t + \theta_5) + \cdots$$

$$x_d(t) = 0.910 \sin (\nu t + \theta_1) + 1.324 \sin (3\nu t + \theta_3) + 0.106 \sin (5\nu t + \theta_5) + \cdots$$

where $\nu = 0.55$

These contain dominantly the third-harmonic components.

On the other hand, another branch of point D^1 may approach meanderingly to the nonperiodic oscillation whose successive images are dispersed in the phase plane and represented by the set of central points, so it was not shown in this figure. Such oscillations can also result in the region of the third-harmonic entrainment, although the area common to both oscillations is too small

to illustrate it in Fig. 4.23.

When the system parameters are set such as B = 2.2 and ν = 0.55, we obtain the homoclinic structure of invariant curves as shown in Fig. 4.34. The details of fixed points are listed in Table 4.28. We can clearly separate the whole phase plane into the two domains of attraction leading to the harmonic and nonperiodic responses, as shown in Fig. 4.33. But the domain of attraction for the stable point S^1 in Fig. 4.34 has an infinite number of narrow tails owing to the homoclinic structure of invariant curves. Hence, a slight disturbance in the system is apt to change the initial points from the dispersed points of the nonperiodic oscillation onto the narrow tails of the harmonic oscillation, when the mapping T is applied repeatedly. Then the complicated nonperiodic oscillation can scarcel sustain in the physical system. So, we can obtain an unique harmonic oscillation ultimately, even if we set the initial condition at any state.

If the system parameters are set near the region where the homoclinic structure appears as the previous case (Fig. 4.33), the movement of the successive images correlated to the nonperiodic oscillation is affected by its indication. The further details of the relation between the doubly asymptotic structure of invariant curves and the nonperiodic oscillation whose successive images of the mapping T are dispersed in the phase plane will be considered in Chap. 5.

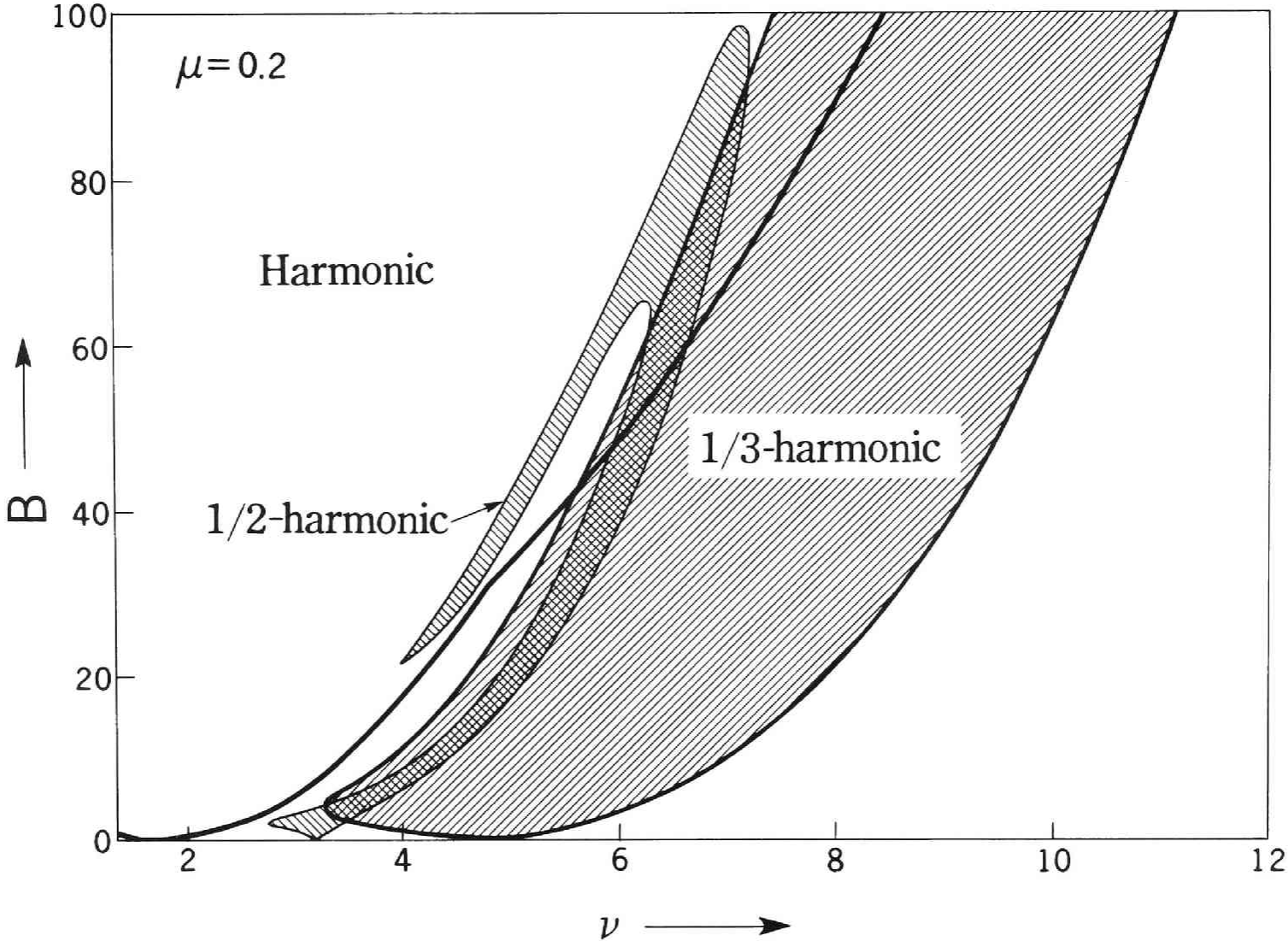

Fig. 4.1 Regions of frequency entrainment for Eq. (4.1).

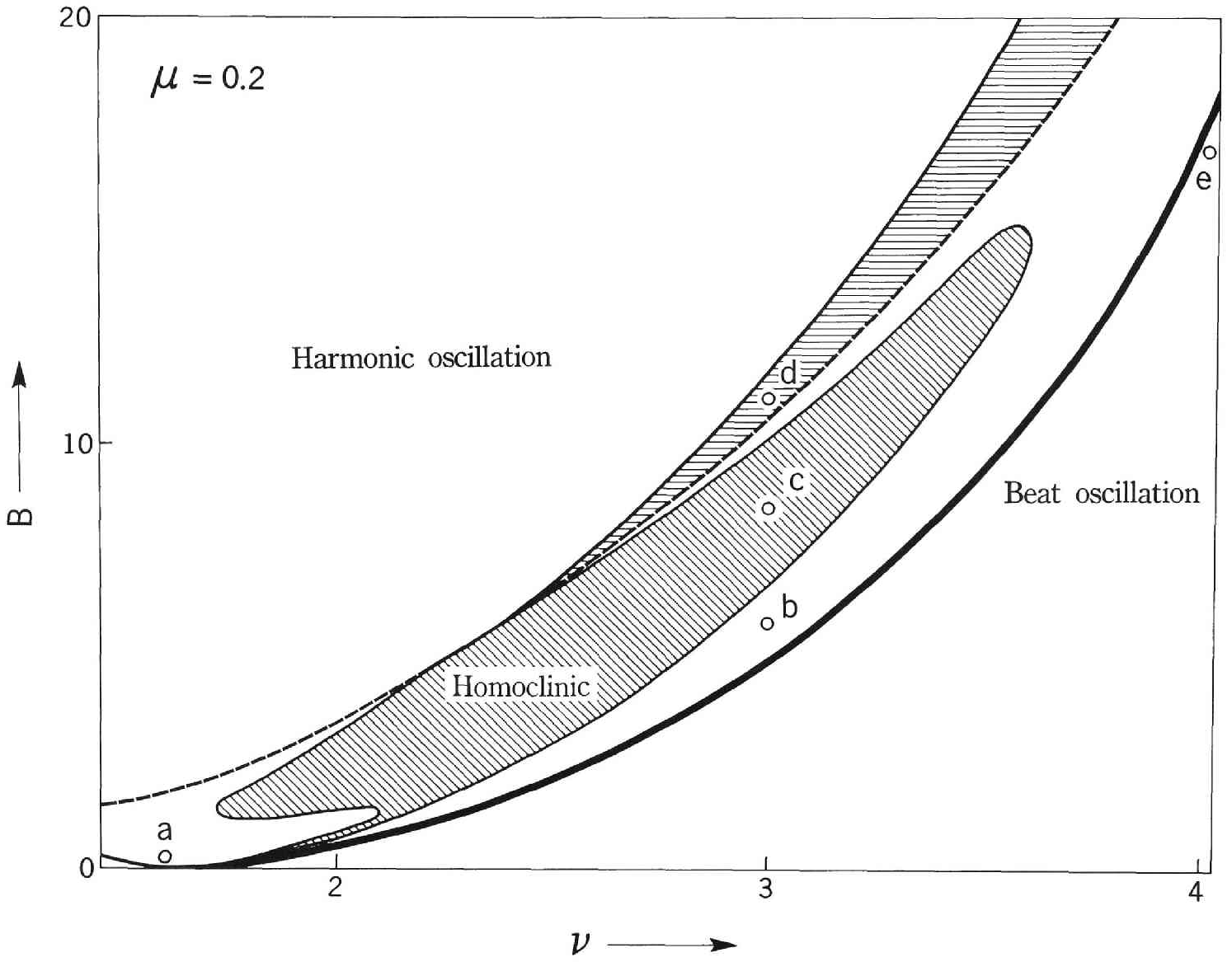

Fig. 4.2 Regions in which different types of the harmonic oscillations

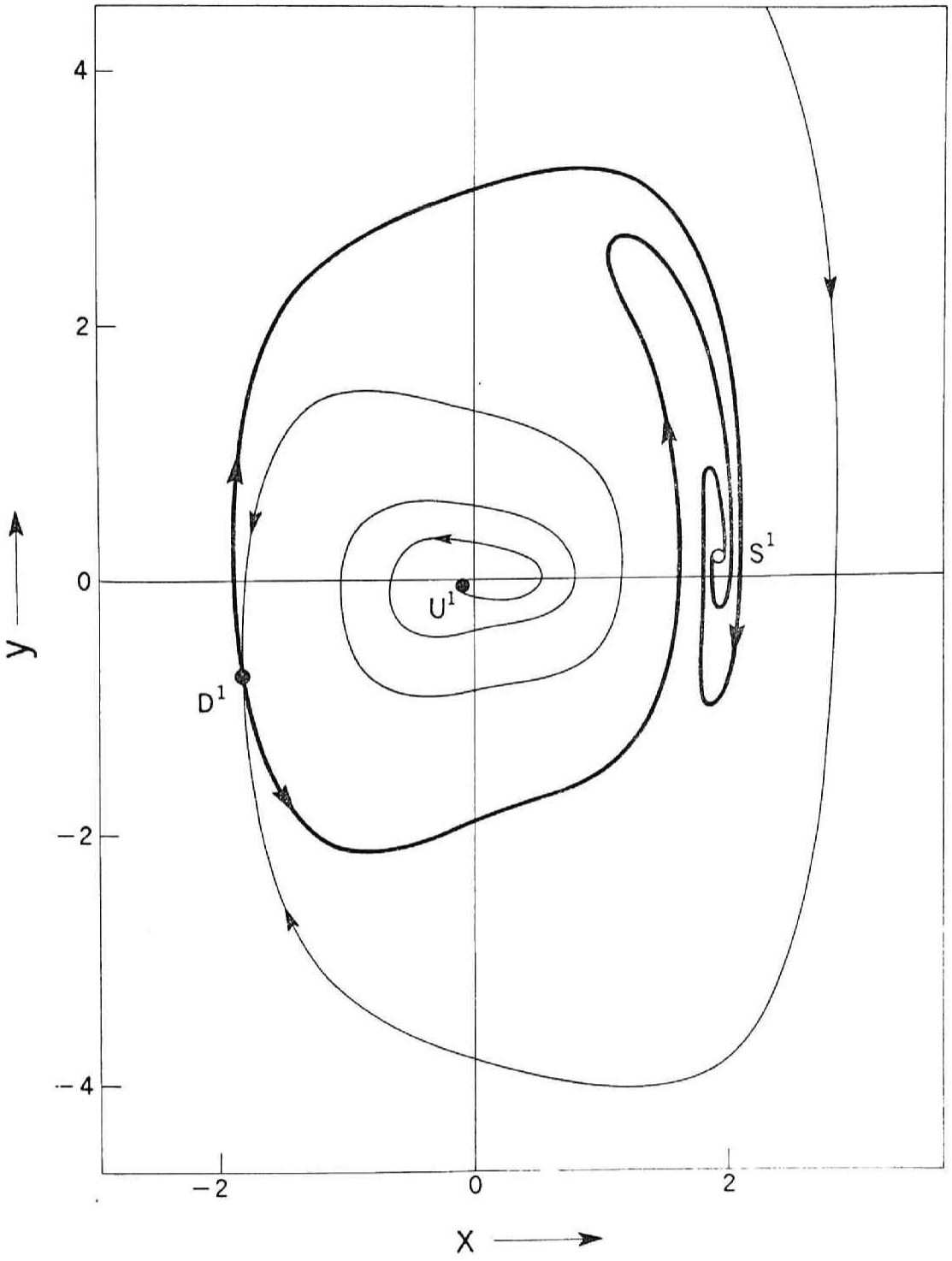

Fig. 4.3 Fixed points and invariant curves of the mapping for Eq. (4.1).

(a) B = 0.2, ν = 1.6

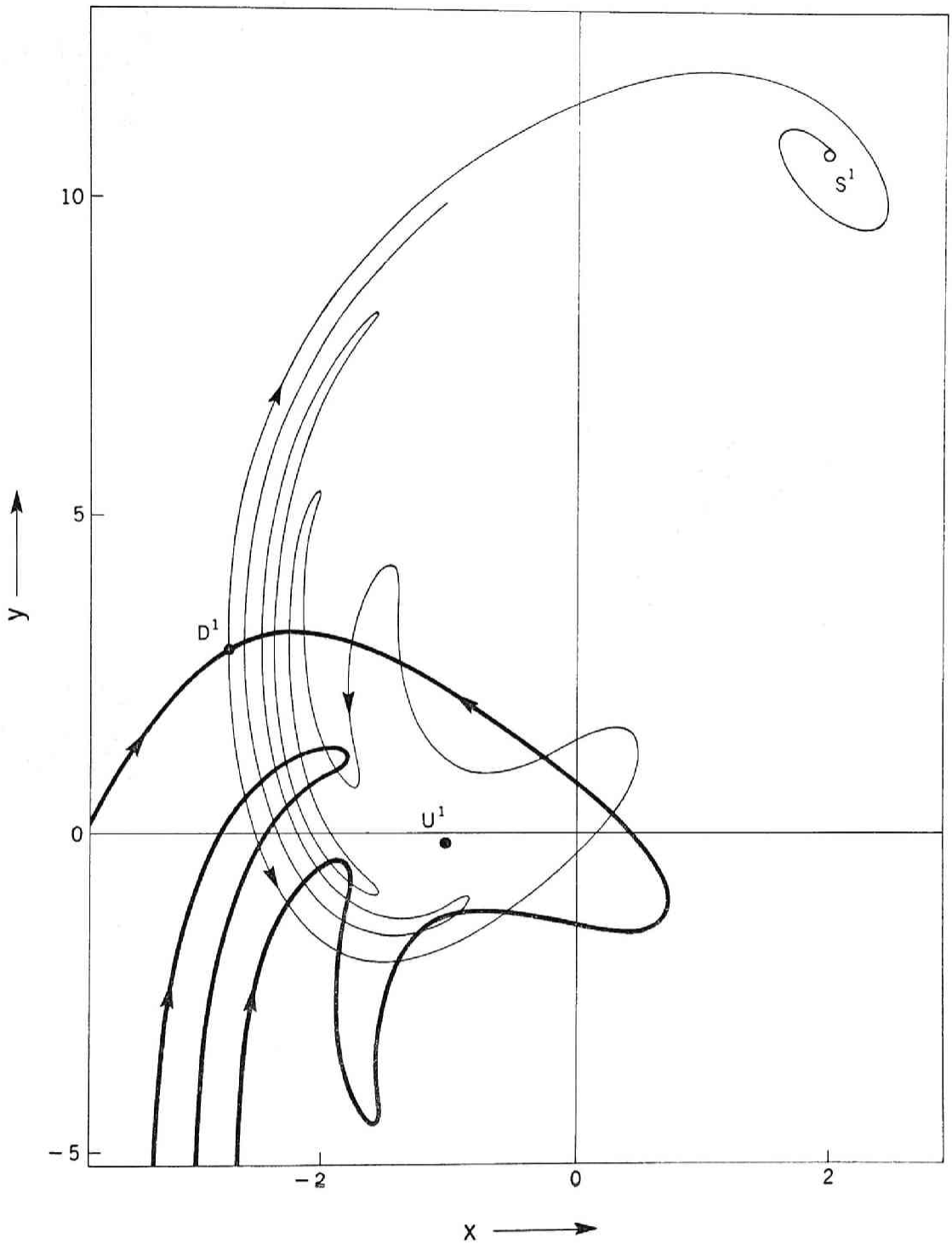

Fig. 4.4 Fixed points and invariant curves of the mapping for Eq. (4.1).

(c) B = 8.5, ν = 3.0

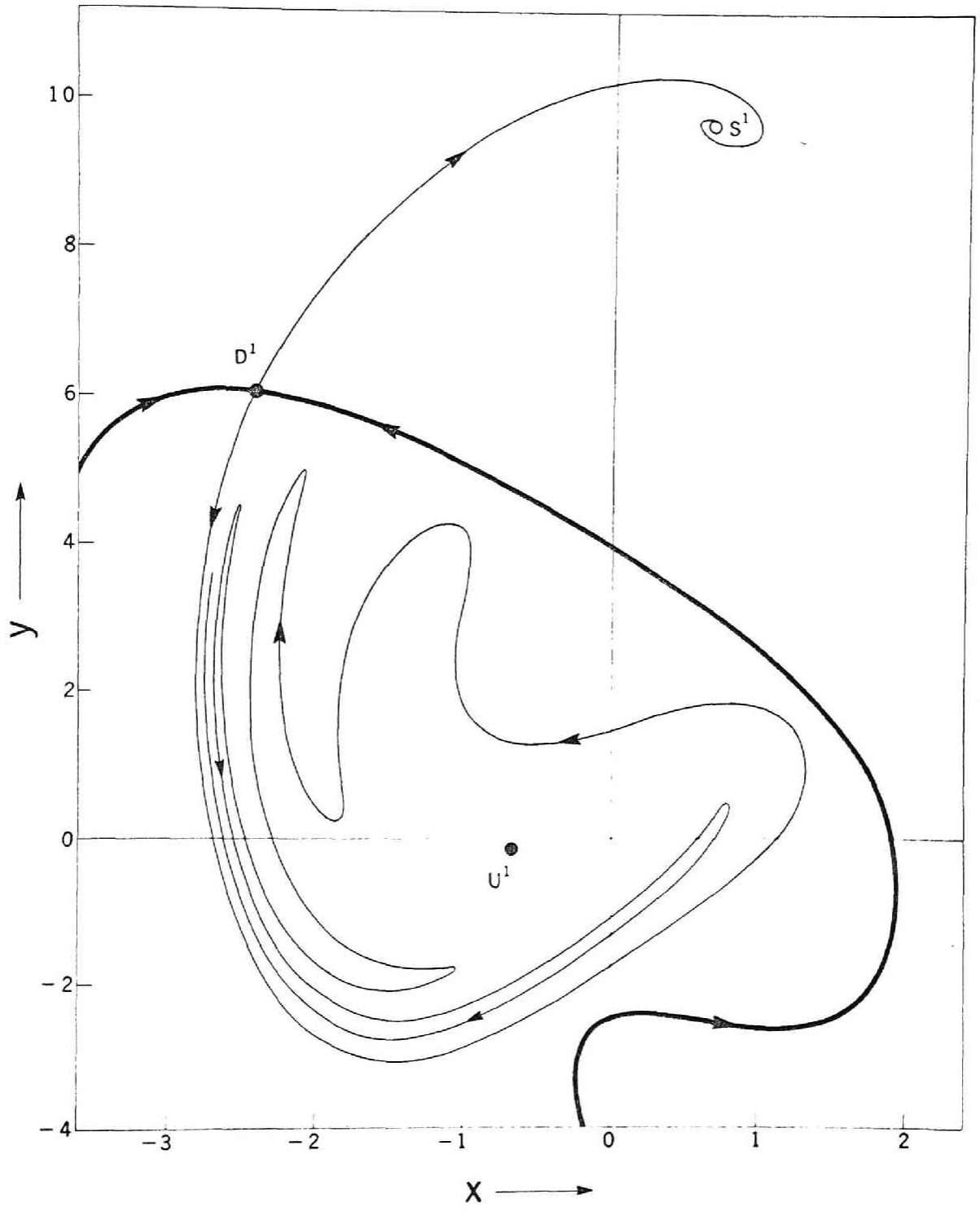

Fig. 4.5 Fixed points and invariant curves of the mapping for Eq. (4.1).
(b) B = 5.8, ν = 3.0

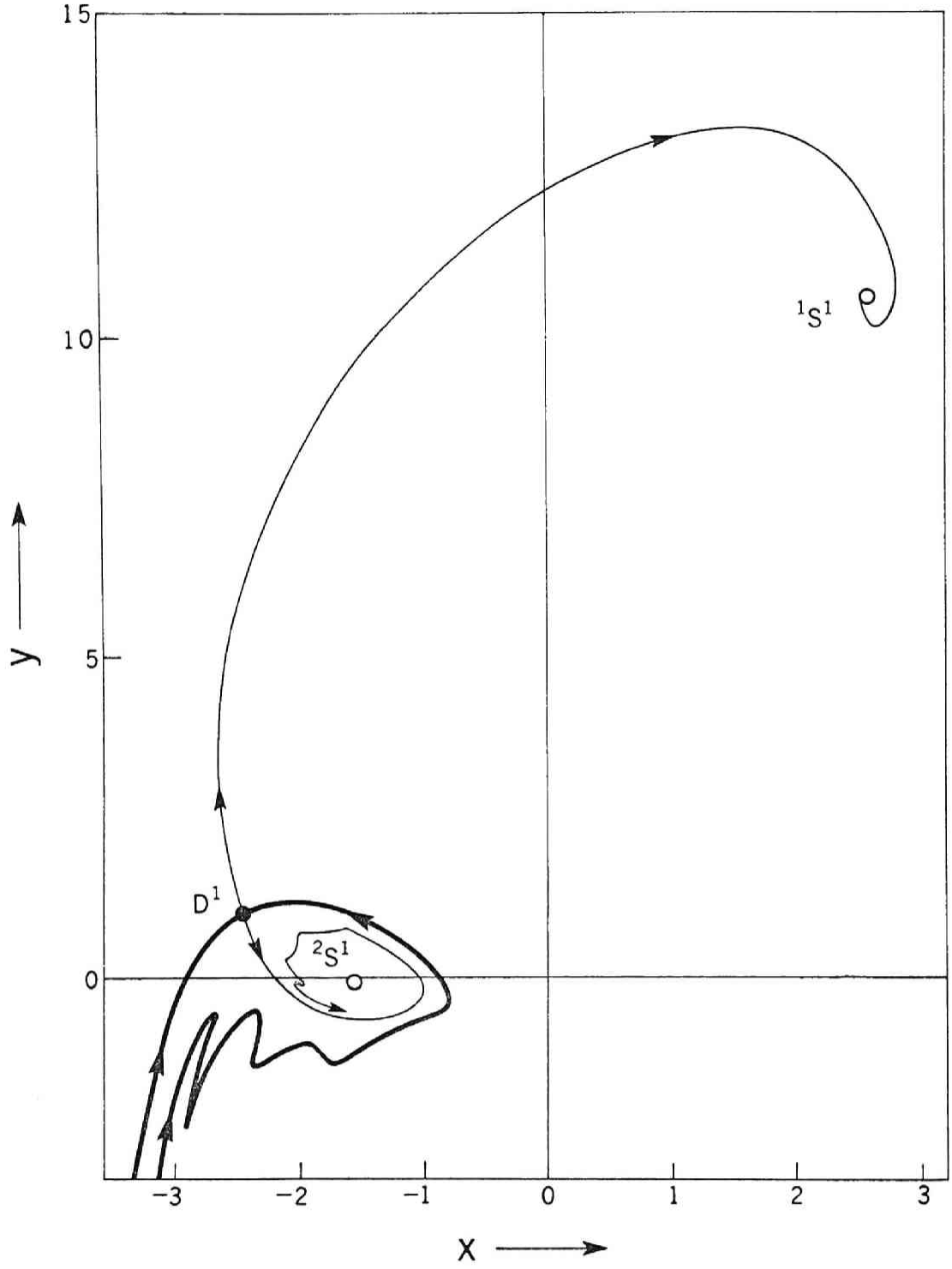

Fig. 4.6 Fixed points and invariant curves of the mapping for Eq. (4.1).

(d) B = 11.0, ν = 3.0

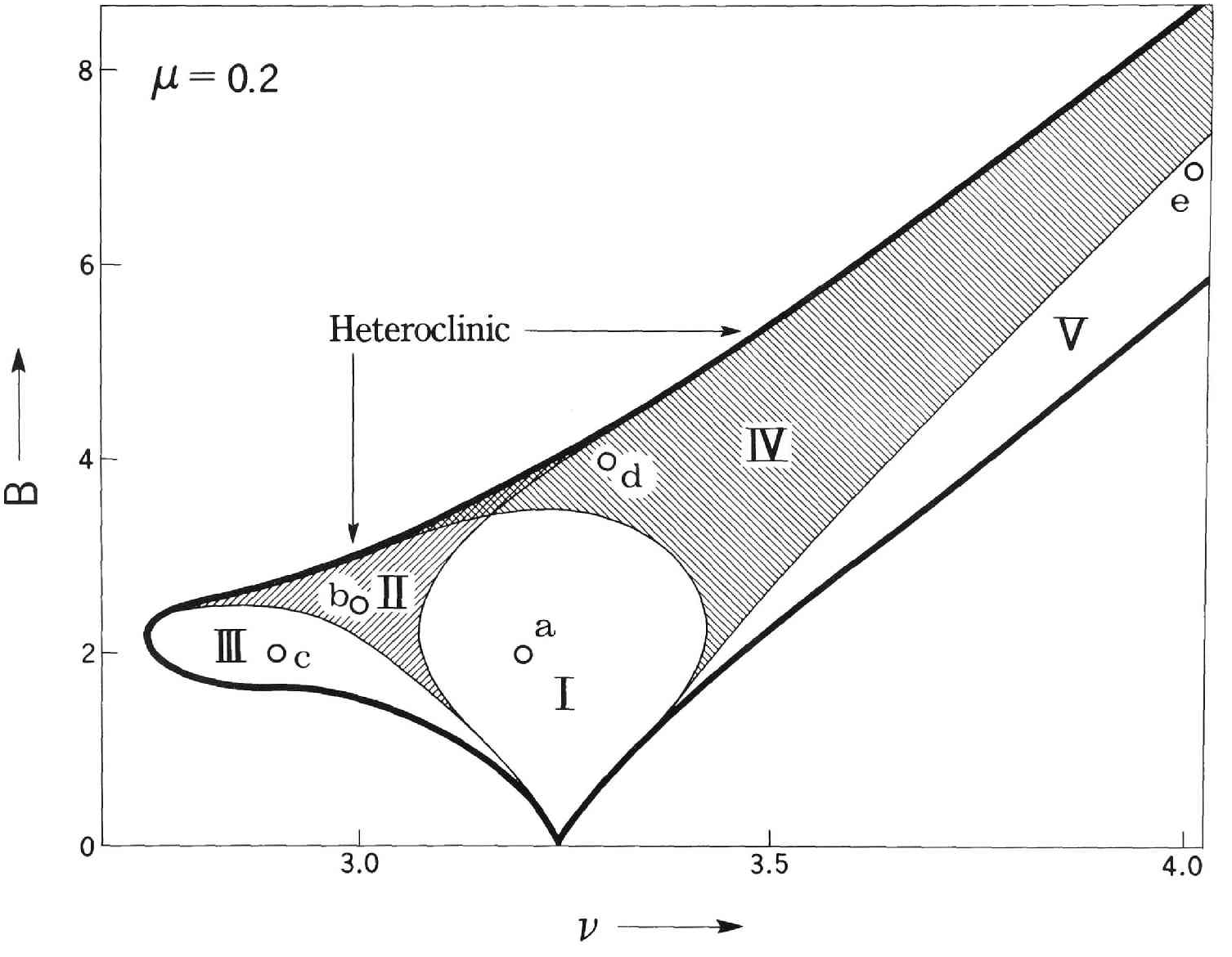

Fig. 4.7 Regions in which different types of the 1/2-harmonic oscillations are resulted in Eq. (4.1).

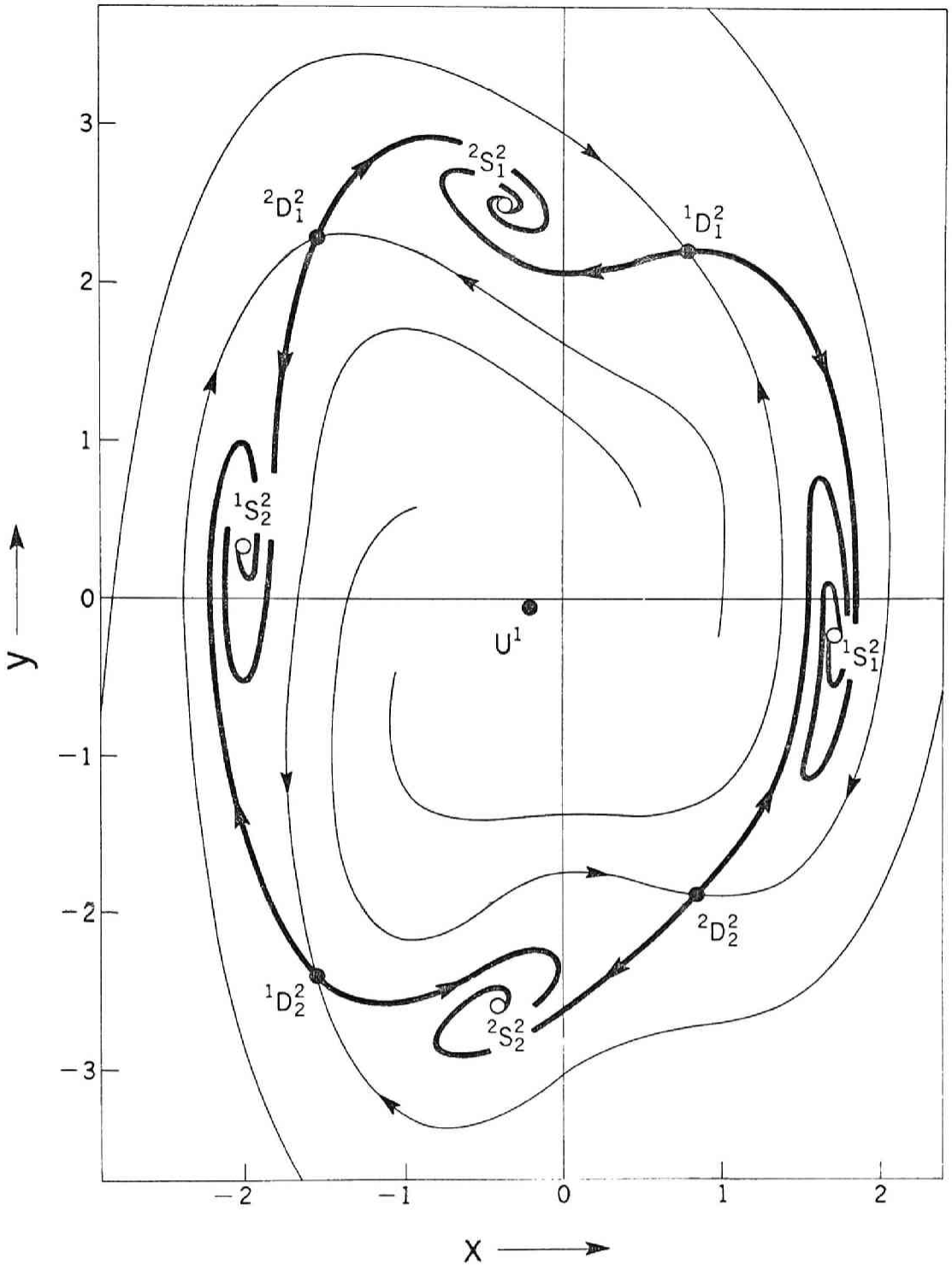

Fig. 4.8 Fixed points and invariant curves of the mapping for Type I of the 1/2-harmonic oscillations. (a) B = 2.0, ν = 3.2

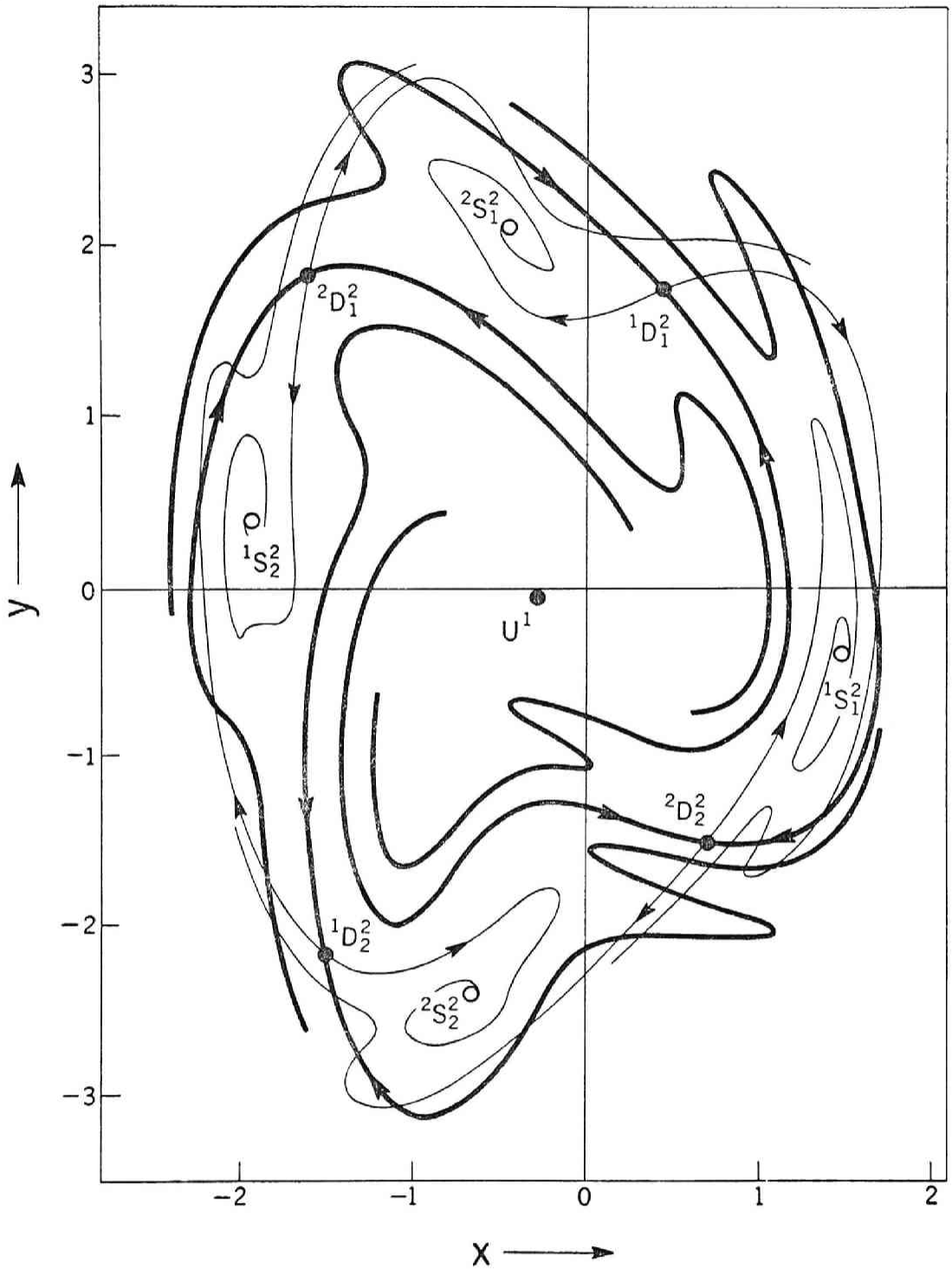

Fig. 4.9 Fixed points and invariant curves of the mapping for Type II of the 1/2-harmonic oscillations. (b) B = 2.5, ν = 3.0

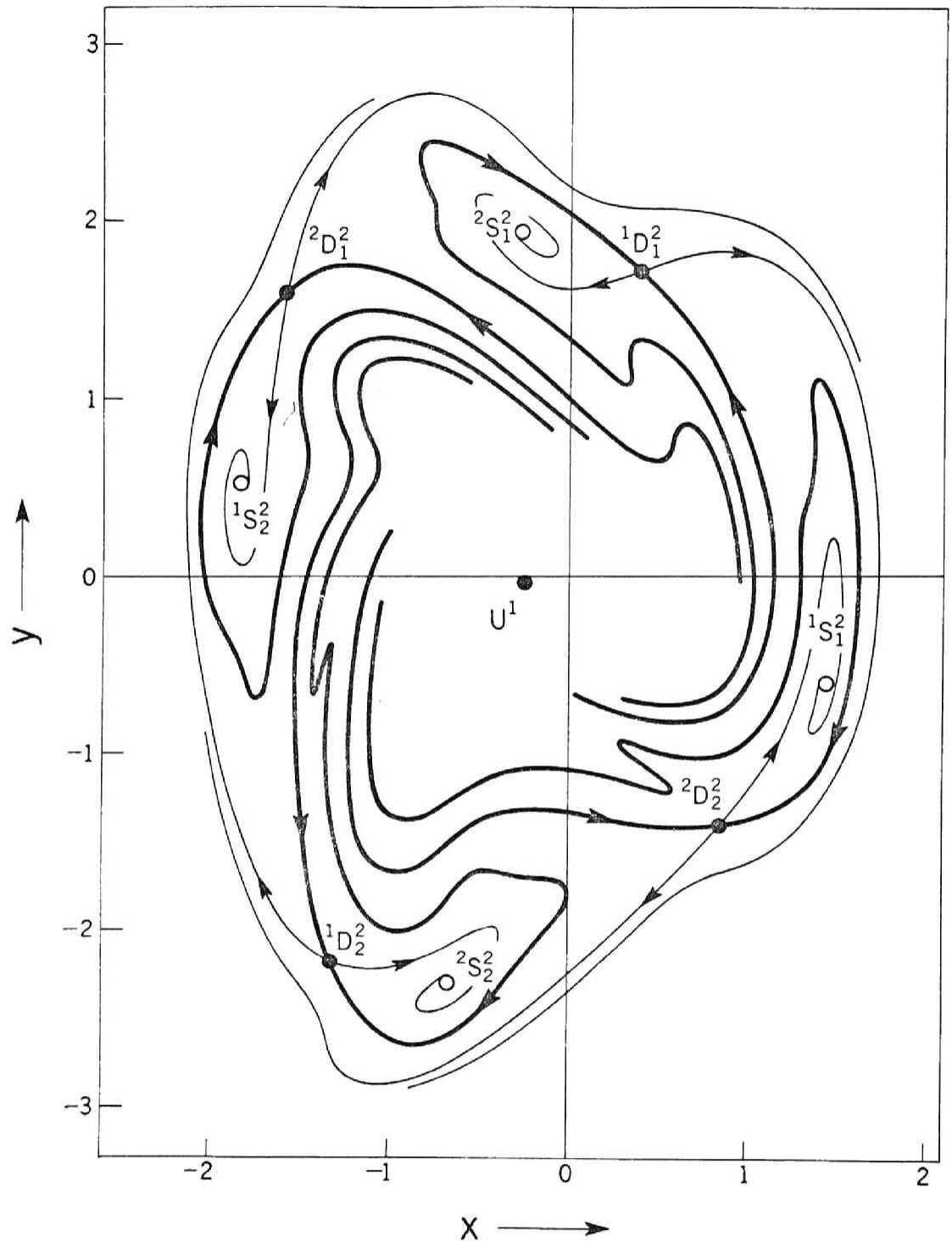

Fig. 4.10 Fixed points and invariant curves of the mapping for Type III of the 1/2-harmonic oscillations. (c) B = 2.0, ν = 2.9

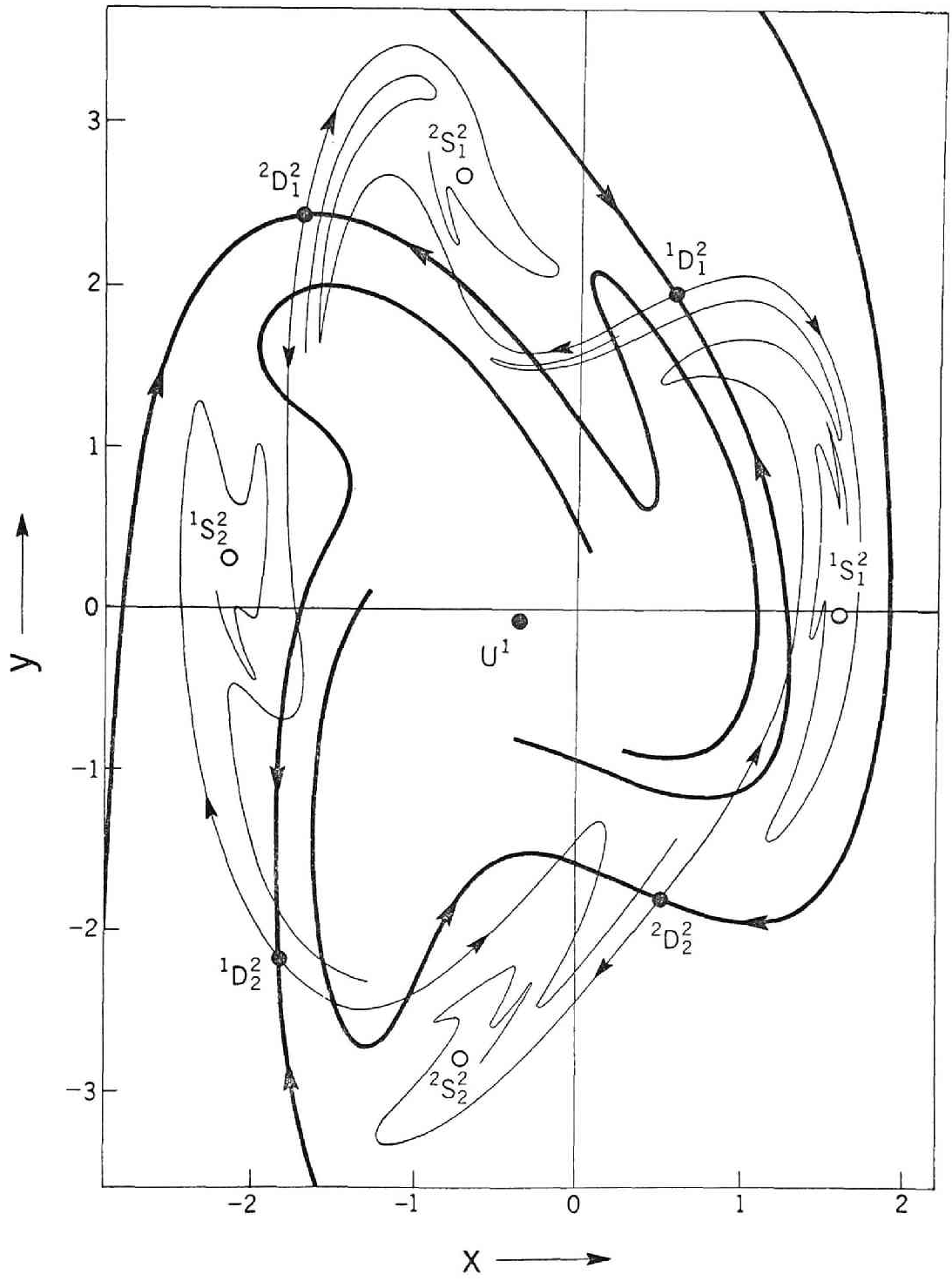

Fig. 4.11 Fixed points and invariant curves of the mapping for Type IV of the 1/2-harmonic oscillations. (d) B = 4.0, ν = 3.3

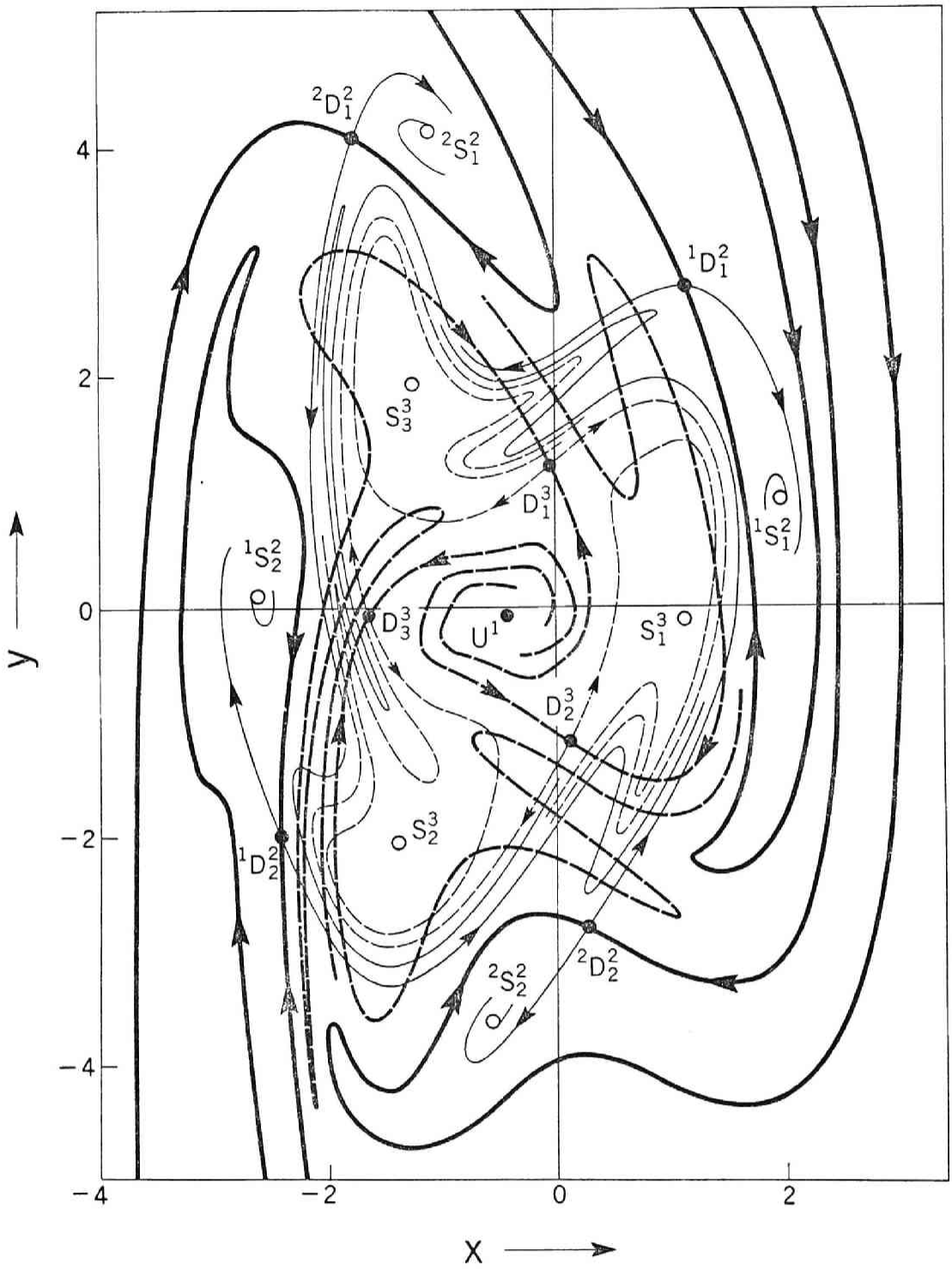

Fig. 4.12 Fixed points and invariant curves of the mapping for Type V of the 1/2-harmonic oscillations. (e) B = 7.0, ν = 4.0

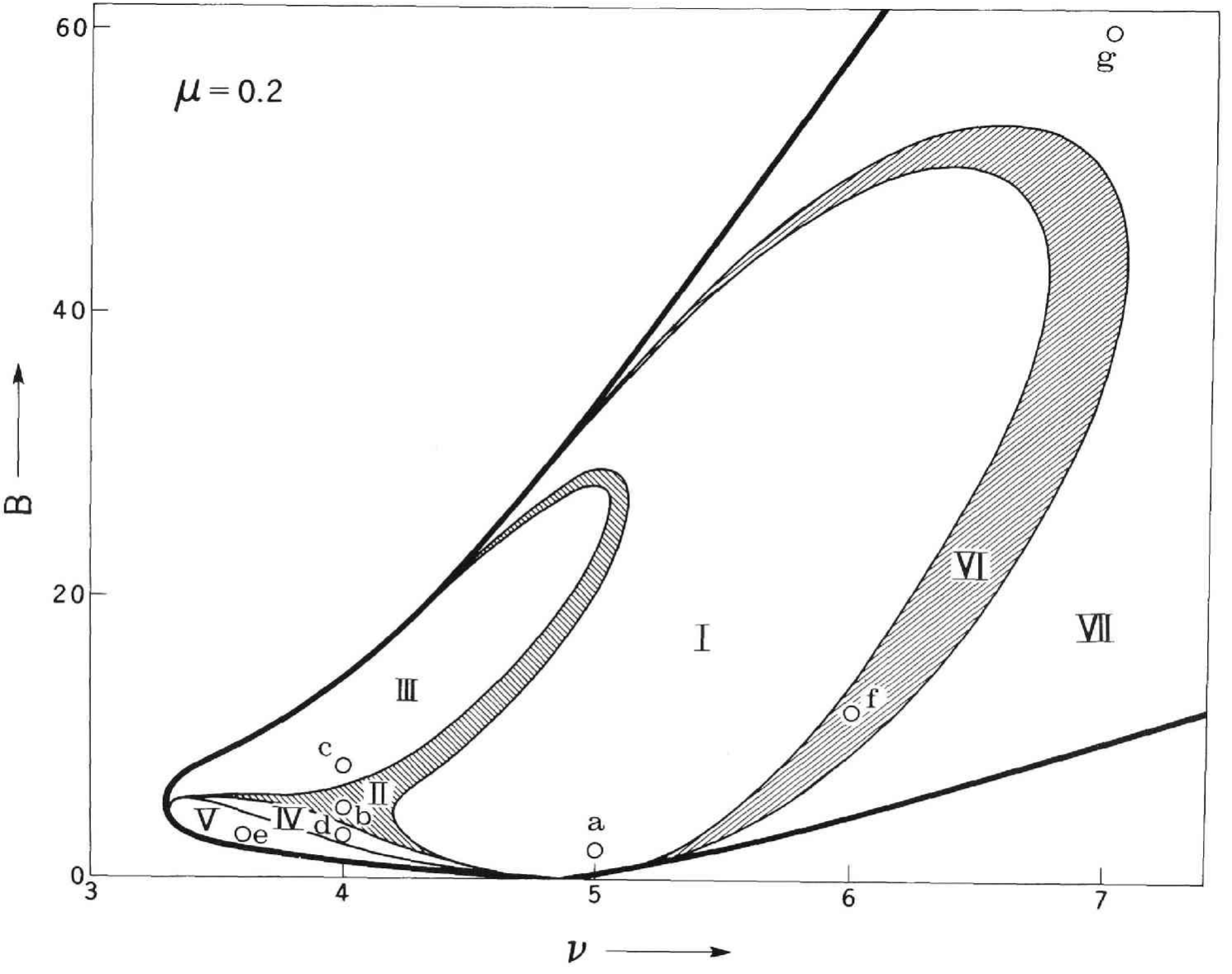

Fig. 4.13 Regions in which different types of the 1/3-harmonic oscillations

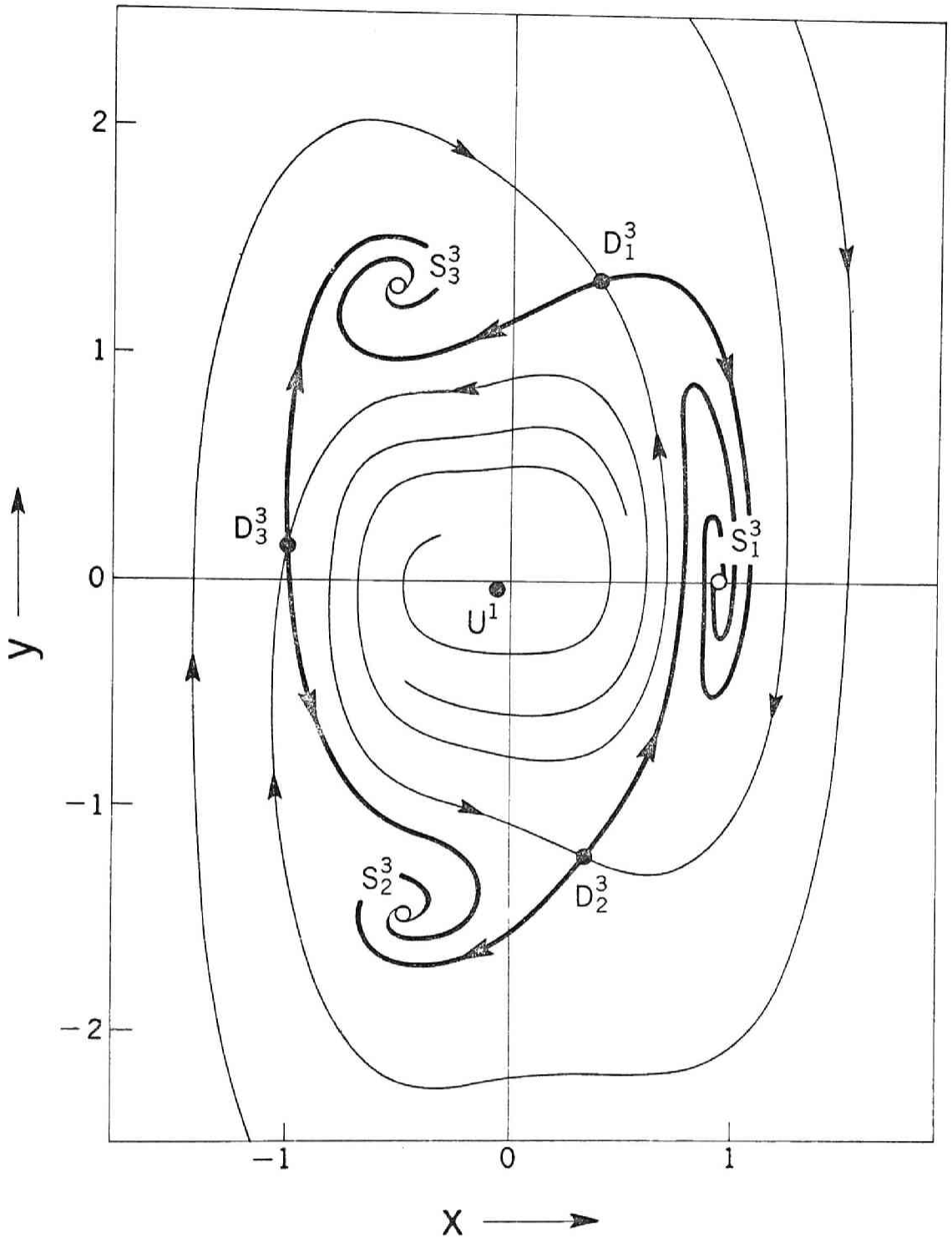

Fig. 4.14 Fixed points and invariant curves of the mapping for Type I of the 1/3-harmonic oscillations. (a) B = 2.0, ν = 5.0

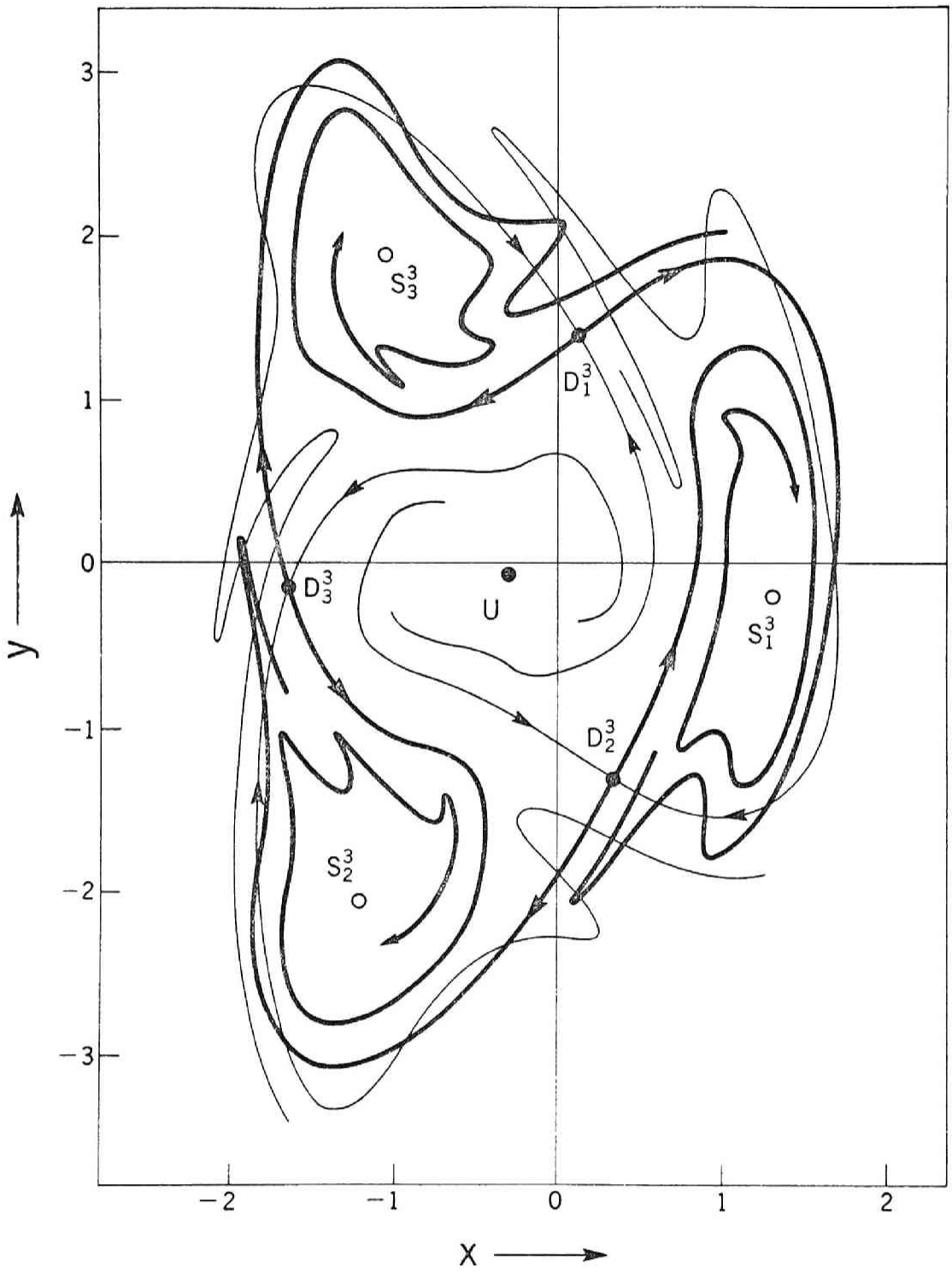

Fig. 4.15 Fixed points and invariant curves of the mapping for Type II of the 1/3-harmonic oscillations. (b) B = 5.0, ν = 4.0

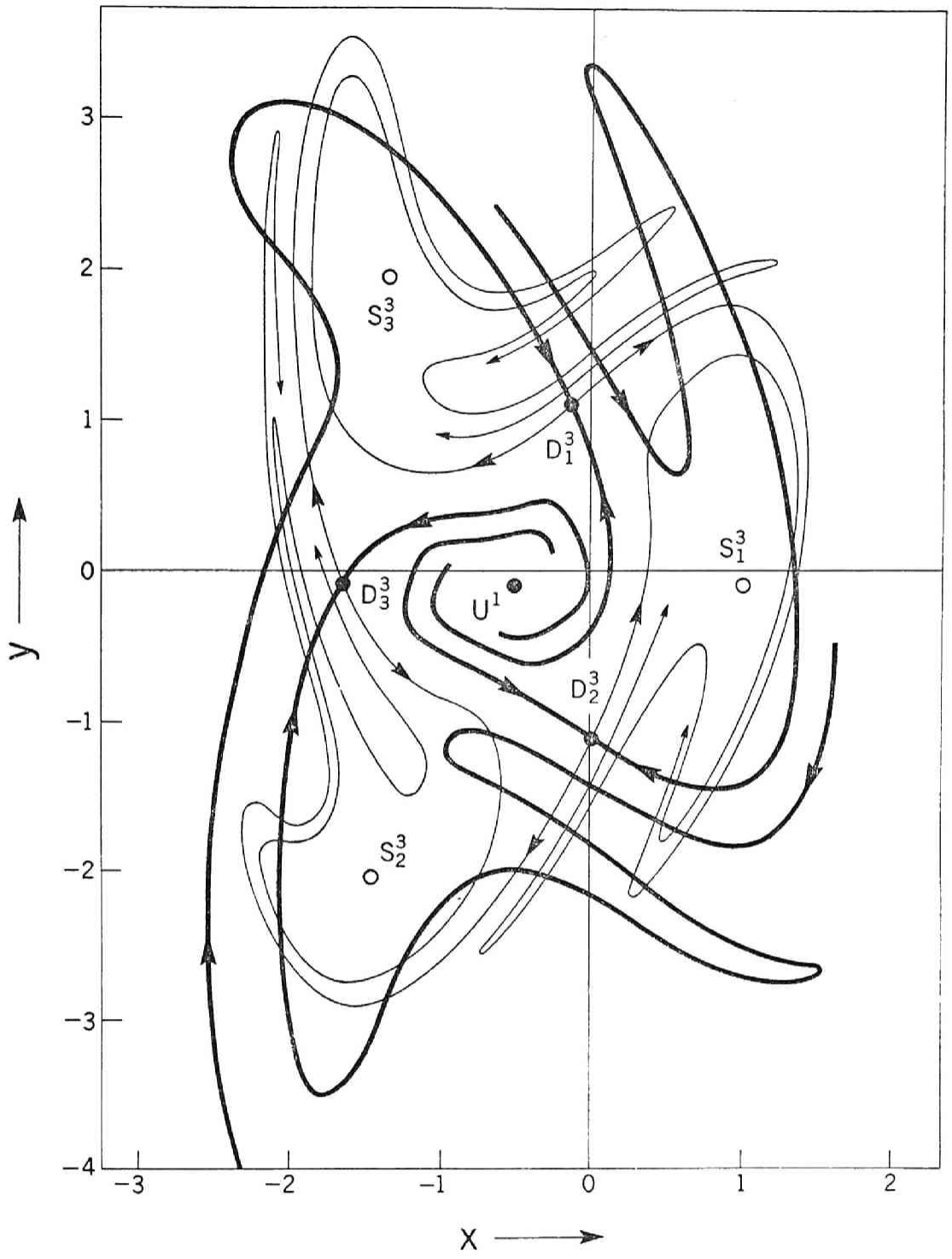

Fig. 4.16 Fixed points and invariant curves of the mapping for Type III of the 1/3-harmonic oscillations. (c) B = 8.0, ν = 4.0

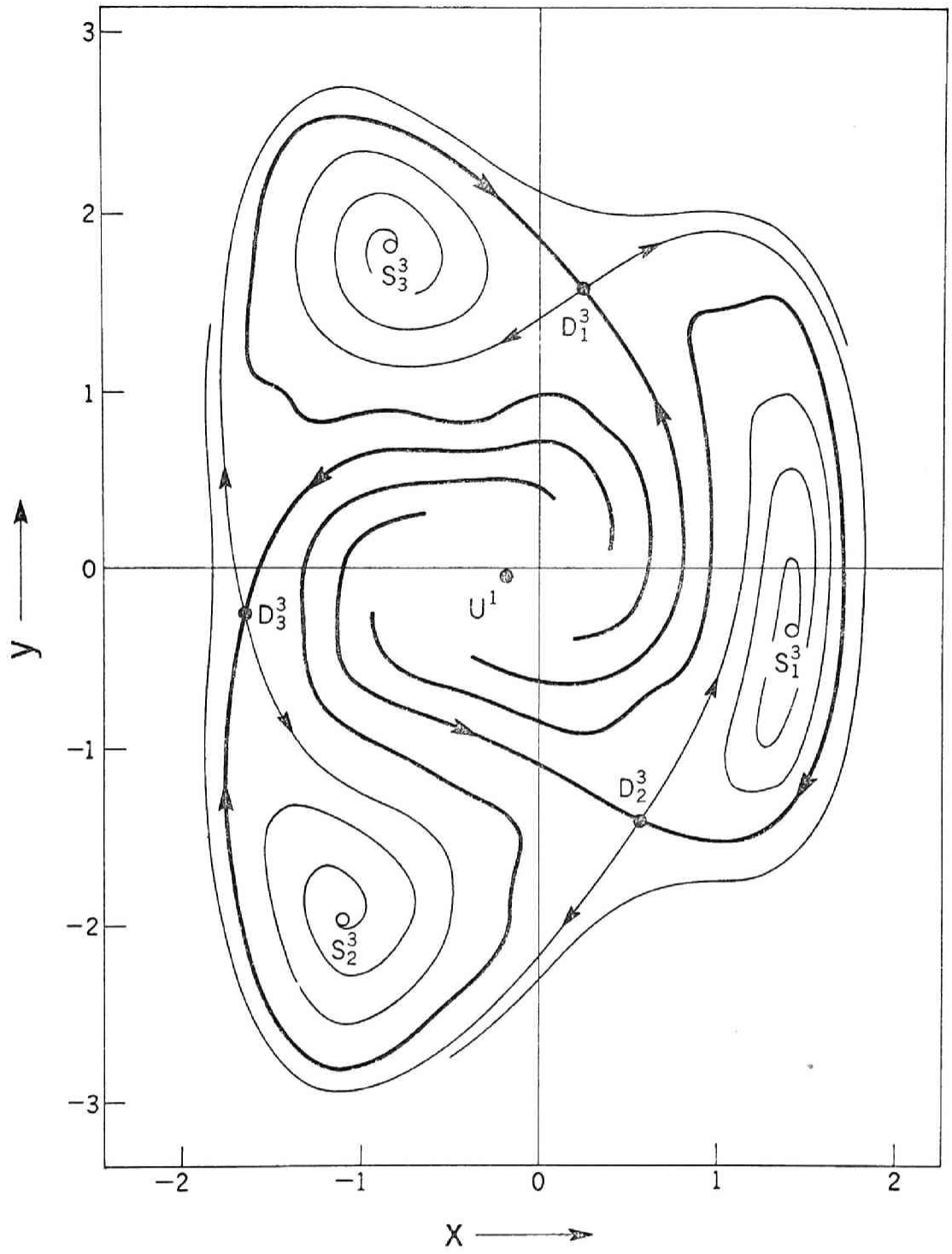

Fig. 4.17 Fixed points and invariant curves of the mapping for Type IV of the 1/3-harmonic oscillations. (d) B = 3.0, ν = 4.0

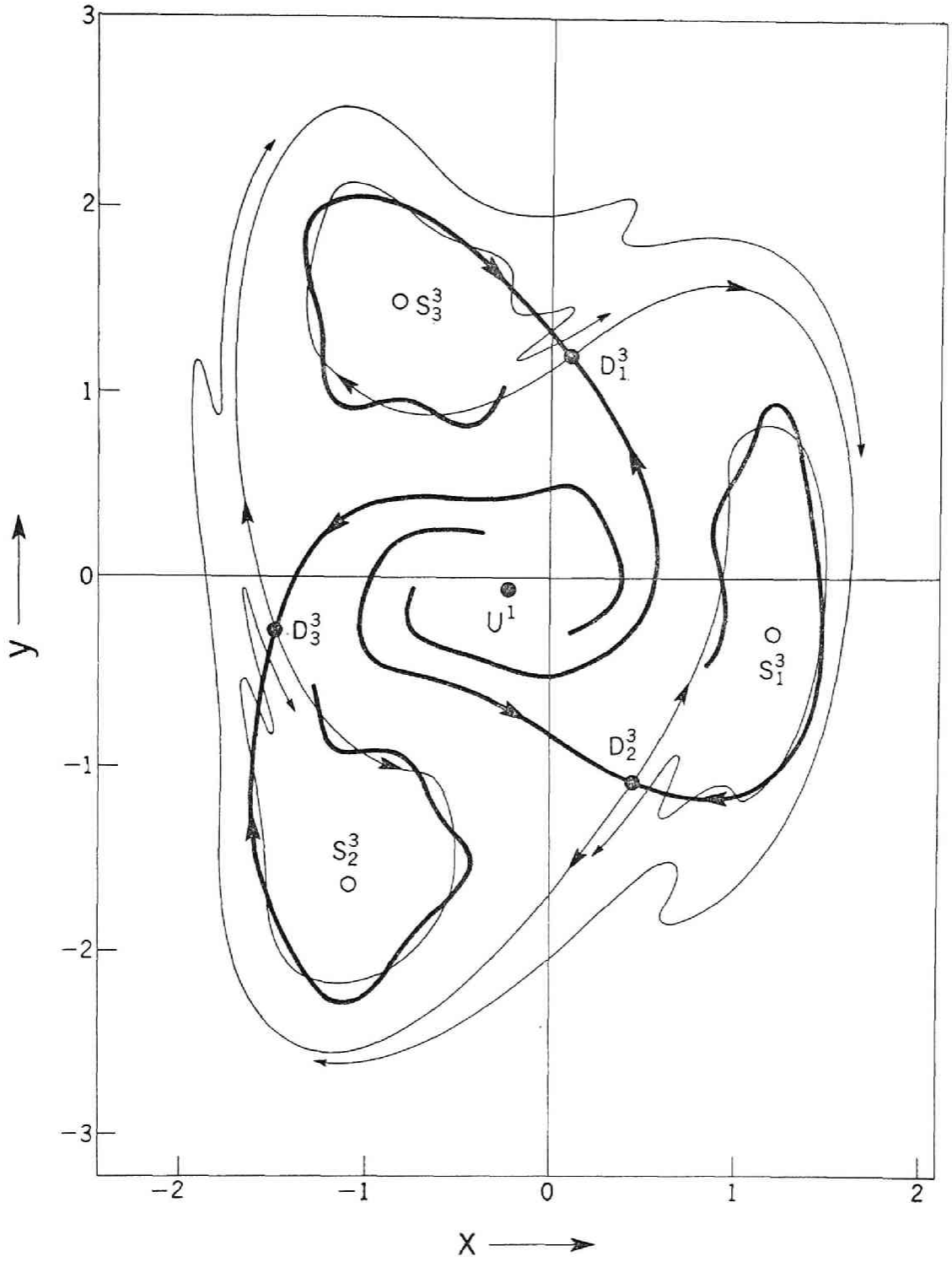

Fig. 4.18 Fixed points and invariant curves of the mapping for Type V of the 1/3-harmonic oscillations. (e) B = 3.0, ν = 3.6

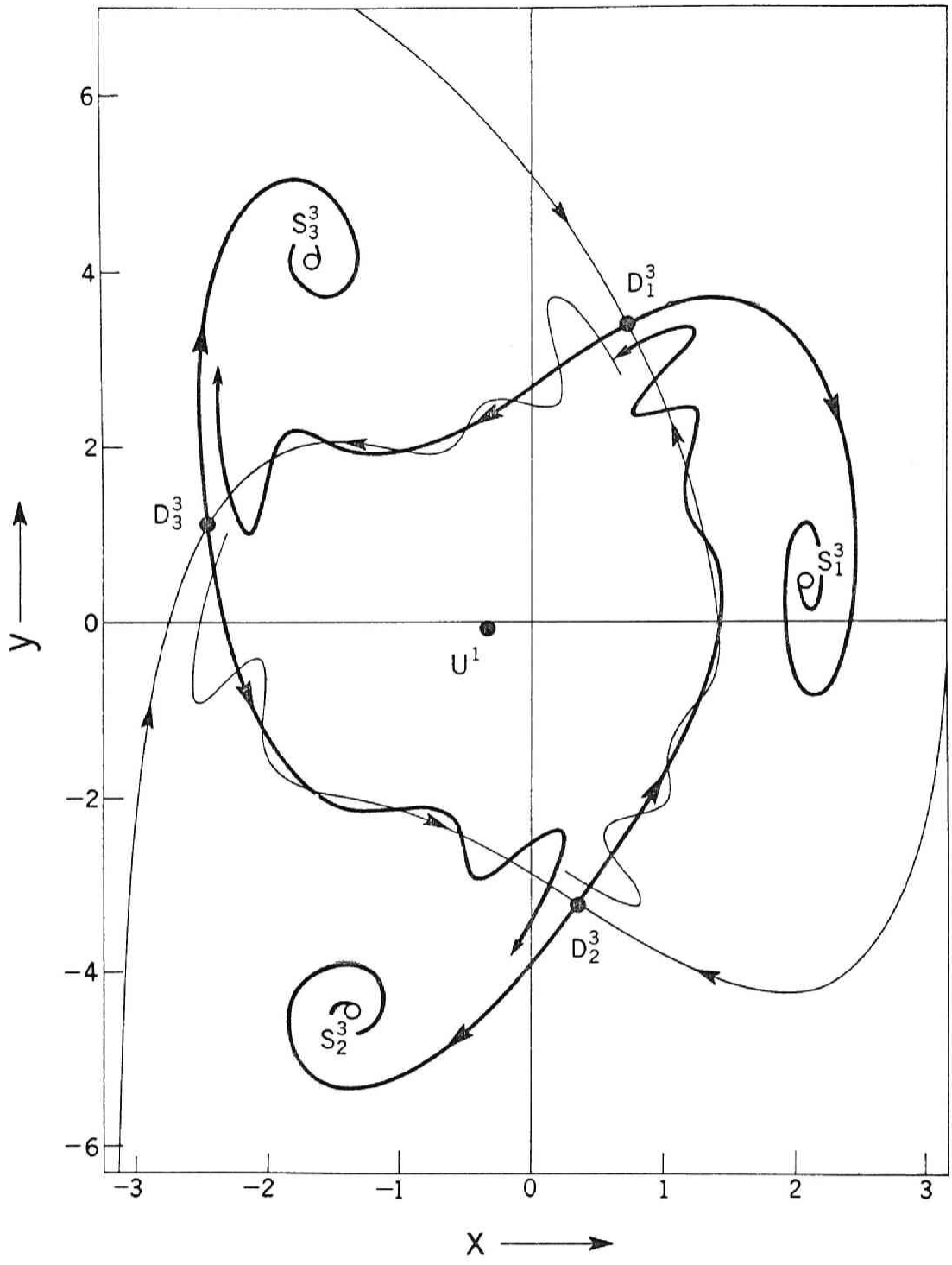

Fig. 4.19 Fixed points and invariant curves of the mapping for Type VI of the 1/3-harmonic oscillations. (f) B = 12.0, ν = 6.0

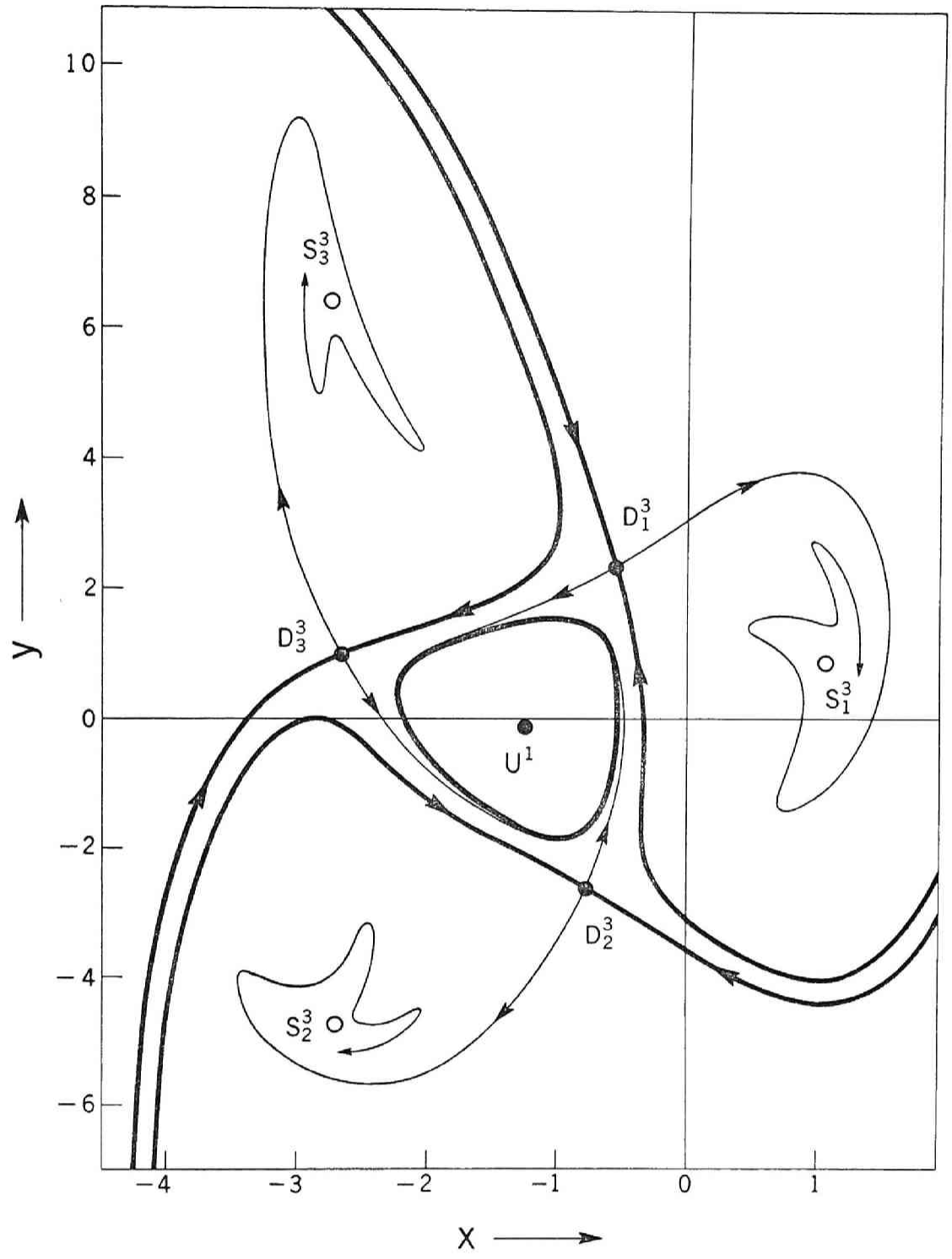

Fig. 4.20 Fixed points and invariant curves of the mapping for Type VII of the 1/3-harmonic oscillations. (g) B = 60.0, ν = 7.0

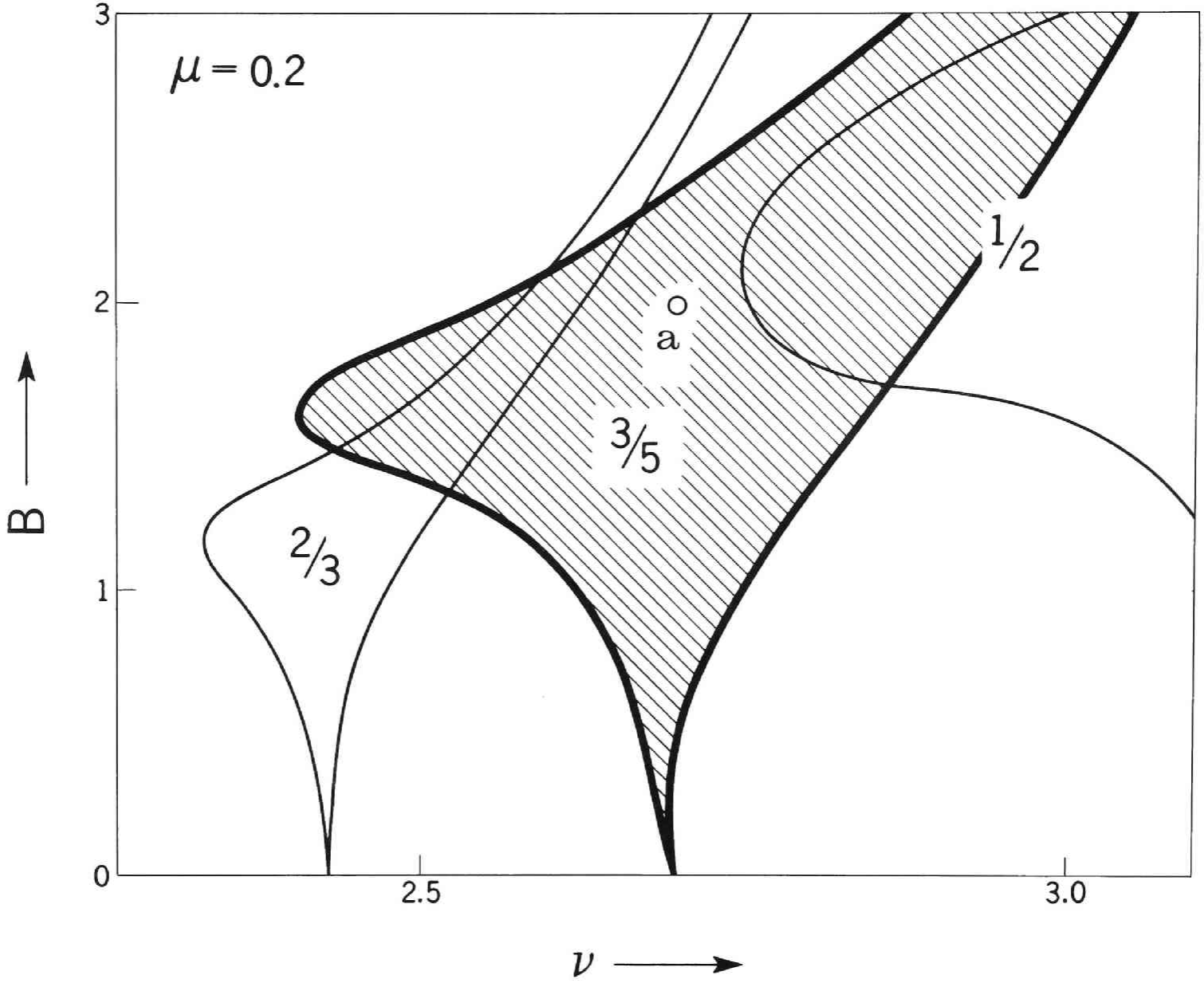

Fig. 4.21 Regions of ultra-subharmonic entrainment for Eq. (4.1).

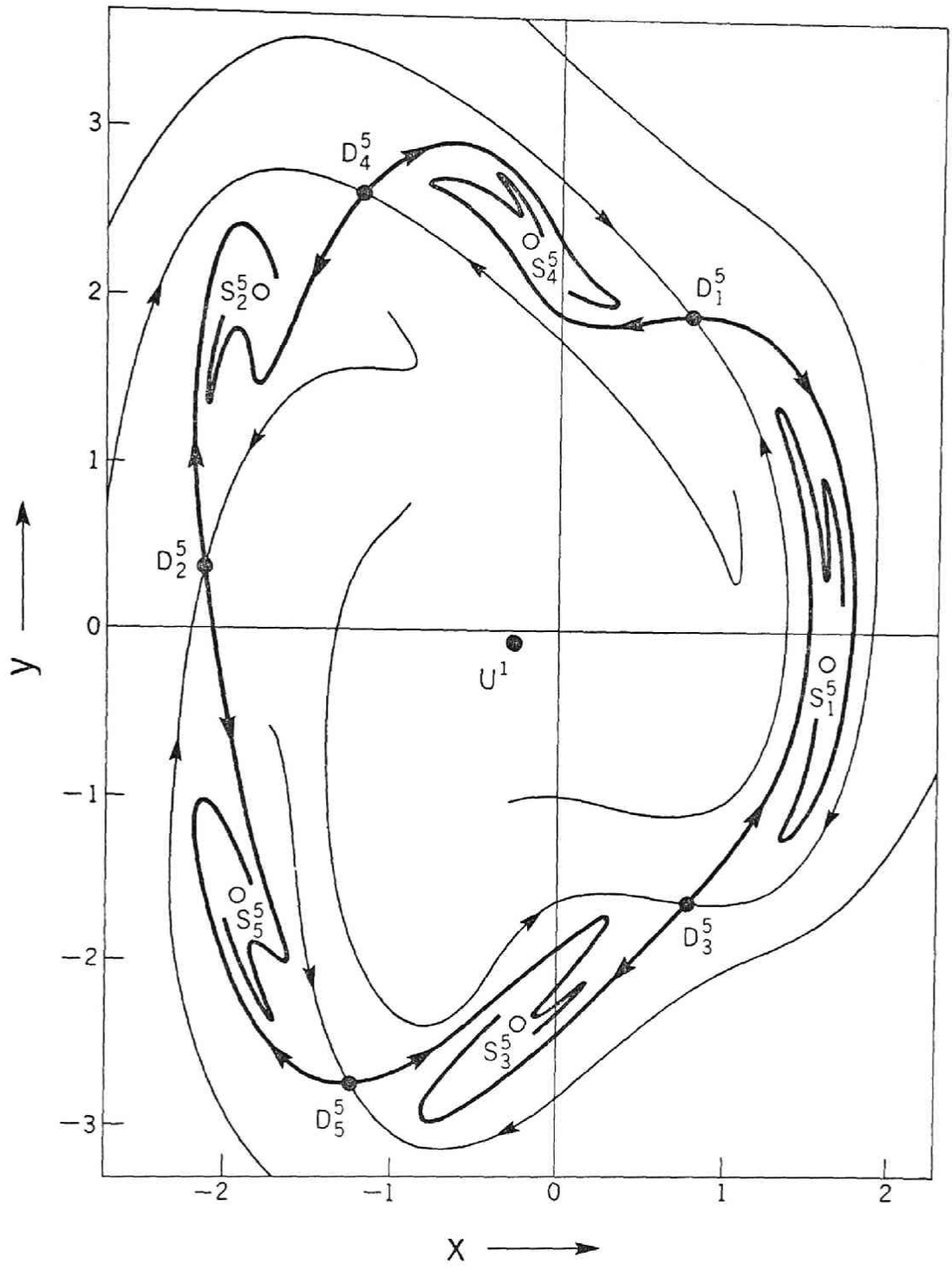

Fig. 4.22 Fixed points and invariant curves of the mapping for Eq. (4.1).

(a) B = 2.0, ν = 2.7

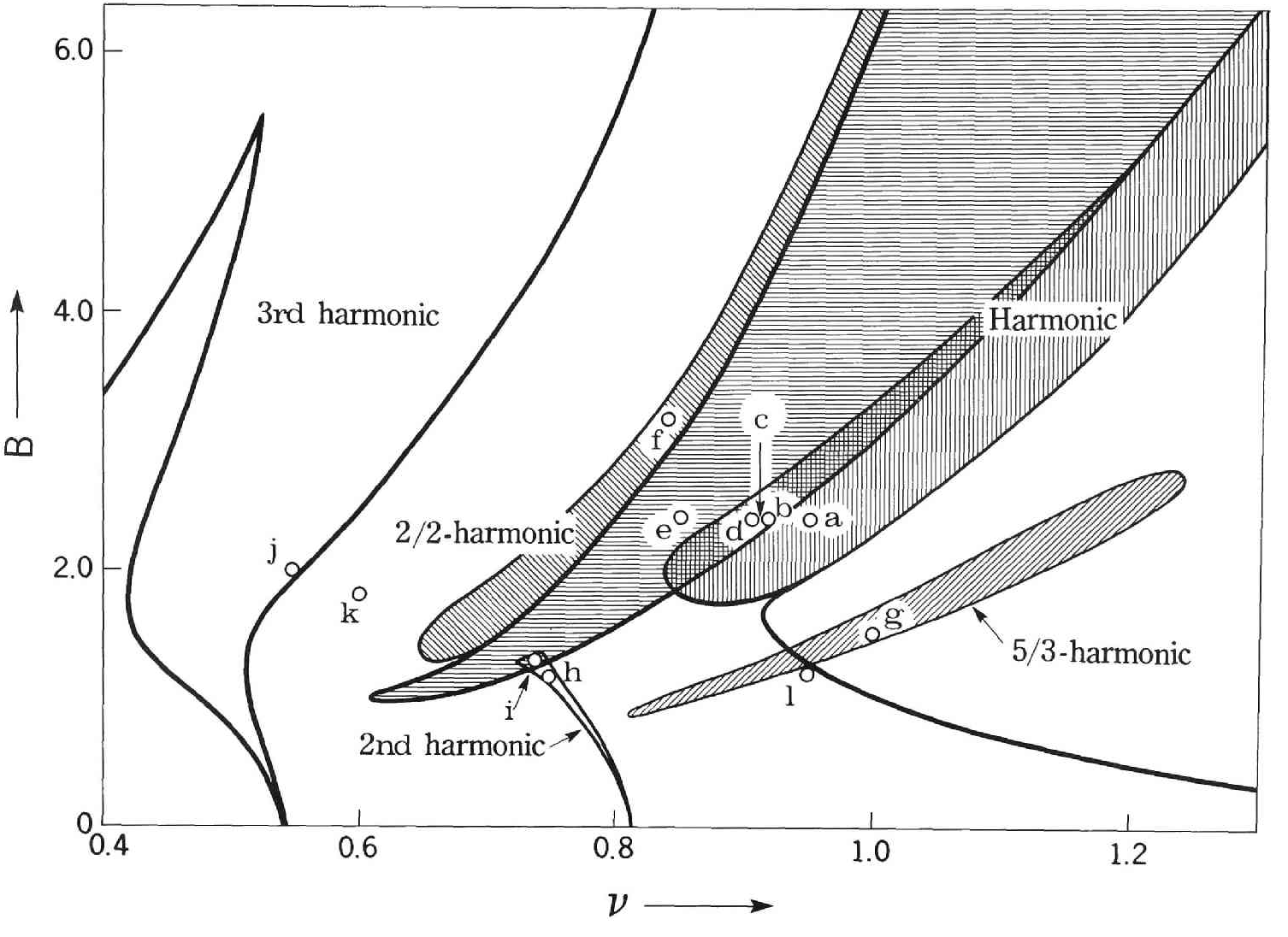

Fig. 4.23 Regions of harmonic and higher-harmonic entrainments for Eq. (4.1).

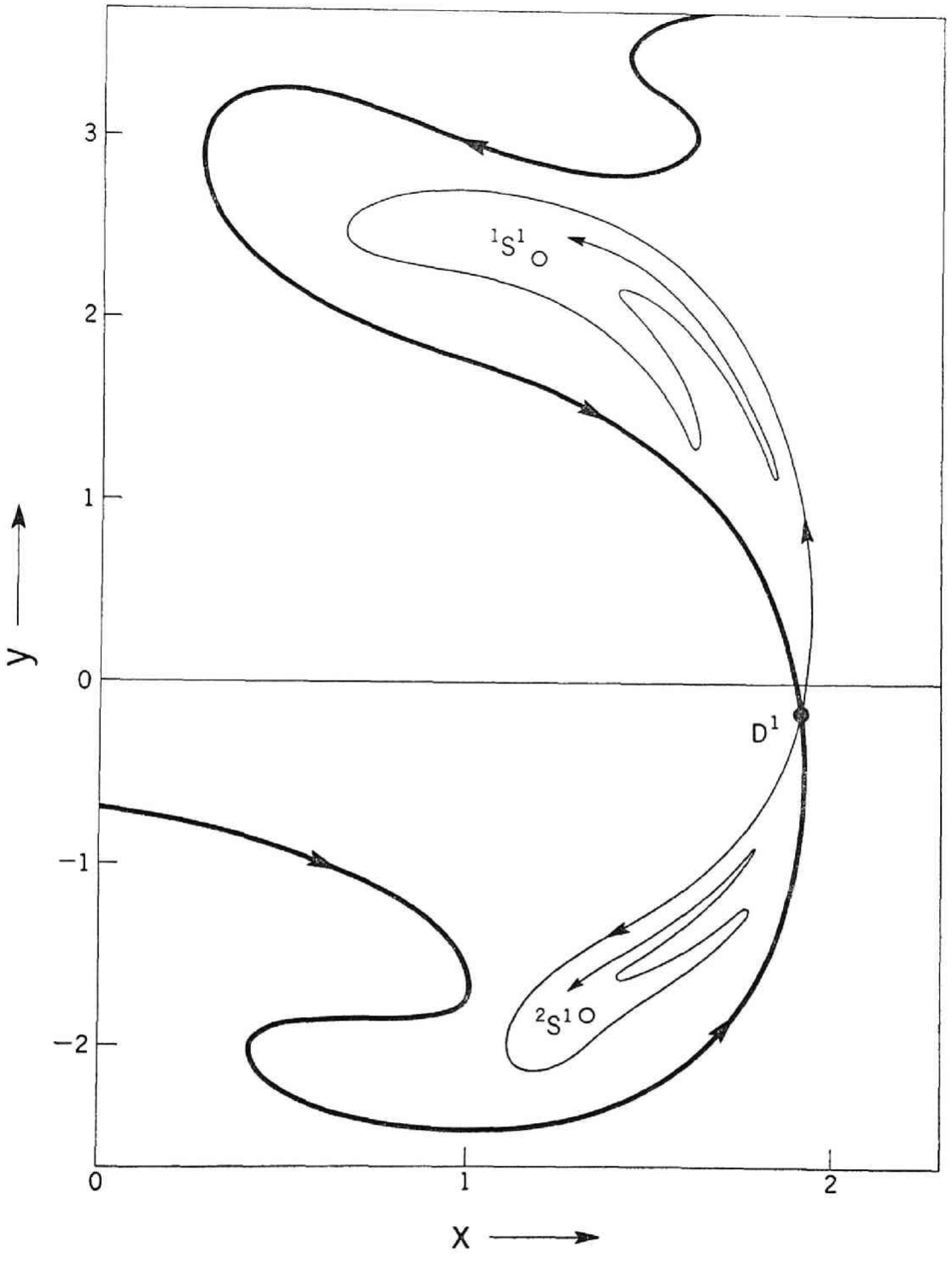

Fig. 4.24 Fixed points and invariant curves of the mapping for Eq. (4.1).

(a) $B = 2.4$, $\nu = 0.95$

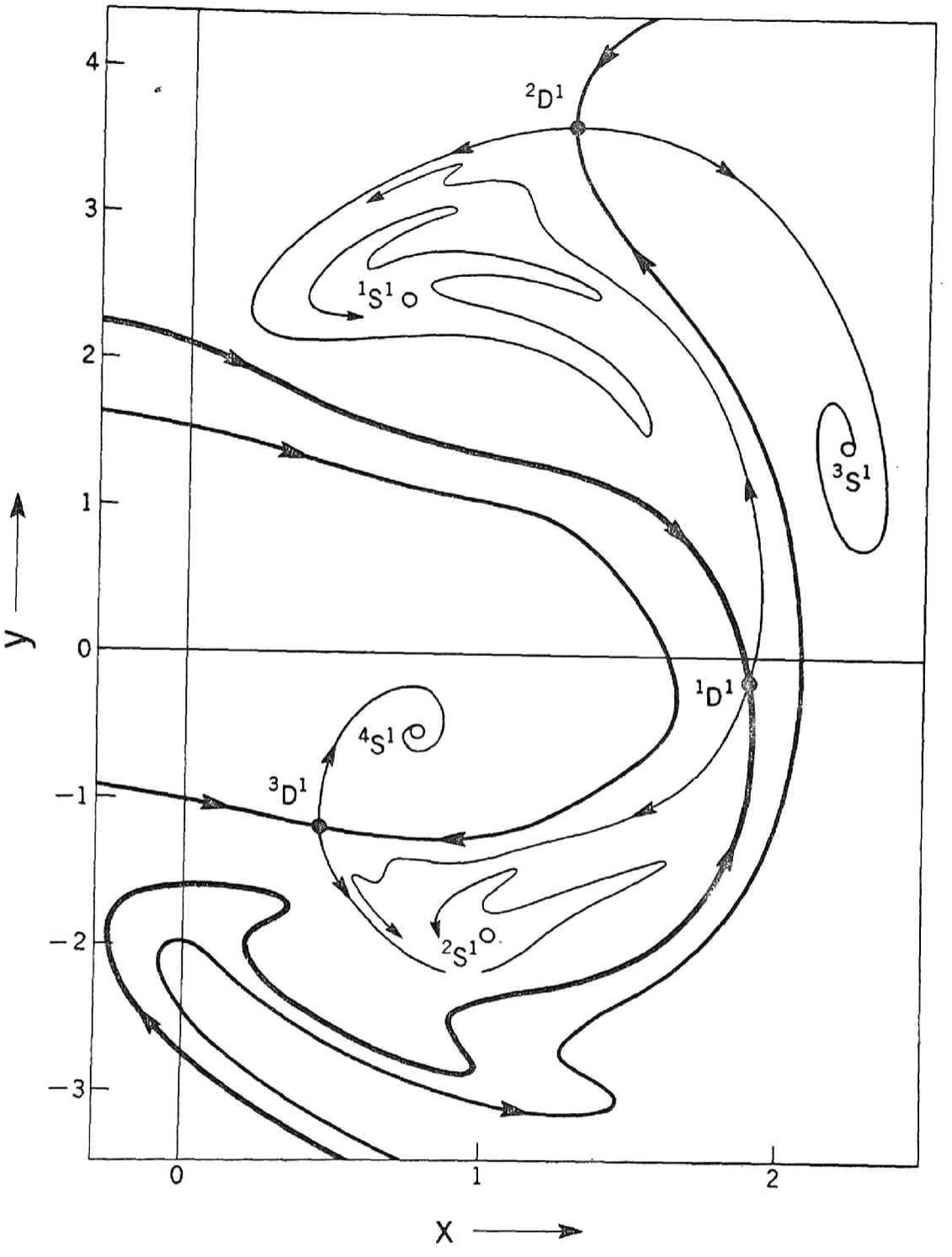

Fig. 4.25 Fixed points and invariant curves of the mapping for Eq. (4.1).
(b) B = 2.4, ν = 0.912

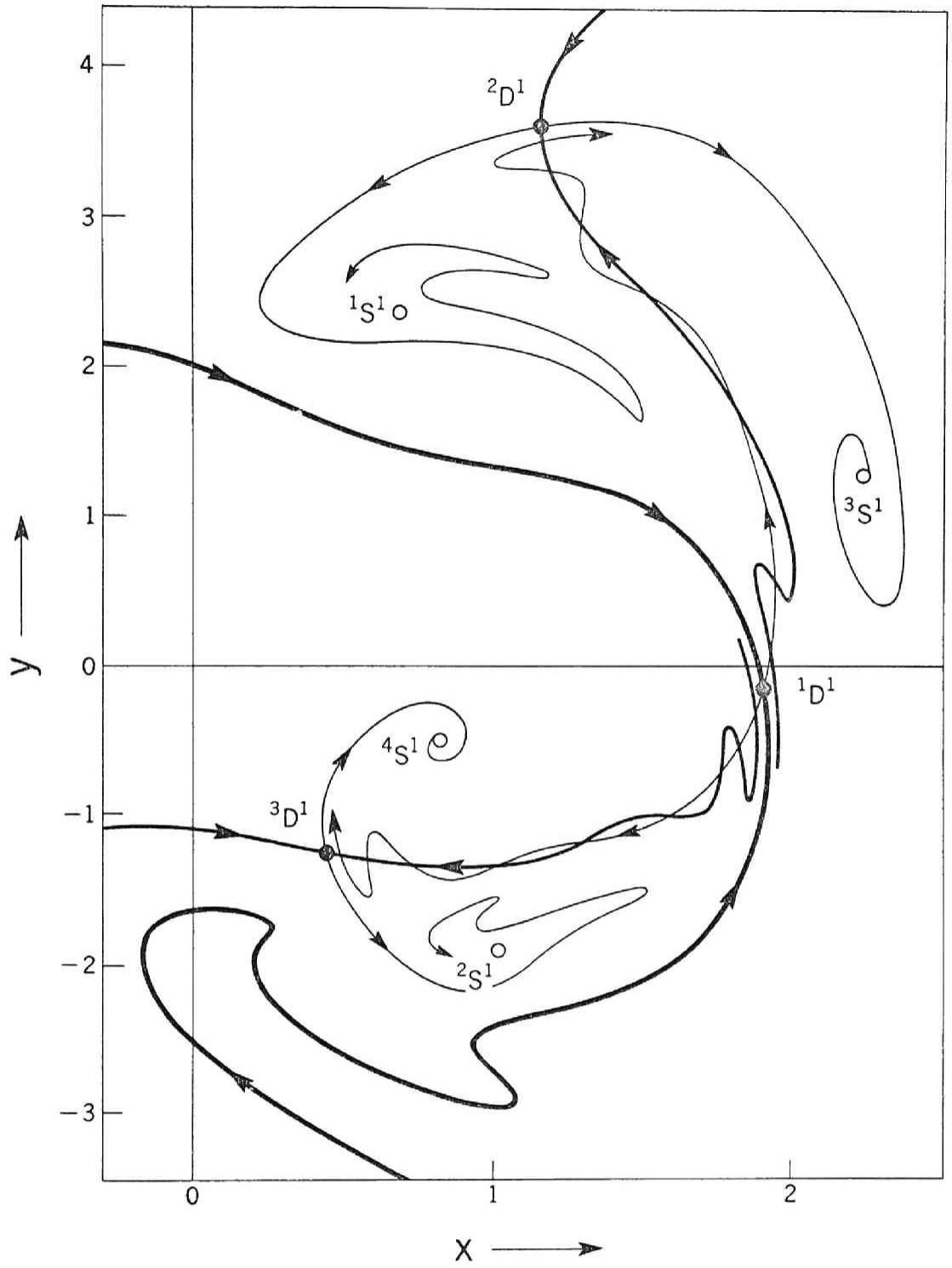

Fig. 4.26 Fixed points and invariant curves of the mapping for Eq. (4.1).
(c) B = 2.4, ν = 0.908

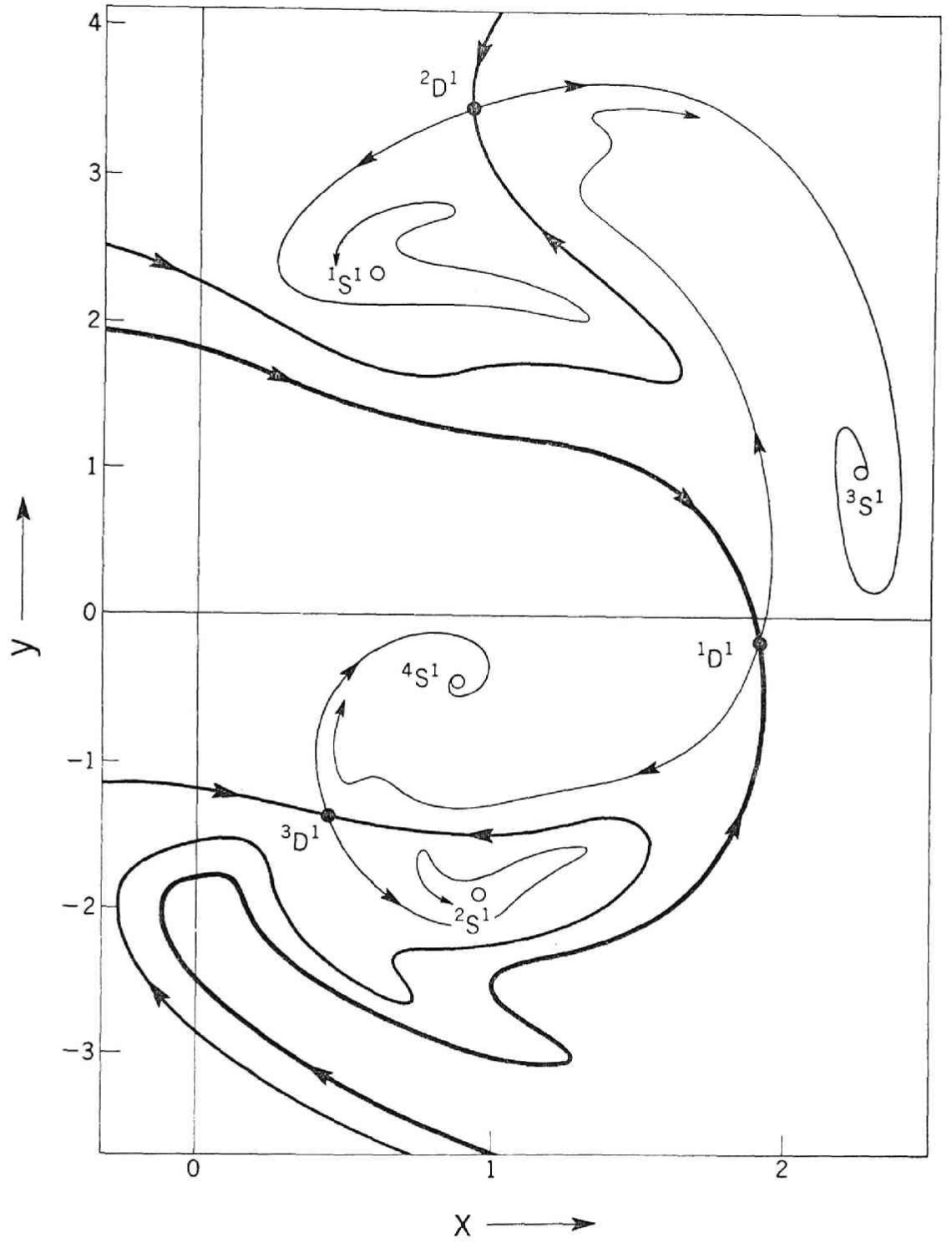

Fig. 4.27 Fixed points and invariant curves of the mapping for Eq. (4.1).

(d) B = 2.4, ν = 0.90

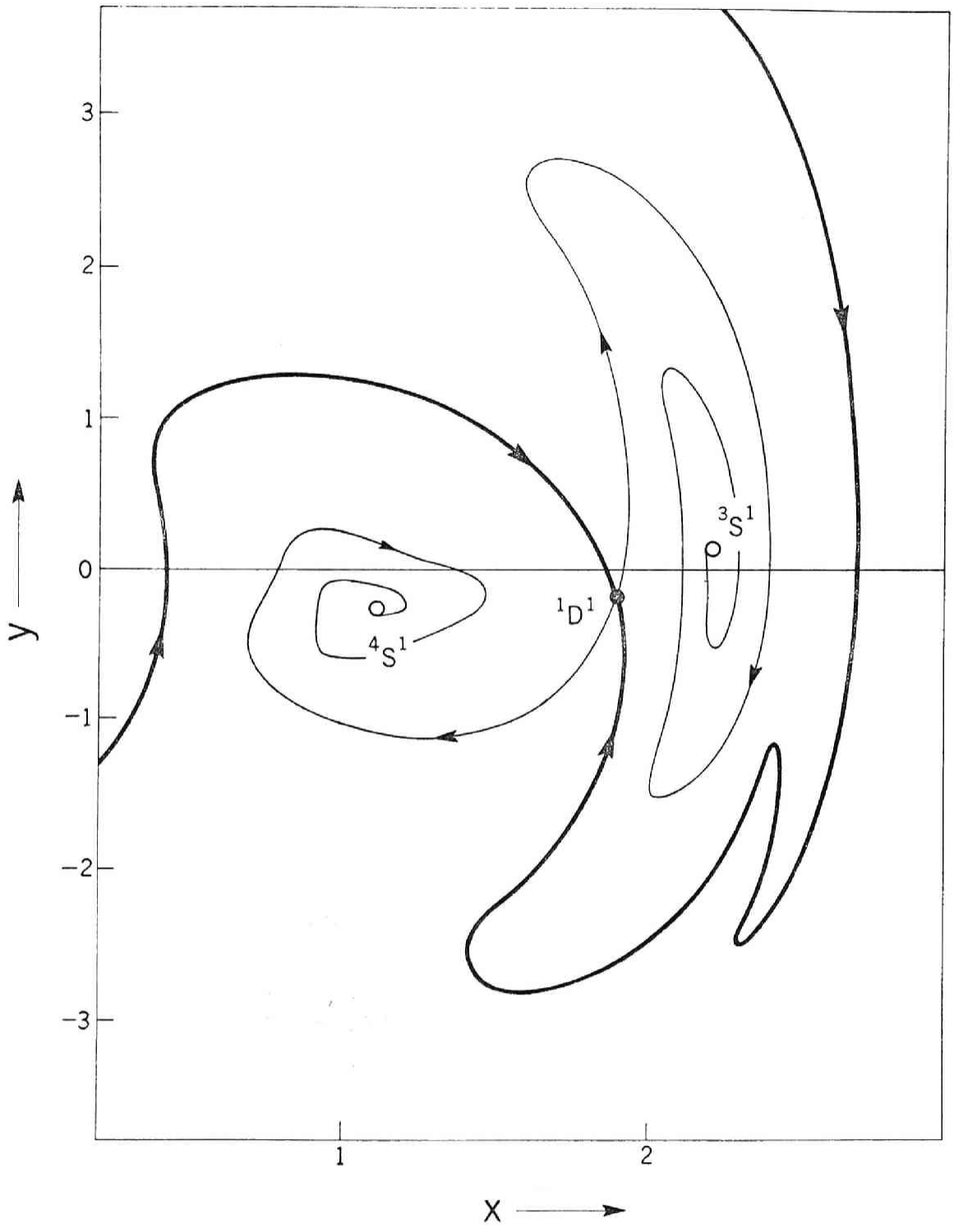

Fig. 4.28 Fixed points and invariant curves of the mapping for Eq. (4.1).
(e) B = 2.4, ν = 0.85

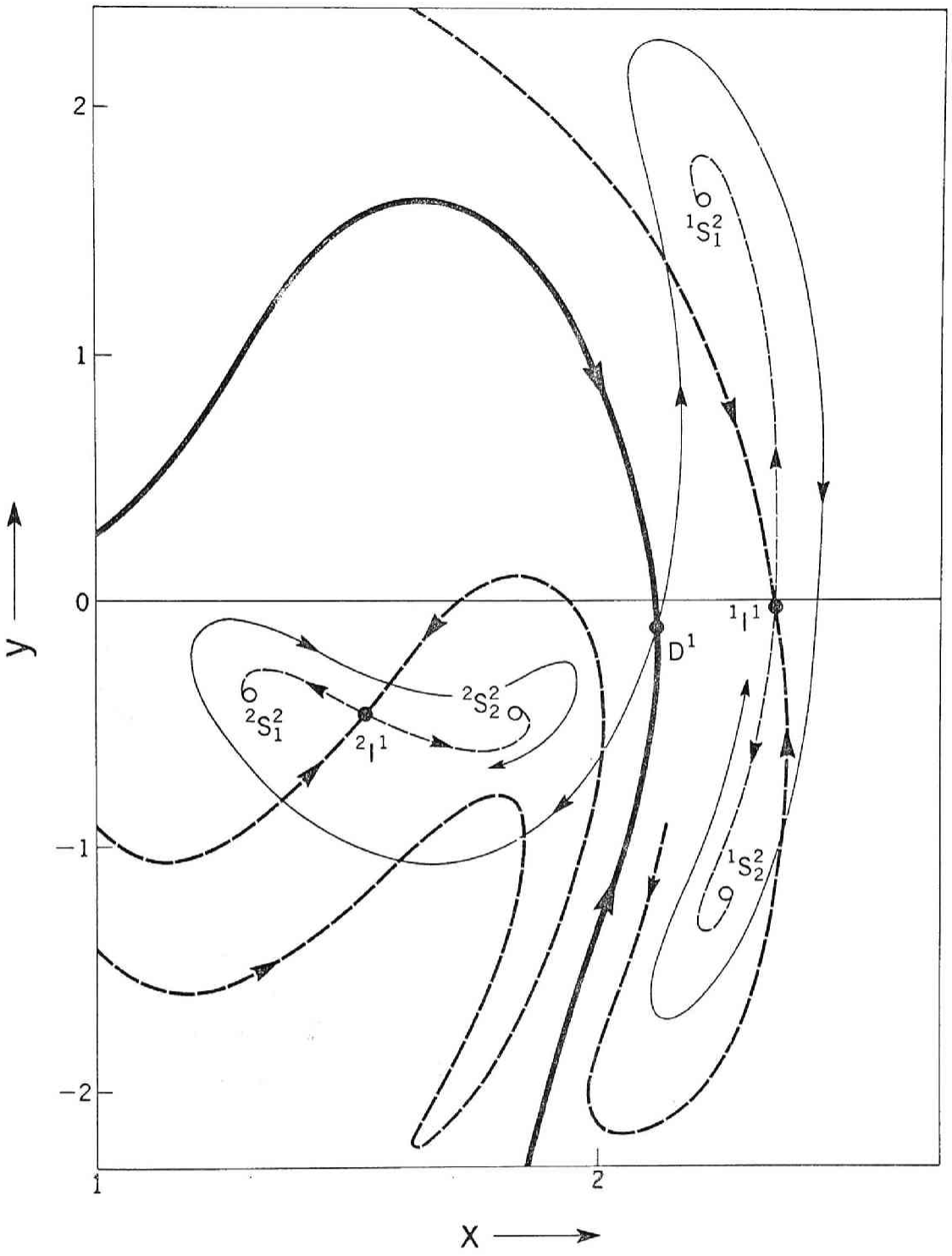

Fig. 4.29 Fixed points and invariant curves of the mapping for Eq. (4,1).
(f) B = 3.2, ν = 0.84

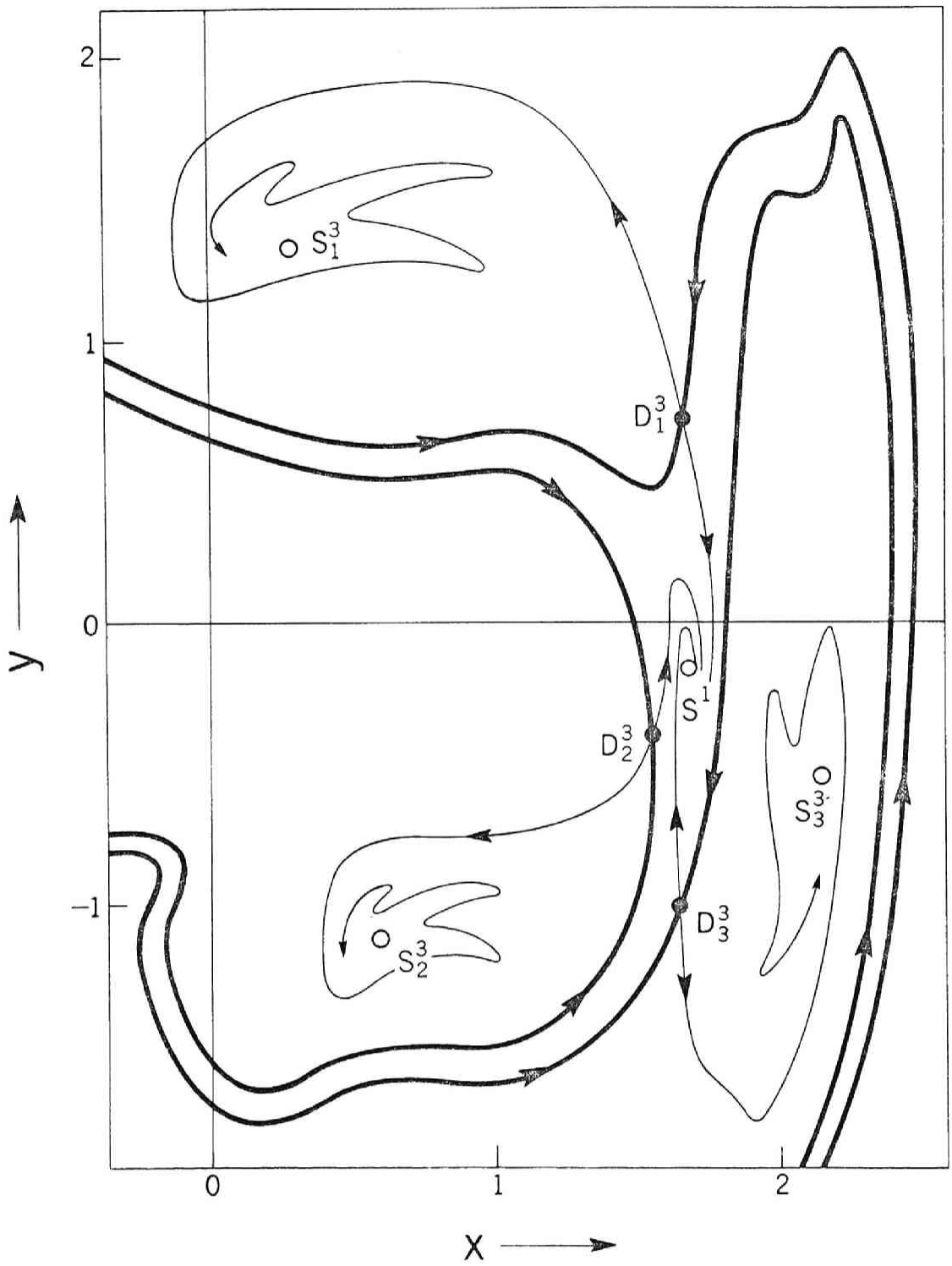

Fig. 4.30 Fixed points and invariant curves of the mapping for Eq. (4.1).
(g) B = 1.5, ν = 1.0

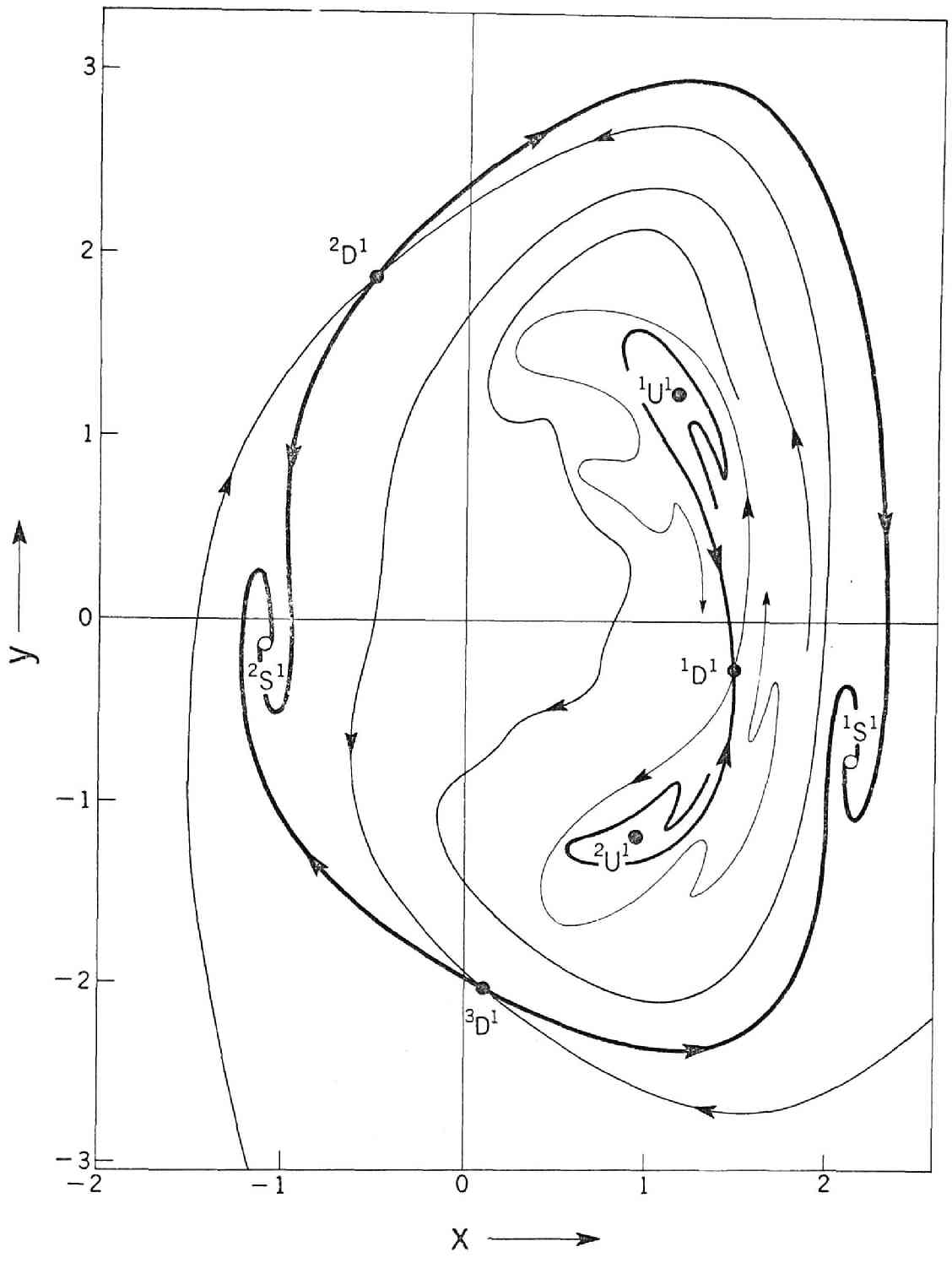

Fig. 4.31 Fixed points and invariant curves of the mapping for Eq. (4.1).
(h) B = 1.16, ν = 0.75

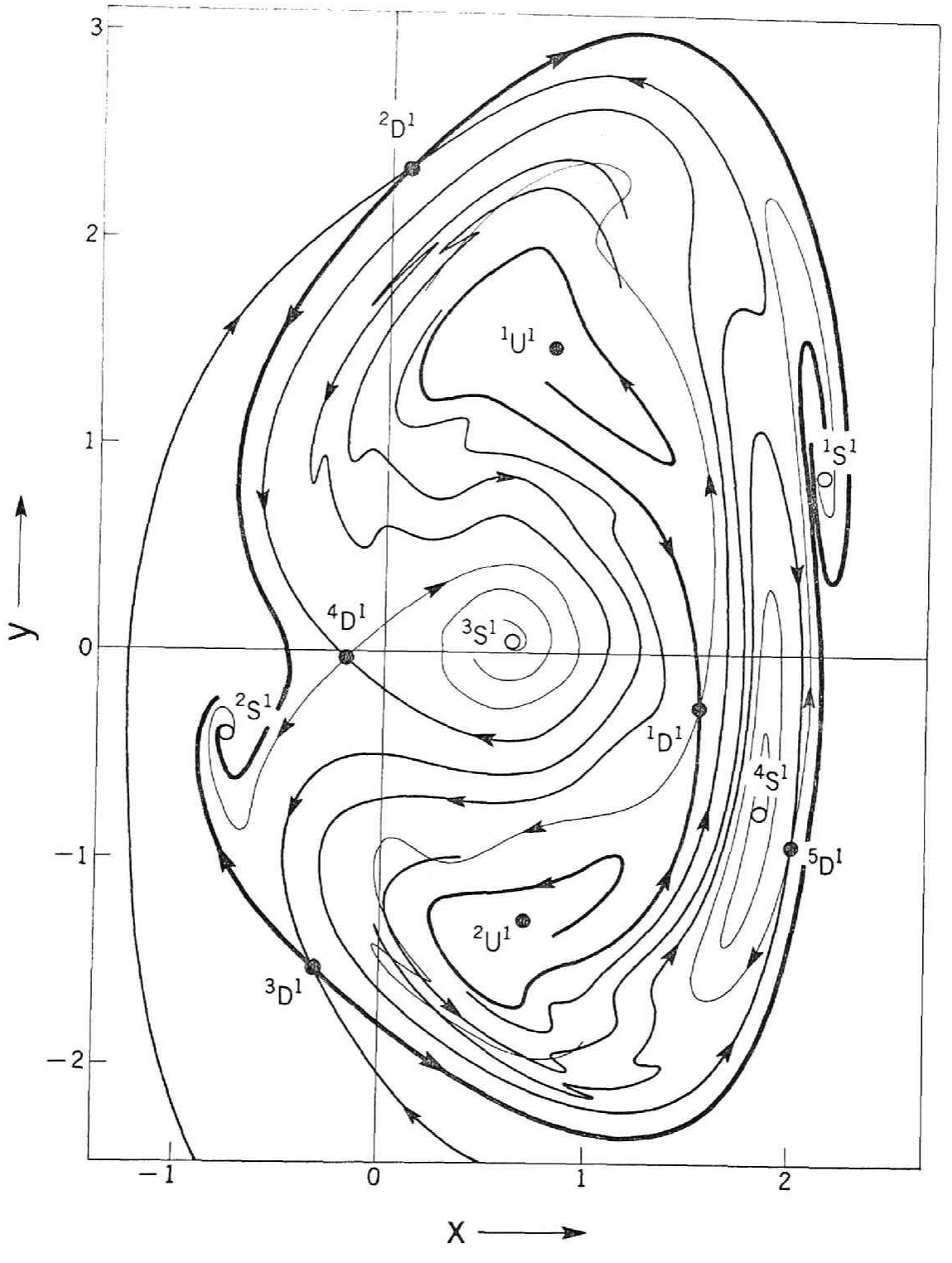

Fig. 4.32 Fixed points and invariant curves of the mapping for Eq. (4.1).

(i) B = 1.3, ν = 0.74

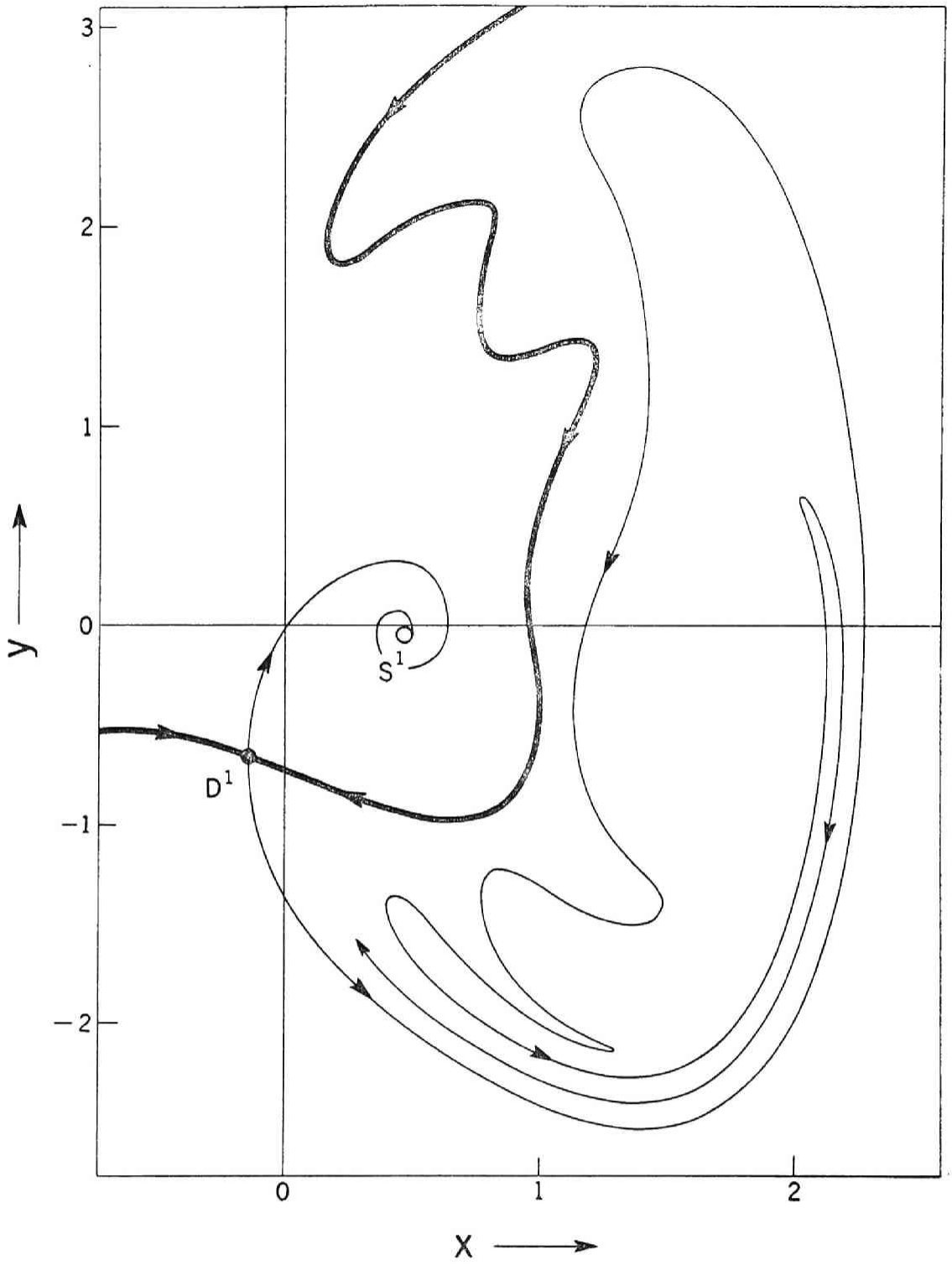

Fig. 4.33 Fixed points and invariant curves of the mapping for Eq. (4.1).

(j) B = 2.0, ν = 0.55

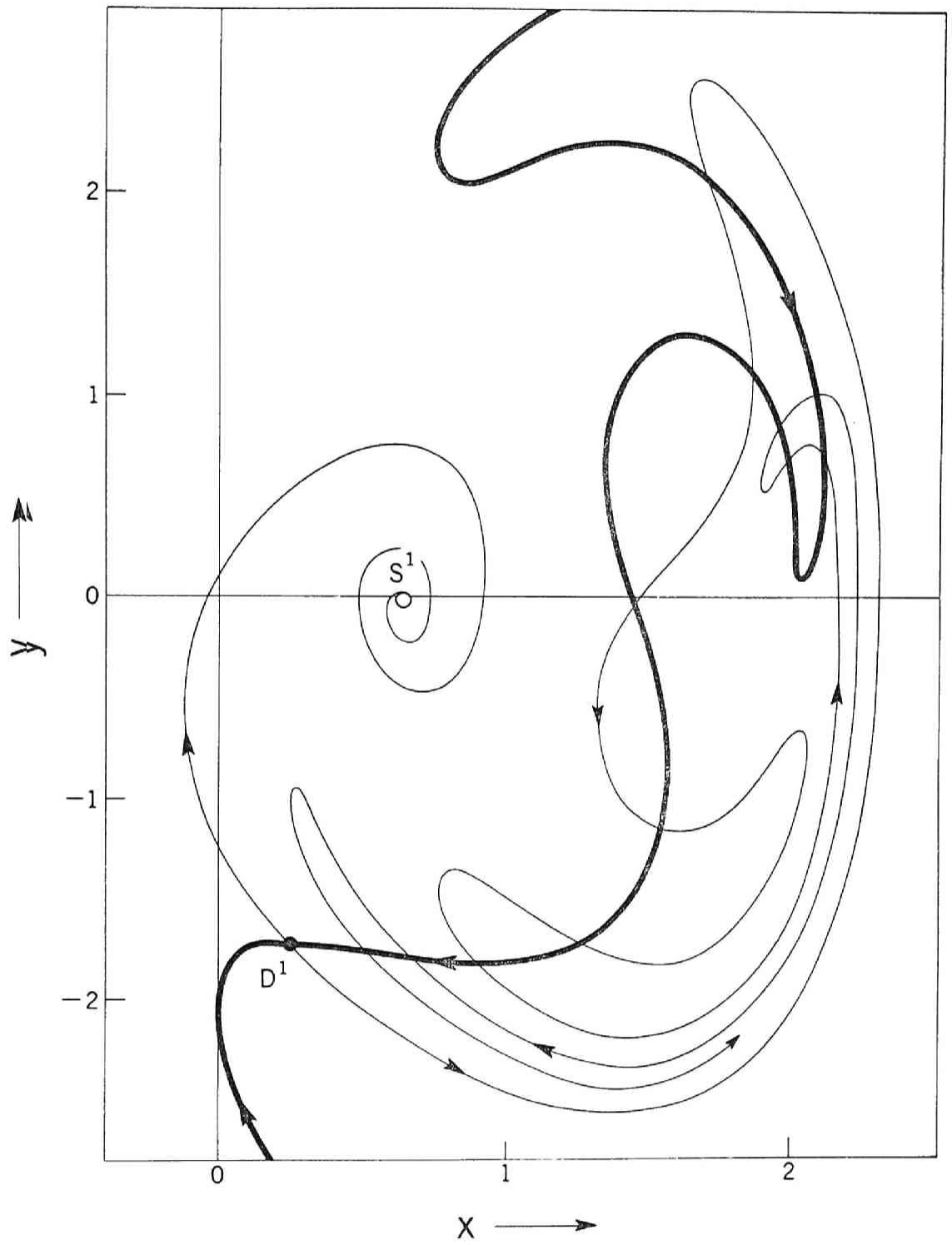

Fig. 4.34 Fixed points and invariant curves of the mapping for Eq. (4.1).
(B = 2.2, ν = 0.55)

Table 4.1 Fixed Points and Related Properties in Fig. 4.3 (B = 0.2, ν = 1.6)

Fixed point	x	y	m_1 , m_2	$\|m\|$
S^1	1.930	0.181	0.581±0.490i	0.760
D^1	-1.812	-0.670	0.367 , 1.746	
U^1	-0.079	-0.016	1.317 , 1.662	

Table 4.2 Fixed Points and Related Properties in Fig. 4.4 (B = 8.5, ν = 3.0)

Fixed point	x	y	m_1 , m_2	$\|m\|$
S^1	1.986	10.566	0.057±0.302i	0.308
D^1	-2.741	2.875	0.099 , 2.930	
U^1	-1.039	-0.152	-0.993±0.478i	1.102

Table 4.3 Fixed Points and Related Properties in Fig. 4.5 (B = 5.8, ν = 3.0)

Fixed point	x	y	m_1 , m_2	$\|m\|$
S^1	0.674	9.707	0.285±0.199i	0.348
D^1	-2.415	6.047	0.109 , 1.833	
U^1	-0.667	-0.119	-0.169±1.164i	1.177

Table 4.4 Fixed Points and Related Properties in Fig. 4.6 (B = 11.0, ν = 3.0)

Fixed point	x	y	m_1 , m_2	$\|m\|$
$^1S^1$	2.569	10.527	-0.057±0.276i	0.282
$^2S^1$	-1.520	-0.102	-0.610±0.755i	0.971
D^1	-2.450	0.967	0.137 , 3.244	

Table 4.5 Fixed Points and Related Properties in Fig. 4.8 (B = 2.0, ν = 3.2)

Fixed point	x	y	m_1 , m_2	|m|
$^1S_1^2$	1.721	-0.247	0.273±0.723i	0.773
$^1S_2^2$	-2.003	0.326	0.273±0.723i	0.773
$^2S_1^2$	-0.357	2.483	0.273±0.723i	0.773
$^2S_2^2$	-0.409	-2.619	0.273±0.723i	0.773
$^1D_1^2$	0.803	2.183	0.249 , 2.545	
$^1D_2^2$	-1.559	-2.403	0.249 , 2.545	
$^2D_1^2$	-1.526	2.284	0.249 , 2.545	
$^2D_2^2$	0.856	-1.902	0.249 , 2.545	
U^1	-0.196	-0.039	1.103±0.504i	1.212

Table 4.6 Fixed Points and Related Properties in Fig. 4.9 (B = 2.5, ν = 3.0)

Fixed point	x	y	m_1 , m_2	|m|
$^1S_1^2$	1.486	-0.378	-0.262±0.775i	0.818
$^1S_2^2$	-1.925	0.385	-0.262±0.775i	0.818
$^2S_1^2$	-0.455	2.120	-0.262±0.775i	0.818
$^2S_2^2$	-0.653	-2.410	-0.262±0.775i	0.818
$^1D_1^2$	0.450	1.760	0.177 , 4.237	
$^1D_2^2$	-1.508	-2.174	0.177 , 4.237	
$^2D_1^2$	-1.610	1.844	0.177 , 4.237	
$^2D_2^2$	0.720	-1.511	0.177 , 4.237	
U^1	-0.278	-0.055	0.945±0.776i	1.233

Table 4.7 Fixed Points and Related Properties in Fig. 4.10 (B = 2.0, ν = 2.9)

Fixed point	x	y	m_1 , m_2	|m|
$^1S_1^2$	1.434	-0.587	0.053±0.851i	0.853
$^1S_2^2$	-1.833	0.515	0.053±0.851i	0.853
$^2S_1^2$	-0.286	1.939	0.053±0.851i	0.853
$^2S_2^2$	-0.668	-2.300	0.053±0.851i	0.853
$^1D_1^2$	0.382	1.719	0.230 , 3.407	
$^1D_2^2$	-1.329	-2.193	0.230 , 3.407	
$^2D_1^2$	-1.593	1.597	0.230 , 3.407	
$^2D_2^2$	0.861	-1.406	0.230 , 3.407	
U^1	-0.240	-0.047	1.021±0.694i	1.234

Table 4.8 Fixed Points and Related Properties in Fig. 4.11 (B = 4.0, ν = 3.3)

Fixed point	x	y	m_1 , m_2	$\|m\|$
$^1S_1^2$	1.578	-0.024	-0.611±0.406i	0.734
$^1S_2^2$	-2.153	0.309	-0.611±0.406i	0.734
$^2S_1^2$	-0.746	2.676	-0.611±0.406i	0.734
$^2S_2^2$	-0.708	-2.788	-0.611±0.406i	0.734
$^1D_1^2$	0.558	1.978	0.125 , 5.172	
$^1D_2^2$	-1.837	-2.184	0.125 , 5.172	
$^2D_1^2$	-1.714	2.435	0.125 , 5.172	
$^2D_2^2$	0.510	-1.787	0.125 , 5.172	
U^1	-0.370	-0.072	0.792±0.894i	1.194

Table 4.9 Fixed Points and Related Properties in Fig. 4.12 (B = 7.0, ν = 4.0)

Fixed point	x	y	m_1 , m_2	$\|m\|$
$^1S_1^2$	1.868	1.051	-0.157±0.584i	0.605
$^1S_2^2$	-2.588	0.063	-0.157±0.584i	0.605
$^2S_1^2$	-1.127	4.190	-0.157±0.584i	0.605
$^2S_2^2$	-0.534	-3.626	-0.157±0.584i	0.605
$^1D_1^2$	1.127	2.790	0.126 , 3.377	
$^1D_2^2$	-2.411	-2.041	0.126 , 3.377	
$^2D_1^2$	-1.779	4.094	0.126 , 3.377	
$^2D_2^2$	0.267	-2.794	0.126 , 3.377	
S_1^3	1.115	-0.120	-0.591±0.544i	0.803
S_2^3	-1.383	-2.075	-0.591±0.544i	0.803
S_3^3	-1.251	1.946	-0.591±0.544i	0.803
D_1^3	-0.049	1.205	0.063 , 19.899	
D_2^3	0.116	-1.191	0.063 , 19.899	
D_3^3	-1.655	-0.093	0.063 , 19.899	
U^1	-0.441	-0.083	0.771±0.856i	1.152

Table 4.10 Fixed Points and Related Properties in Fig. 4.14 (B = 2.0, ν = 5.0)

Fixed point	x	y	m_1 , m_2	$\|m\|$
S_1^3	1.920	0.049	0.114±0.713i	0.722
S_2^3	-0.897	-2.948	0.114±0.713i	0.722
S_3^3	-1.046	2.631	0.114±0.713i	0.722
D_1^3	0.819	2.700	0.189 , 3.176	
D_2^3	0.668	-2.482	0.189 , 3.176	
D_3^3	-1.997	0.436	0.189 , 3.176	
U^1	-0.084	-0.016	1.110 , 1.157	

Table 4.11 Fixed Points and Related Properties in Fig. 4.15 (B = 5.0, ν = 4.0)

Fixed point	x	y	m_1 , m_2	$\|m\|$
S_1^3	1.288	-0.198	-0.821±0.117i	0.829
S_2^3	-1.232	-2.060	-0.821±0.117i	0.829
S_3^3	-1.064	1.893	-0.821±0.117i	0.829
D_1^3	0.115	1.401	0.074 , 15.528	
D_2^3	0.327	-1.310	0.074 , 15.528	
D_3^3	-1.662	-0.136	0.074 , 15.528	
U^1	-0.313	-0.061	0.968±0.641i	1.161

Table 4.12 Fixed Points and Related Properties in Fig. 4.16 (B = 8.0, ν = 4.0)

Fixed point	x	y	m_1 , m_2	$\|m\|$
S_1^3	1.010	-0.099	-0.447±0.660i	0.797
S_2^3	-1.456	-2.055	-0.447±0.660i	0.797
S_3^3	-1.332	1.956	-0.447±0.660i	0.797
D_1^3	-0.137	1.104	0.064 , 20.640	
D_2^3	0.012	-1.127	0.064 , 20.640	
D_3^3	-1.643	-0.084	0.064 , 20.640	
U^1	-0.505	-0.094	0.654±0.942i	1.147

Table 4.13 Fixed Points and Related Properties in Fig. 4.17 (B = 3.0, ν = 4.0)

Fixed point	x	y	m_1 , m_2	$\|m\|$
S_1^3	1.413	-0.344	-0.680 $\pm$ 0.540i	0.869
S_2^3	-1.102	-1.968	-0.680 $\pm$ 0.540i	0.869
S_3^3	-0.834	1.810	-0.680 $\pm$ 0.540i	0.869
D_1^3	0.244	1.588	0.112 , 9.155	
D_2^3	0.564	-1.417	0.112 , 9.155	
D_3^3	-1.645	-0.252	0.112 , 9.155	
U^1	-0.188	-0.037	1.105 $\pm$ 0.374i	1.167

Table 4.14 Fixed Points and Related Properties in Fig. 4.18 (B = 3.0, ν = 3.6)

Fixed point	x	y	m_1 , m_2	$\|m\|$
S_1^3	1.201	-0.293	-0.921 $\pm$ 0.244i	0.953
S_2^3	-1.093	-1.636	-0.921 $\pm$ 0.244i	0.953
S_3^3	-0.829	1.493	-0.921 $\pm$ 0.244i	0.953
D_1^3	0.104	1.209	0.097 , 13.439	
D_2^3	0.439	-1.094	0.097 , 13.439	
D_3^3	-1.494	-0.271	0.097 , 13.439	
U^1	-0.232	-0.046	1.059 $\pm$ 0.532i	1.185

Table 4.15 Fixed Points and Related Properties in Fig. 4.19 (B = 12.0, ν = 6.0)

Fixed point	x	y	m_1 , m_2	$\|m\|$
S_1^3	2.090	0.464	-0.474 $\pm$ 0.260i	0.540
S_2^3	-1.350	-4.473	-0.474 $\pm$ 0.260i	0.540
S_3^3	-1.653	4.122	-0.474 $\pm$ 0.260i	0.540
D_1^3	0.735	3.413	0.065 , 7.706	
D_2^3	0.352	-3.250	0.065 , 7.706	
D_3^3	-2.445	1.117	0.065 , 7.706	
U^1	-0.334	-0.064	1.009 $\pm$ 0.447i	1.104

Table 4.16 Fixed Points and Related Properties in Fig. 4.20 (B = 60, ν = 7)

Fixed point	x	y	m_1 , m_2	|m|
S_1^3	1.060	0.861	-0.212±0.350i	0.409
S_2^3	-2.712	-4.764	-0.212±0.350i	0.409
S_3^3	-2.757	6.423	-0.212±0.350i	0.409
D_1^3	-0.566	2.348	0.068 , 9.738	
D_2^3	-0.780	-2.621	0.068 , 9.738	
D_3^3	-2.688	0.999	0.068 , 9.738	
U^1	-1.256	-0.124	0.190±1.001i	1.019

Table 4.17 Fixed Points and Related Properties in Fig. 4.22 (B = 2.0, ν = 2.7)

Fixed point	x	y	m_1 , m_2	|m|
S_1^5	1.605	-0.179	0.010±0.461i	0.461
S_2^5	-1.800	2.016	0.010±0.461i	0.461
S_3^5	-0.232	-2.377	0.010±0.461i	0.461
S_4^5	-0.201	2.353	0.010±0.461i	0.461
S_5^5	-1.912	-1.604	0.010±0.461i	0.461
D_1^5	0.781	1.906	0.014 , 17.817	
D_2^5	-2.115	0.390	0.014 , 17.817	
D_3^5	0.787	-1.647	0.014 , 17.817	
D_4^5	-1.186	2.627	0.014 , 17.817	
D_5^5	-1.246	-2.744	0.014 , 17.817	
U^1	-0.275	-0.054	0.912±0.857i	1.251

Table 4.18 Fixed Points and Related Properties in Fig. 4.24 (B = 2.4, ν = 0.95

Fixed point	x	y	m_1 , m_2	$\|m\|$
$^1S^1$	1.183	2.334	$-0.425 \pm 0.702i$	0.821
$^2S^1$	1.330	-1.840	$-0.425 \pm 0.702i$	0.821
D^1	1.917	-0.171	0.229 , 2.801	

Table 4.19 Fixed Points and Related Properties in Fig. 4.25 (B = 2.4, ν = 0.912

Fixed point	x	y	m_1 , m_2	$\|m\|$
$^1S^1$	0.730	2.425	$-0.595 \pm 0.584i$	0.834
$^2S^1$	1.019	-1.894	$-0.595 \pm 0.584i$	0.834
$^3S^1$	2.229	1.456	$0.334 \pm 0.563i$	0.654
$^4S^1$	0.794	-0.534	$0.334 \pm 0.563i$	0.654
$^1D^1$	1.912	-0.178	0.178 , 3.763	
$^2D^1$	1.290	3.618	0.244 , 1.926	
$^3D^1$	0.449	-1.194	0.244 , 1.926	

Table 4.20 Fixed Points and Related Properties in Fig. 4.26 (B = 2.4, ν = 0.908

Fixed point	x	y	m_1 , m_2	$\|m\|$
$^1S^1$	0.691	2.360	$-0.613 \pm 0.571i$	0.838
$^2S^1$	1.024	-1.908	$-0.613 \pm 0.571i$	0.838
$^3S^1$	2.241	1.273	$0.278 \pm 0.594i$	0.656
$^4S^1$	0.827	-0.498	$0.278 \pm 0.594i$	0.656
$^1D^1$	1.911	-0.179	0.174 , 3.870	
$^2D^1$	1.157	3.599	0.236 , 2.035	
$^3D^1$	0.442	-1.254	0.236 , 2.035	

Table 4.21 Fixed Points and Related Properties in Fig. 4.27 (B = 2.4, ν = 0.90

Fixed point	x	y	m_1 , m_2	|m|
$^1S^1$	0.599	2.351	$-0.489 \pm 0.680i$	0.838
$^2S^1$	0.959	-1.901	$-0.489 \pm 0.680i$	0.838
$^3S^1$	2.252	0.998	$0.175 \pm 0.637i$	0.660
$^4S^1$	0.883	-0.443	$0.175 \pm 0.637i$	0.660
$^1D^1$	1.910	-0.180	0.167 , 4.086	
$^2D^1$	0.914	3.474	0.230 , 2.195	
$^3D^1$	0.441	-1.364	0.230 , 2.195	

Table 4.22 Fixed Points and Related Properties in Fig. 4.28 (B = 2.4, ν = 0.85

Fixed point	x	y	m_1 , m_2	|m|
$^3S^1$	2.221	0.167	$-0.320 \pm 0.615i$	0.693
$^4S^1$	1.124	-0.285	$-0.320 \pm 0.615i$	0.693
$^1D^1$	1.911	-0.186	0.132 , 5.565	

Table 4.23 Fixed Points and Related Properties in Fig. 4.29 (B = 3.2, ν = 0.84

Fixed point	x	y	m_1 , m_2	|m|
D^1	2.128	-0.111	0.081 , 7.540	
$^1I^1$	2.370	-0.004	-1.361 , -0.296	
$^2I^1$	1.538	-0.468	-1.361 , -0.296	
$^1S_1^2$	2.219	1.639	$-0.398 \pm 0.160i$	0.429
$^1S_2^2$	2.269	-1.210	$-0.398 \pm 0.160i$	0.429
$^2S_1^2$	1.308	-0.384	$-0.398 \pm 0.160i$	0.429
$^2S_2^2$	1.840	-0.468	$-0.398 \pm 0.160i$	0.429

Table 4.24 Fixed Points and Related Properties in Fig. 4.30 (B = 1.5, ν = 1.0)

Fixed point	x	y	m_1 , m_2	|m|
S^1	1.703	-0.247	-0.244±0.859i	0.893
S_1^3	0.291	1.337	-0.139±0.733i	0.746
S_2^3	0.592	-1.128	-0.139±0.733i	0.746
S_3^3	2.144	-0.541	-0.139±0.733i	0.746
D_1^3	1.685	0.860	0.195 , 2.585	
D_2^3	1.563	-0.341	0.195 , 2.585	
D_3^3	1.642	-1.037	0.195 , 2.585	

Table 4.25 Fixed Points and Related Properties in Fig. 4.31 (B = 1.16, ν = 0.7

Fixed point	x	y	m_1 , m_2	|m|
$^1S^1$	2.126	-0.765	0.748±0.155i	0.764
$^2S^1$	-1.096	-0.144	0.748±0.155i	0.764
$^1D^1$	1.491	-0.263	0.354 , 3.793	
$^2D^1$	-0.455	1.921	0.488 , 1.177	
$^3D^1$	0.080	-2.025	0.488 , 1.177	
$^1U^1$	1.160	1.260	-0.556±1.045i	1.184
$^2U^1$	0.945	-1.189	-0.556±1.045i	1.184

Table 4.26 Fixed Points and Related Properties in Fig. 4.32 (B = 1.3, ν = 0.74)

Fixed point	x	y	m_1 , m_2	$\|m\|$
$^1S^1$	2.126	0.876	0.776±0.301i	0.833
$^2S^1$	-0.772	-0.395	0.776±0.301i	0.833
$^3S^1$	0.617	0.058	0.335±0.874i	0.936
$^4S^1$	1.846	-0.764	0.335±0.874i	0.936
$^1D^1$	1.546	-0.256	0.243 , 5.298	
$^2D^1$	0.104	2.373	0.486 , 1.359	
$^3D^1$	-0.324	-1.545	0.486 , 1.359	
$^4D^1$	-0.198	-0.029	0.473 , 1.818	
$^5D^1$	2.010	-0.935	0.473 , 1.818	
$^1U^1$	0.805	1.494	-0.277±1.306i	1.335
$^2U^1$	0.699	-1.304	-0.277±1.306i	1.335

Table 4.27 Fixed Points and Related Properties in Fig. 4.33 (B = 2.0, ν = 0.55)

Fixed point	x	y	m_1 , m_2	$\|m\|$
S^1	0.468	-0.027	0.022±0.708i	0.708
D^1	-0.142	-0.654	0.276 , 1.806	

Table 4.28 Fixed Points and Related Properties in Fig. 4.34 (B = 2.2, ν = 0.55)

Fixed point	x	y	m_1 , m_2	$\|m\|$
S^1	0.641	-0.008	-0.463±0.476i	0.664
D^1	0.237	-1.724	0.198 , 2.322	

Chapter 5 Nonperiodic Oscillations

5.1 Introduction

In the preceding chapter, we have chiefly considered the periodic oscillations occurring in the various regions of frequency entrainments. If the external force in the system has been prescribed outside the entrained region, there result nonperiodic oscillations whose steady states do not correspond simply to fixed or periodic points in the phase plane.

In the present chapter, we shall devote ourself to study nonperiodic oscillations of Eq. (4.1), especially to consider the reason why they are generated, because their details have not yet known.

The nonperiodic oscillations divide themselves into two different kinds, according to the configuration of the set of central points as mentioned in Sec. 2.3. That is, they are an almost periodic oscillation whose successive images of the mapping in the steady state move along a simple invariant closed curve, and a nonperiodic oscillation whose successive images do not move along a simple closed curve but they are dispersed in the phase plane.

5.2 Almost Periodic Oscillations

To begin with, we shall consider, as a specific example of almost periodic oscillations defined by H. Bohr [23], the case where $\mu = 0.2$, $B = 0.5$ and $\nu = 1.3$ in Eq. (3.1). Thus we are dealing with

$$\frac{d^2x}{dt^2} - 0.2\,(1 - x^2)\,\frac{dx}{dt} + x = 0.5 \cos 1.3t \quad . \quad (5.1)$$

The unique stable solution of Eq. (5.1) is considered to be almost periodic. The successive images of the mapping T move along a simple invariant closed curve C. Therefore, the configuration of its phase-portrait is topologically similar to the one shown in Fig. 3.3. The rotation number ρ which characterizes this curve C is computed to be 0.7706.... Judging from the numerical result, this invariant closed curve C may be assumed to be smooth and not to exhibit a singular nature at all [24]. We now confine our attention upon the solutions of Eq. (5.1) emanating from C at t = 0. These solution curves between t = 0 and t = L constitute one surface, as shown in Fig. 5.1, which is homeomorphous to a torus. This surface is described by the following equations:

$$
\begin{aligned}
x &= f(\theta,t) \\
&= -0.077 \sin 2\pi\theta + 1.675 \cos 2\pi\theta + \ldots \\
&\quad + (\ 0.312 - 0.811 \sin 2\pi\theta - 0.053 \cos 2\pi\theta + \ldots) \\
&\quad \times \sin 1.3t \\
&\quad + (-0.558 - 0.243 \sin 2\pi\theta - 0.026 \cos 2\pi\theta + \ldots) \\
&\quad \times \cos 1.3t + \ldots \\
y &= g(\theta,t) \\
&= -1.694 \sin 2\pi\theta + 0.019 \cos 2\pi\theta + \ldots \\
&\quad + (\ 0.825 - 0.011 \sin 2\pi\theta - 0.814 \cos 2\pi\theta + \ldots) \\
&\quad \times \sin 1.3t \\
&\quad + (\ 0.231 - 0.004 \sin 2\pi\theta - 0.256 \cos 2\pi\theta + \ldots) \\
&\quad \times \cos 1.3t + \cdots
\end{aligned}
\tag{5.2}
$$

in which the parameter θ has been taken to be proportional to the arc length of this surface, while t is kept constant, and $\theta = 0$ is chosen, without loss of generality, at points $y = 0$ and $x > 0$ on the surface.

By using Eqs (5.1) and (5.2), we can obtain the differential equation on a torus whose solution curves are expanded into the $t\theta$ plane in Fig. 5.2. Owing to Eq. (2.7) the solution of this equation is concretely formulated by the following equaton;*

$$\begin{aligned}\theta(t) = {} & \frac{1.3}{2\pi}\rho t - 0.008 + 0.003 \sin 1.3\rho t - 0.007 \cos 1.3\rho t + \ldots \\ & \ldots + (-0.068 + 0.028 \sin 1.3\rho t + 0.009 \cos 1.3\rho t + \ldots) \\ & \times \sin 1.3t \\ & + (-0.019 + 0.009 \sin 1.3\rho t + 0.011 \cos 1.3\rho t + \ldots) \\ & \times \cos 1.3t + \ldots \end{aligned} \tag{5.3}$$

where $\rho = 0.7706\ldots$

Substituting Eq. (5.3) into Eq. (5.2), we can obtain the expressions for x(t) and y(t) which contain only time t. Thus, these functions precisely express the almost periodic oscillation.

---

* The reduction of Eq. (5.3) has been given in Ref. [9].

5.3 Nonperiodic Oscillations Whose Phase-Portraits Are Given by Dispersed Points in the Phase Plane

In the system with linear restoring force there appear almost periodic oscillations whose successive images keep on moving along the invariant closed curve under the repeated iterations of the mapping T. However, we can obtain the nonperiodic oscillations whose successive images of the mapping do not lie on a simple invariant closed curve but are dispersed in the phase plane, when the system contains nonlinear restoring force. In this case, the successive images which start from any initial points approach the dispersed region, after the mapping T is applied indefinitely. Such a region may be considered as a 'set of central points' defined by G. D. Birkhoff [5]. But, until now little attention has been given to such nonperiodic oscillations.

In order to know briefly the movement of successive images under the mapping and the shape of central points, we shall show the sequence of one hundred points which is counted after the suffifient lapse of time t. We can conjecture that the distribution of these points is similar to the one of the set of central points. These types of oscillations appear near the region where the doubly asymptotic points appear. It is conjectured that from the theorem proved by G. D. Birkhoff, there exists an infinite number of periodic points, probably unstable ones, in the neighborhood of homoclinic points. In

---

*This theorem has been mentioned in Sec. 2.6.

fact, we can discover many directly and inversely unstable periodic points among the sequence of points, when such complicated nonperiodic oscillation occurs. Since the movements of successive images under iterations of the mapping may be closely related to the behavior of the invariant curves, α- and ω-branches, passing through the unstable points D and I, we shall also show them minutely.

In the following, we shall confine our attention to study three different types of these oscillations, according to the structure of phase-portrait.

(a) Nonperiodic Oscillations Occurring near the Harmonic Entrainment

To begin with, let us consider a case in which the nonperiodic oscillation whose successive images are dispersed in the phase plane results in the region between the harmonic and the 1/2-harmonic entrainments.

As an example of this case, we choose the system parameters at point e ($B = 17$, $\nu = 4$) which is prescribed just below the region of harmonic entrainment as shown in Fig. 4.2. In Fig. 5.3, the sequence of one hundred points obtained by the iterations of the mapping is represented. As the numerals in this figure show the order of the mapping, we can see the movements of the images in the set of central points. Even though the iterations of the mapping are continued, we obtain a similar point set which covers more densely the same domain as shown in Fig. 5.3 and has narrow

tails. We can not image that the sequence of these points moves along a certain simple closed curve, such as shown in Fig. 3.3.

We now investigate the internal structure in the set of central points. G. D. Birkhoff [16] has stated that an arbitrary small neighborhood of a homoclinic point contains an infinite number of periodic points.* Therefore, we conjecture that many periodic points still exist when such nonperiodic oscillation occurs. In fact, we have discovered the directly unstable 2-periodic points D^2 and the inversely unstable ones I^2, whose locations besides the invariant curves connected to them are shown in Fig. 5.4. The details of fixed and periodic points are listed in Table 5.1.** With regard to the locations of the points in Fig. 5.4, we can recognize that the movements of successive images are greatly influenced by their existences and the moving points keep away from the vicinity of point U^1. The α-branches (drawn in heavy lines) and the ω-ones (drawn in fine lines) of points D^2 and I^2 in Fig. 5.4 intersect each other, producing an infinite number of homoclinic and heteroclinic points still further.

When the system parameters are given in the region of harmonic entrainment, we can obtain the homoclinic structure of invariant

---

* Some examples of periodic points and corresponding periodic solutions are shown in Ref. [25].

** Moreover, the details of points I^4 whose positions were not indicated in Fig. 5.4 have also been listed in this table.

curves as shown in Fig. 4.4. A decrease or increase in B from this case results in the decomposition of the homoclinic structure. However, there rests the indication of the homoclinic structure as represented in Fig. 4.5. In this case, the one of the α-branch connected to point D^1 continues to move around the unstable point U^1 under the repeated applications of the mapping without tending to any simple closed curve. When the system parameters B and ν are changed, two points S^1 and D^1 coalesced on the boundary of harmonic entrainment disappear in its outside. Thus, if we set B and ν just outside the entrained region (for instance, B = .17 and ν = 4), there solely rests the nonperiodic oscillations whose successive images are dispersed in the phase plane as shown in Fig. 5.3.

(b) Nonperiodic Oscillations Occurring near the Subharmonic Entrainment

As the second example of the complicated nonperiodic oscillations, we shall deal with the oscillation which appears near the region of the subharmonic entrainment.

The system parameters B and ν in Eq. (4.1) are chosen so as to generate a nonperiodic oscillation arising from the 5/3-harmonic oscillations. We select the point 1 (B = 1.2, ν = 0.95) in Fig. 4.23 which is located lust below the region common to the harmonic and 5/3-harmonic entrainments. By the procedure analogous to the previous case, we show the ordered sequence of one hundred points in Fig. 5.5. The distribution of these images under iterations of the mapping is different from Fig. 5.3, because it has a slight regularity that some points, such

as 91, 94, 97, 100, ..., approach each other under the mapping T^3. This fact is due to that such nonperiodic oscillation is derived from the 5/3-harmonic oscillations.

In order to consider the internal structure of this point set, we illustrate the directly unstable periodic points D^3 and the invariant curves passing through them in Fig. 5.6. The locations of fixed and periodic points and their properties are listed in Table 5.2. In this figure the α-branches (drawn in thick lines) of points D^3 can not converge to any points, because there exist no stable points in the phase plane. So they are wandering in a certain region, intersecting the ω-branches (drawn in thin lines). The one of the ω-branches of points D^3 simply converges to the unstable point U^1 under iterations of the inverse mapping $\bar{T}^3$, and the other to the points U^3 or tend to infinity.

Now we discuss the reason why such nonperiodic oscillations occur, reminding of the 5/3-harmonic oscillations whose phase-portrait is shown in Fig. 4.30. However, in this figure the α-branches of points D^3 do not intersect the ω-branches, owing to the comparatively large B (= 1.5). When the system parameters are prescribed in the region common to the harmonic and 5/3-harmonic entrainment shown in Fig. 4.23, the completely stable fixed point S^1 appears besides the completely stable periodic points S^3. If we decrease the amplitude B slightly from this state and settle B and ν just below the overlapped region of the harmonic and 5/3-harmonic entrainments, the stable points S^1 and S^3 turn into the unstable points U^1 and U^3

respectively.* For the sake of the infinite intersections of the α- and ω-branches, successive images of the mapping are greatly disturbed, so they approach the one of the completely unstable periodic points U^3 and leave it proceeding to the other. This meandering movement repeats infinitely. Consequently, we obtain the nonperiodic oscillation whose successive images of the mapping T do not move along a simple closed curve but are dispersed in the phase plane as shown in Fig. 5.5.

(c) Nonperiodic Oscillations Occurring near the Higher-Harmonic Entrainment

We consider the third case of the nonperiodic oscillation whose successive images are dispersed in the phase plane.

In the case where we choose the system parameters at point k ($B = 1.8$, $\nu = 0.6$) in Fig. 4.23, there results a representative example of such oscillations that occur in the region between the second-harmonic and third-harmonic entrainments. Using the same procedure as the preceding case, we obtain the sequence of one hundred points as shown in Fig. 5.7. Comparing this figure with Fig. 5.3, we can notice that the successive images of Fig. 5.3 are

* The characteristic multipliers $|m|$ of points U^1 and U^3 are equal to 1.026 and 1.030 respectively as listed in Table 5.2. These values mean that the stable points S^1 and S^3 turn slightly into the unstable types U^1 and U^3 respectively.

distributed in a ring domain, but the ones of Fig. 5.7 are dispersed in a certain domain without remaining uncovered areas, if we iterate the mapping T infinitely. This phenomenon depends on the existence of unstable fixed and periodic points in the interior of this point set. So, we seek them in the set of central points, in order to investigate the structure of this nonperiodic oscillation. In Fig. 5.8 (a), the directly and inversely unstable fixed points and their invariant curves under the mapping T are illustrated. The behavior of the invariant curves connected to the unstable fixed points D^1, $^1I^1$ and $^2I^1$ of this figure is similar to the one of Fig. 4.29 (the 2/2-harmonic oscillations). However, we can find no completely stable fixed points in Fig. 5.8 (a), such as the stable points S^2 in Fig. 4.29. As mentioned in Sec. 4.5, the multiplication of fixed points proceeds successively, if the system parameters are suitably varied. Hence, the decrease of the frequency ν from the value of Fig. 4.29 has led to the change that the completely stable points, which should terminate such multiplication, turn into the inversely unstable types. Therefore, we consider that such greatly many multiplications may also contribute to the occurrence of these nonperiodic oscillations whose successive images of the mapping T are complicatedly dispersed in the phase plane.

By using the relations (2.5), we can expect the existence of the other periodic points in the phase plane. Thus, the periodic points and their invariant curves under the mapping T^2 and T^3 are shown in Fig. 5.8 (b) and Fig. 5.8 (c) respectively. The precise

locations of the total fixed and periodic points in Fig. 5.8 and their properties are listed in Table 5.3. From these configurations, we can image that the behavior of the α-branches (drawn in heavy lines) passing through points D and I is closely related with the movement of successive images of the mapping T in the set of central points.

By the way, the third-harmonic oscillation represented by point j may influence the nonperiodic one, because the distance between point j and point k is short as shown in Fig. 4.23. In fact, the intersections of the α-branch and the ω-one of point D^1 in Fig. 4.34 have disappeared, when the amplitude B is decreased. However, there still exists the meandering of this α-branch as shown in Fig. 4.33 (at point j of Fig. 4.23). As mentioned in Sec. 4.5, the coalescence of fixed points S^1 and D^1 leads to the disappearance of the third-harmonic oscillation outside the entrained region. Neverthless, there remains the complicated sequence of points which corresponds to the nonperiodic oscillation.

Consequently, the homoclinic structure of invariant curves in addition to the multiplication of periodic points contributes to the appearance of such complicated nonperiodic oscillations.

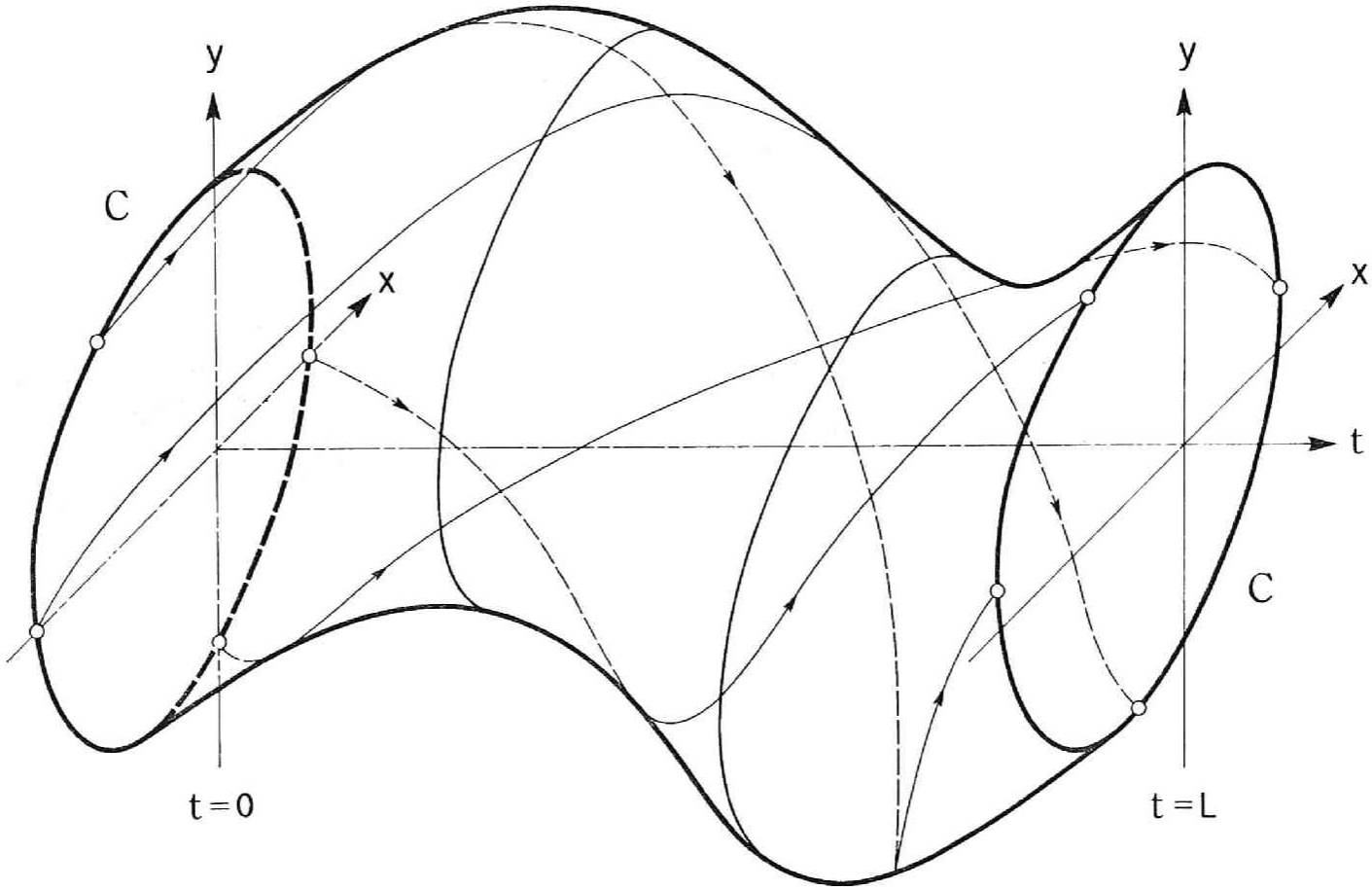

Fig. 5.1 Surface constructed by the solutions of Eq. (5.1) emanating from the invariant closed curve C.

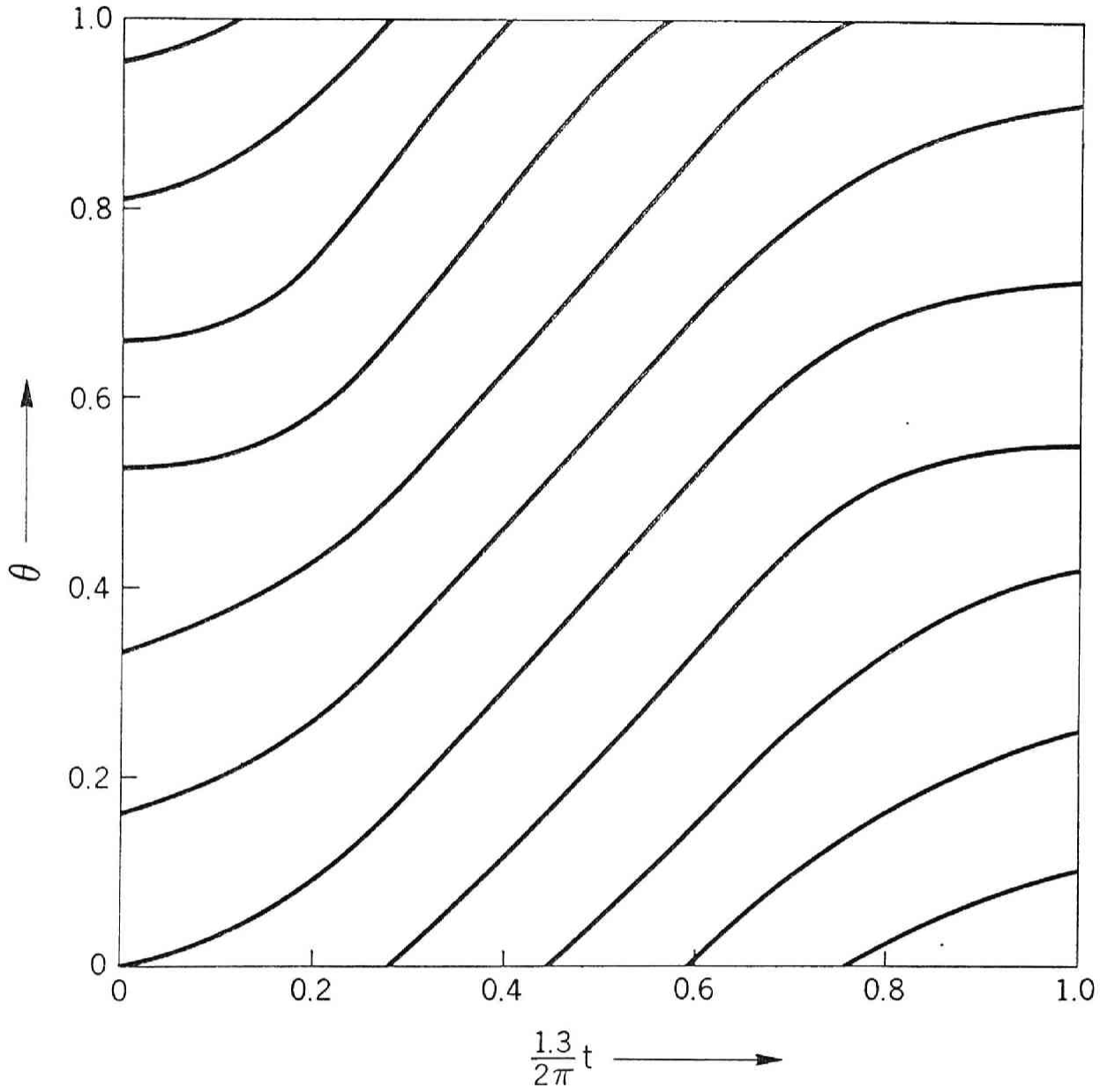

Fig. 5.2 Solution curves of Eq. (5.1) mapped on a torus and developed.

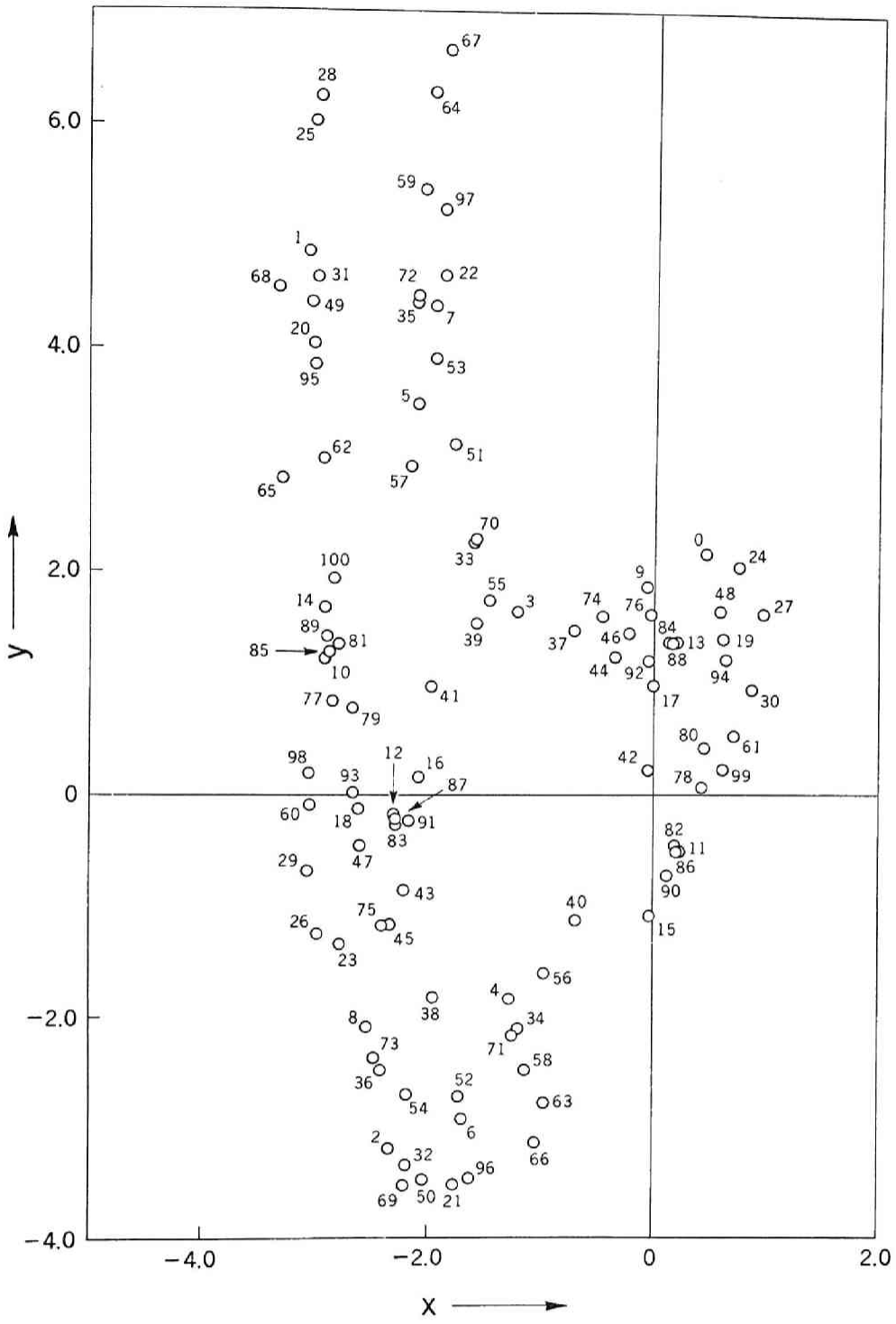

Fig. 5.3 Sequence of points representing the nonperiodic oscillation for Eq. (4.1). (B = 17, ν = 4)

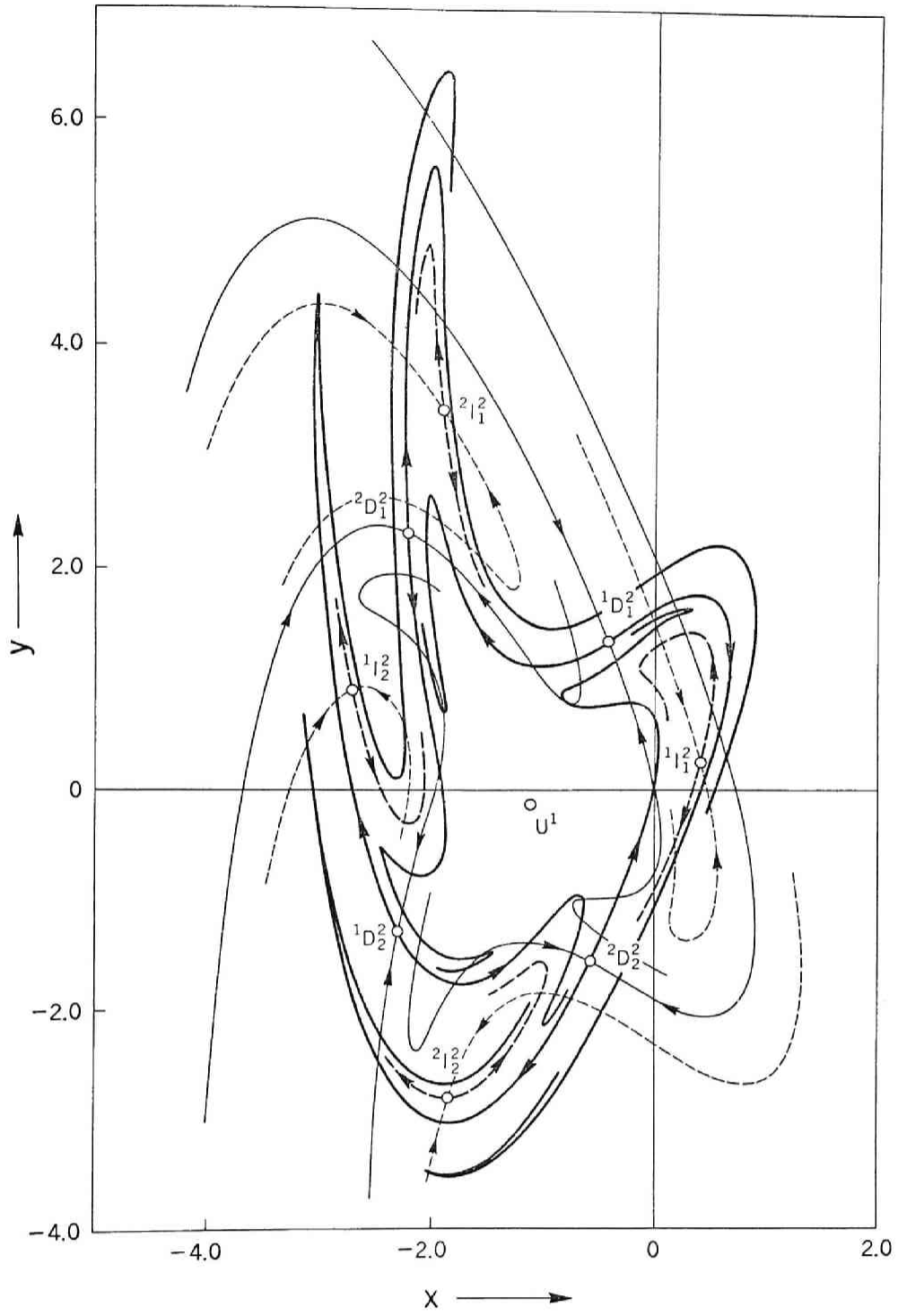

Fig. 5.4 Fixed points and invariant curves of the mapping T^2 for Eq. (4.1
(B = 17, ν = 4)

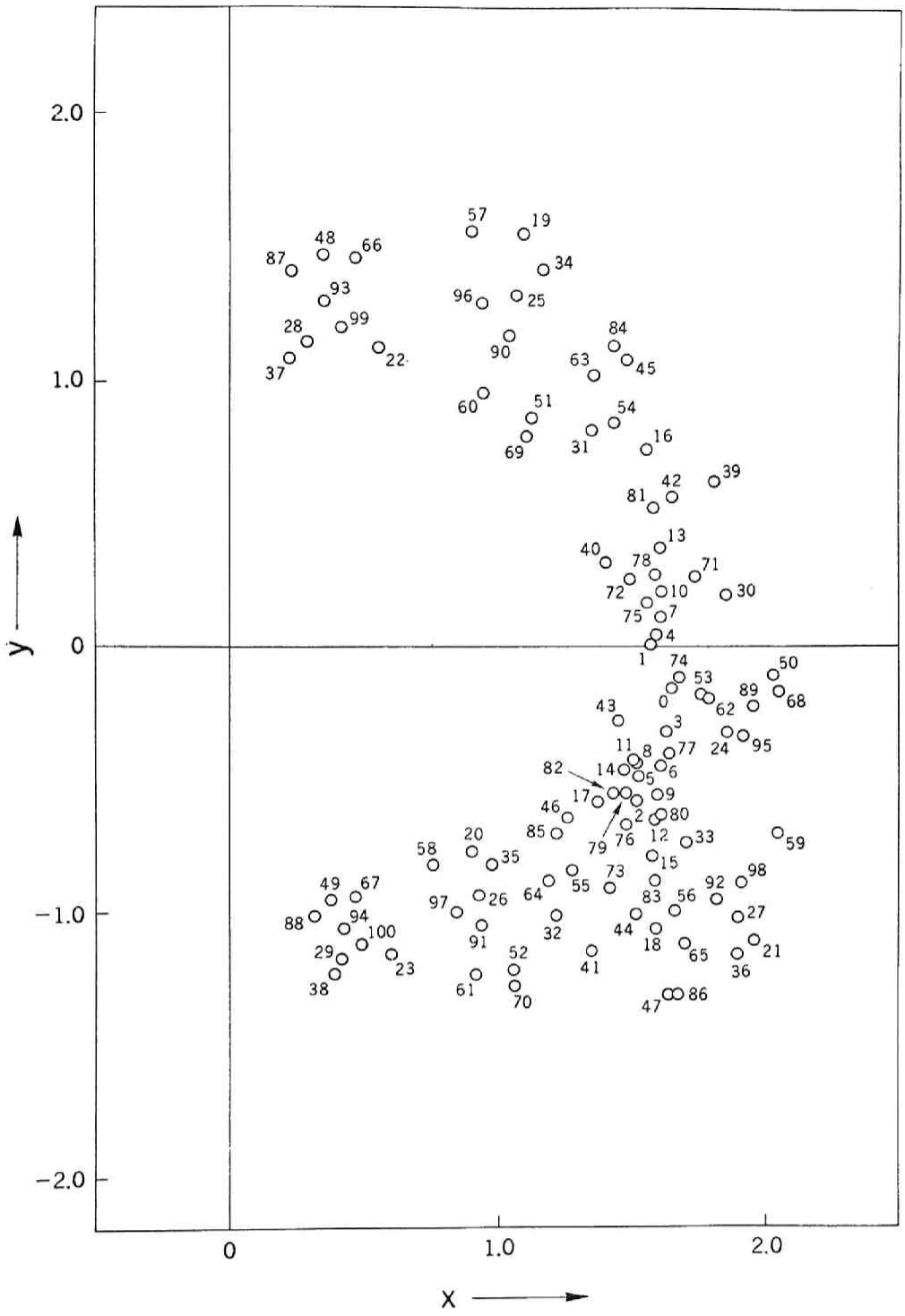

Fig. 5.5 Sequence of points representing the nonperiodic oscillation for Eq. (4.1). (B = 1.2, ν = 0.95)

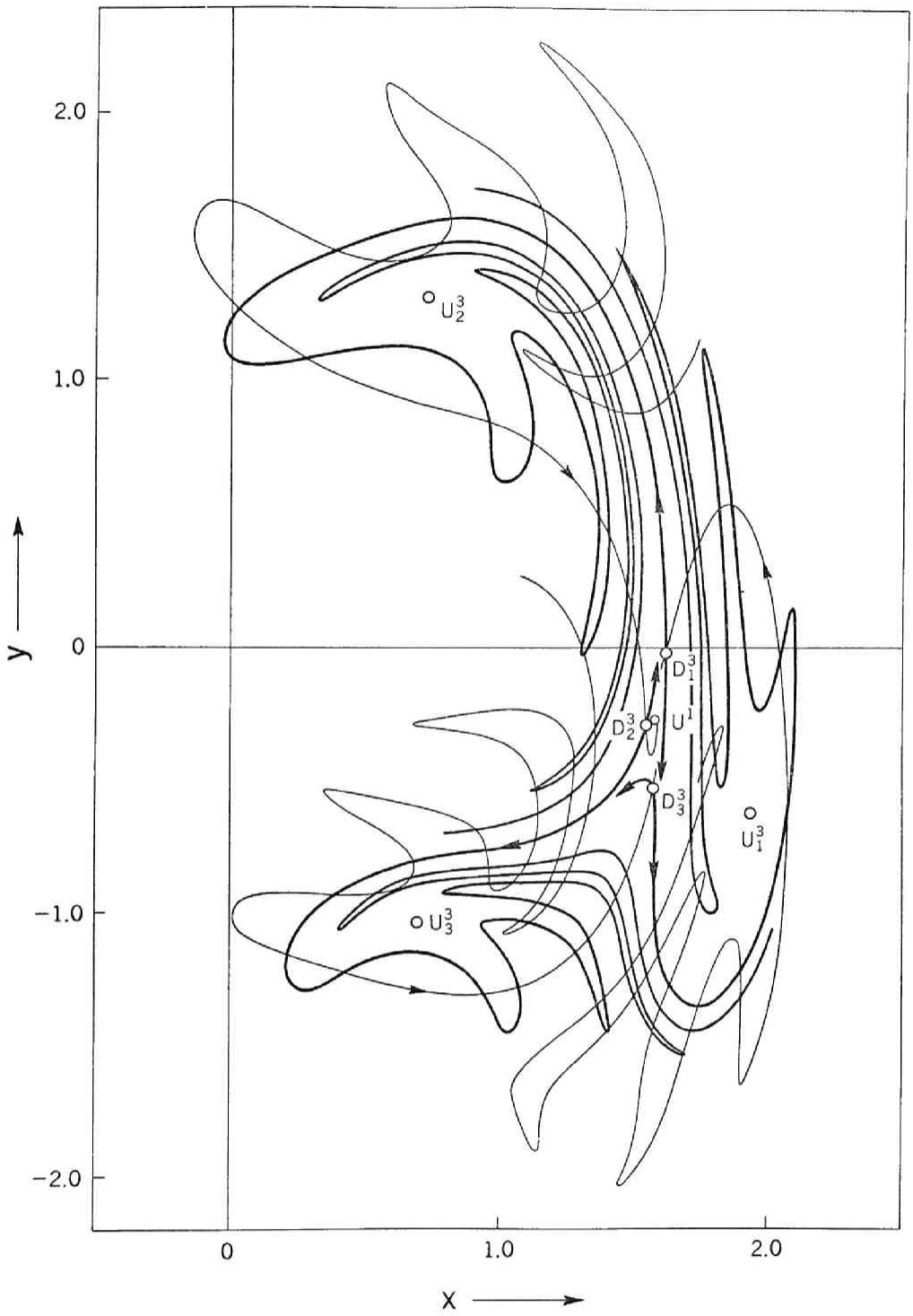

Fig. 5.6 Fixed points and invariant curves of the mapping T^3 for Eq. (4.1). (B = 1.2, ν = 0.95)

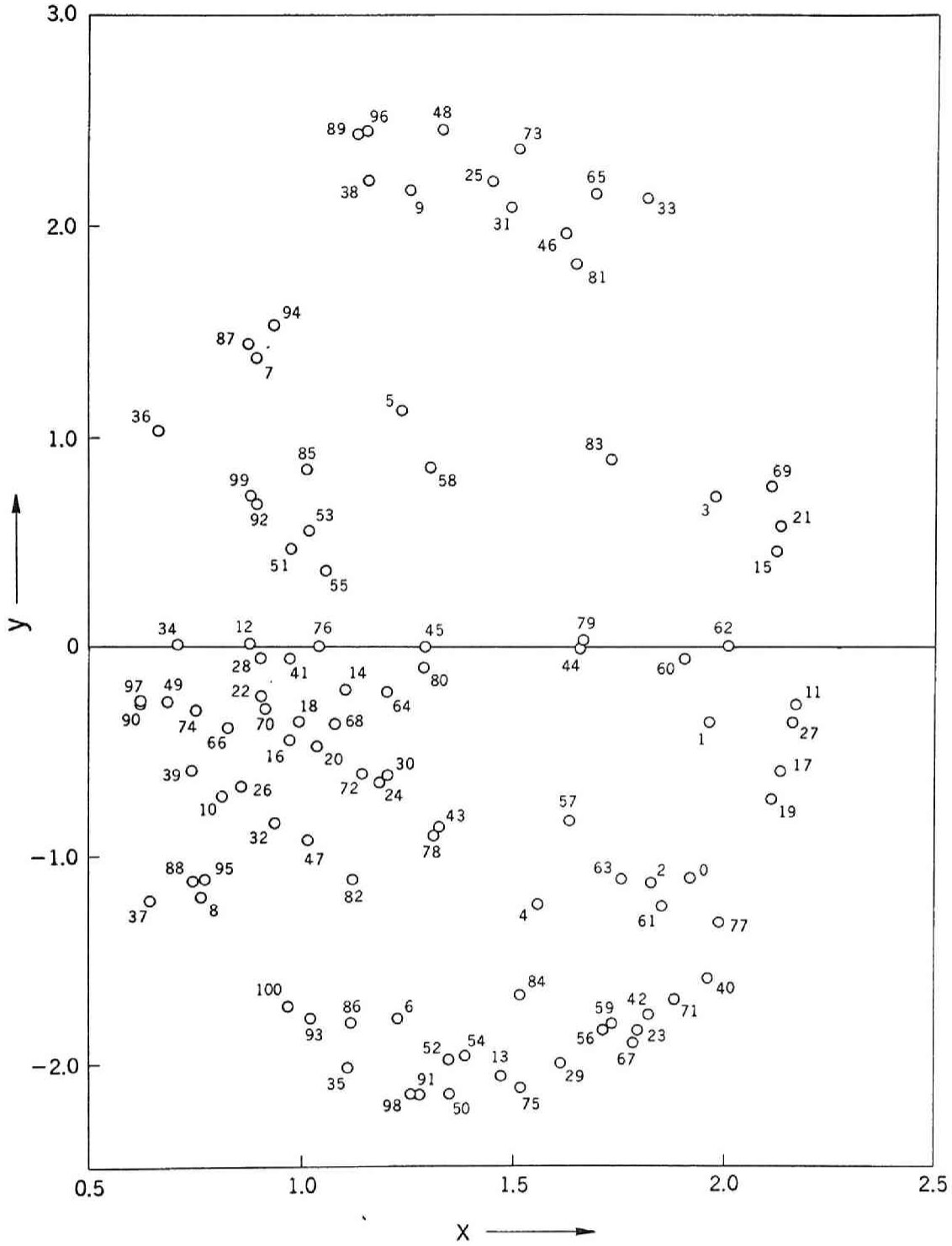

Fig. 5.7 Sequence of points representing the nonperiodic oscillation for Eq. (4.1). (B = 1.8, ν = 0.6)

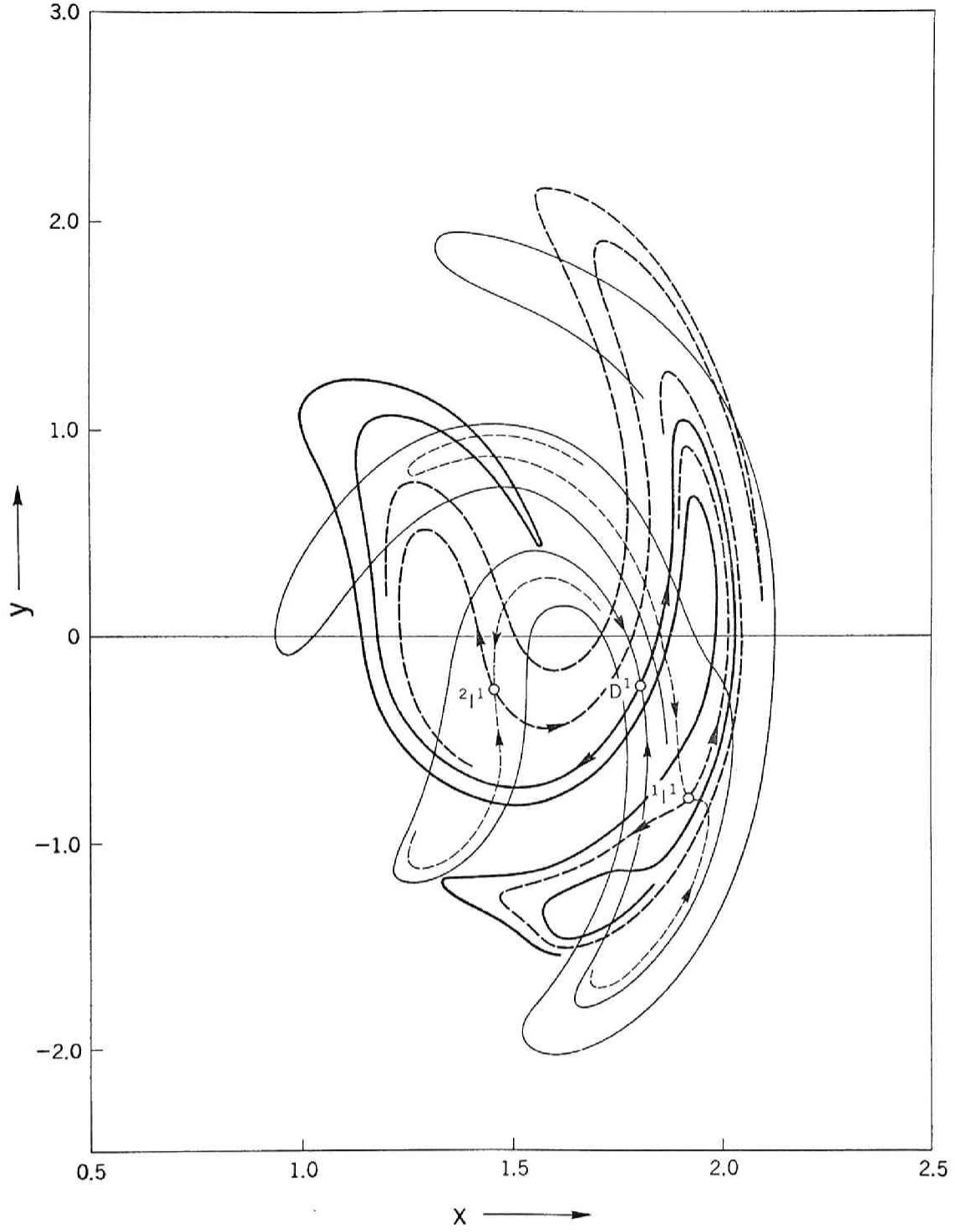

Fig. 5.8 (a) Fixed points and invariant curves of the mapping T for Eq. (4.1) (B = 1.8, ν = 0.6)

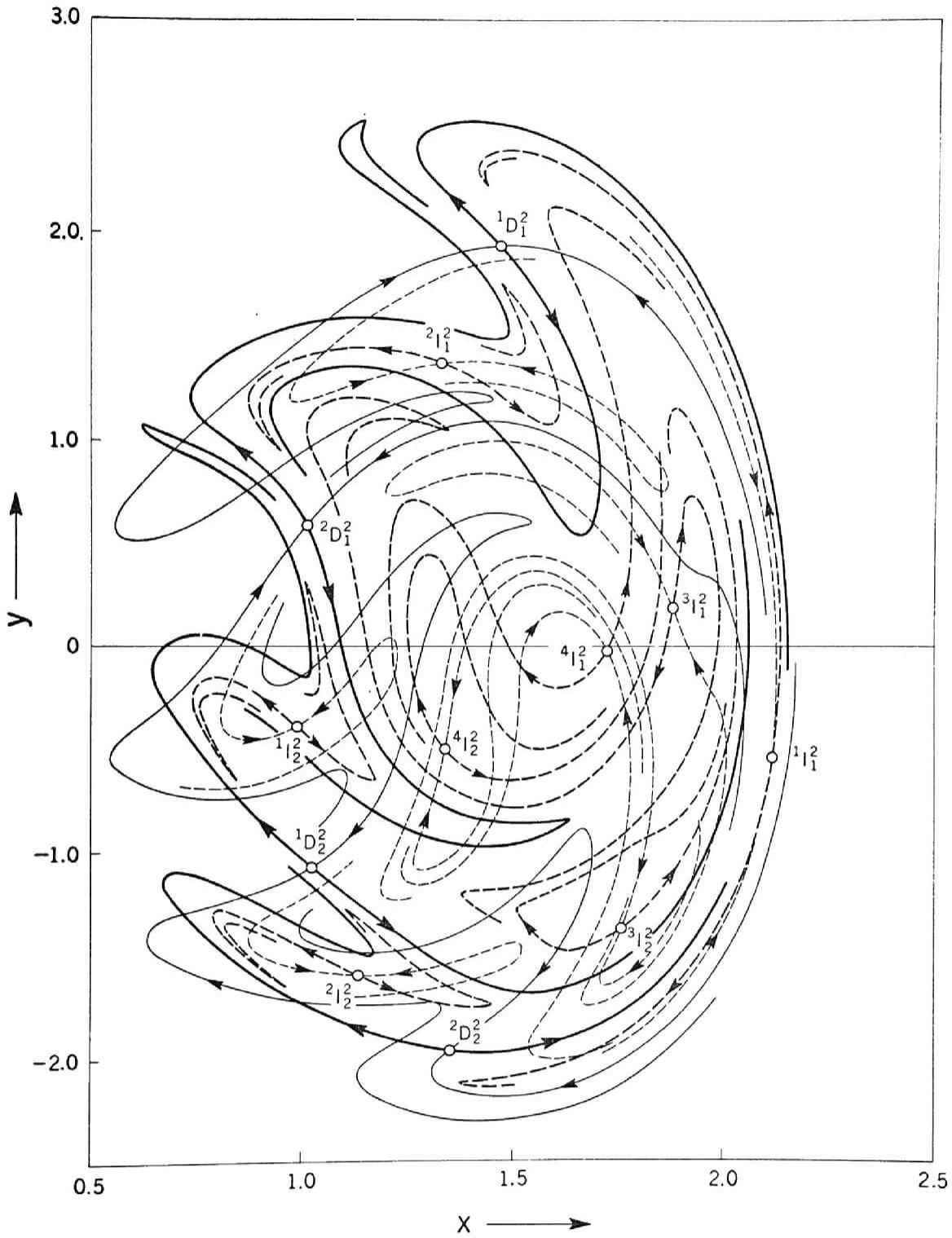

Fig. 5.8 (b) Fixed points and invariant curves of the mapping T^2 for Eq. (4.....
(B = 1.8, ν = 0.6)

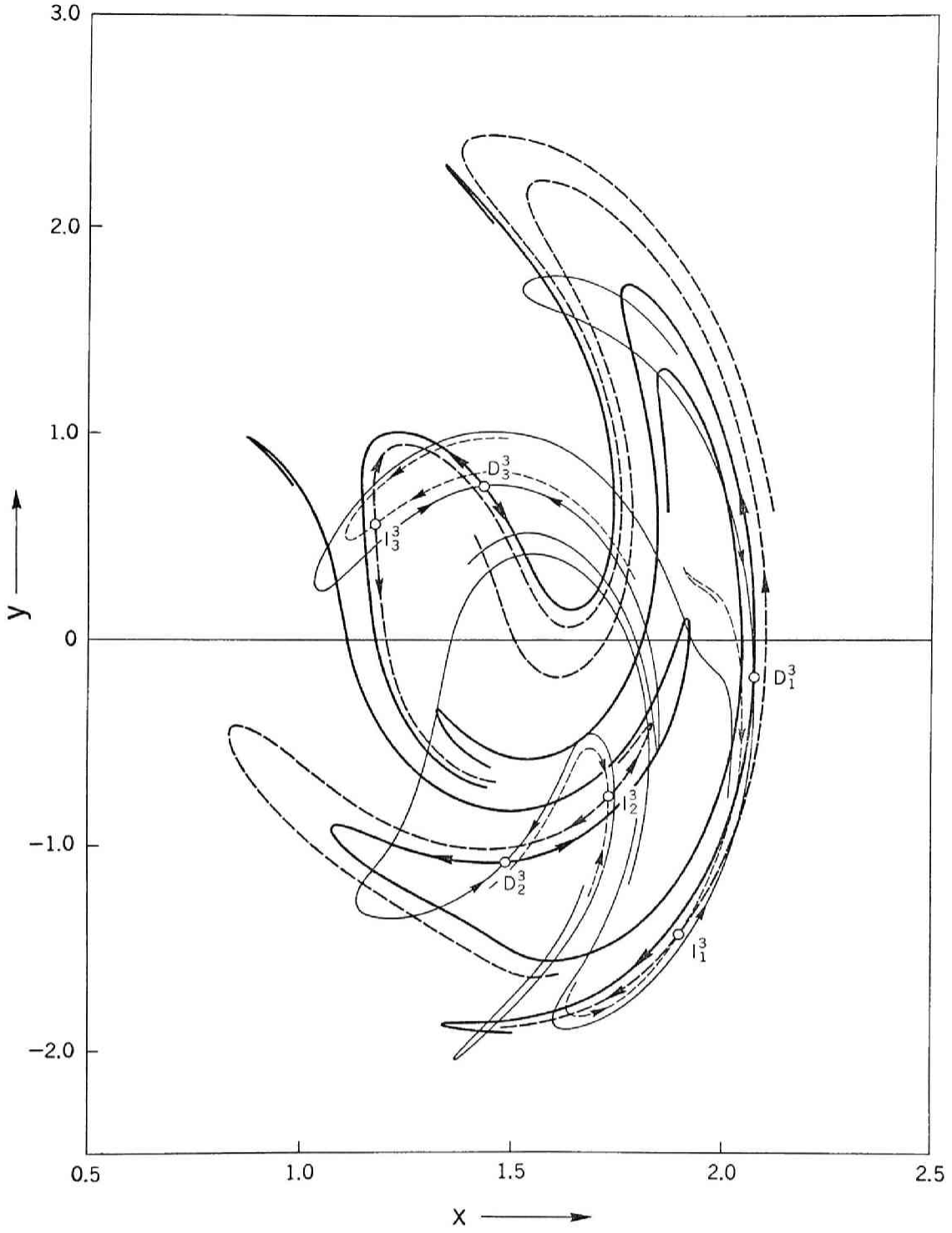

Fig. 5.8 (c) Fixed points and invariant curves of the mapping T^3 for Eq. (4.1

(B = 1.8, ν = 0.6)

Table 5.1 Fixed Points and Related Properties in Fig. 5.4 (B = 17.0, ν = 4

Fixed point	x	y	m_1 , m_2	$\|m\|$
U^1	-1.131	-0.142	$-0.615 \pm 0.861i$	1.059
$^1D_1^2$	-0.421	1.346	0.090 , 7.352	
$^1D_2^2$	-2.305	-1.294	0.090 , 7.352	
$^2D_1^2$	-2.218	2.320	0.090 , 7.352	
$^2D_2^2$	-0.578	-1.569	0.090 , 7.352	
$^1I_1^2$	0.410	0.239	-3.739 , -0.108	
$^1I_2^2$	-2.718	0.905	-3.739 , -0.108	
$^2I_1^2$	-1.910	3.454	-3.739 , -0.108	
$^2I_2^2$	-1.857	-2.809	-3.739 , -0.108	
$^1I_1^4$	-2.284	-0.215	-11.691 , -0.020	
$^1I_2^4$	0.142	1.362	-11.691 , -0.020	
$^1I_3^4$	-2.884	1.302	-11.691 , -0.020	
$^1I_4^4$	0.198	-0.524	-11.691 , -0.020	
$^2I_1^4$	-1.070	-1.935	-11.691 , -0.020	
$^2I_2^4$	-2.169	4.075	-11.691 , -0.020	
$^2I_3^4$	-2.127	-2.877	-11.691 , -0.020	
$^2I_4^4$	-1.638	2.171	-11.691 , -0.020	

Table 5.2 Fixed Points and Related Properties in Fig. 5.6 (B = 1.2, ν = 0.95

Fixed point	x	y	m_1 , m_2	$\|m\|$
U^1	1.585	-0.295	$-0.447 \pm 0.923i$	1.026
D_1^3	1.617	-0.007	0.618 , 1.387	
D_2^3	1.545	-0.297	0.618 , 1.387	
D_3^3	1.571	-0.537	0.618 , 1.387	
U_1^3	1.930	-0.653	$-0.793 \pm 0.658i$	1.030
U_2^3	0.656	1.278	$-0.793 \pm 0.658i$	1.030
U_3^3	0.644	-1.049	$-0.793 \pm 0.658i$	1.030

Table 5.3 Fixed Points and Related Properties in Fig. 5.8 ($B = 1.8$, $\nu = 0.6$

Fixed point	x	y	m_1 , m_2
D^1	1.813	-0.214	0.072 , 22.279
$^1I^1$	1.934	-0.787	-1.353 , -0.775
$^2I^1$	1.465	-0.249	-1.353 , -0.775
$^1D_1^2$	1.478	1.943	0.084 , 10.424
$^1D_2^2$	1.028	-1.076	0.084 , 10.424
$^2D_1^2$	1.016	0.589	0.084 , 10.424
$^2D_2^2$	1.357	-1.962	0.084 , 10.424
$^1I_1^2$	2.136	-0.462	-2.520 , -0.285
$^1I_2^2$	0.999	-0.397	-2.520 , -0.285
$^2I_1^2$	1.347	1.372	-2.520 , -0.285
$^2I_2^2$	1.145	-1.603	-2.520 , -0.285
$^3I_1^2$	1.896	0.182	-29.403 , -0.051
$^3I_2^2$	1.741	-1.442	-29.403 , -0.051
$^4I_1^2$	1.741	-0.010	-29.403 , -0.051
$^4I_2^2$	1.339	-0.481	-29.403 , -0.051
D_1^3	2.089	-0.202	0.056 , 16.928
D_2^3	1.500	-1.076	0.056 , 16.928
D_3^3	1.444	0.747	0.056 , 16.928
I_1^3	1.922	-1.418	-17.897 , -0.064
I_2^3	1.746	-0.760	-17.897 , -0.064
I_3^3	1.181	0.545	-17.897 , -0.064

Chapter 6 Conclusion

In this monograph, we have investigated the essential aspects of the self-oscillatory system with an external force. The system under investigation is governed by the following fundamental equation in dimensionless form;

$$\frac{d^2x}{dt^2} - \mu(1 - x^2)\frac{dx}{dt} + c_1 x + c_3 x^3 = B \cos \nu t \qquad (6.1)$$

By applying the mapping method based on the transformation theory of differential equations to the fundamental equation, we can obtain various types of phase-portraits in Eq. (6.1). We have first determined the regions of harmonic, subharmonic and higher-harmonic entrainments, in order to study the deformation of the phase-portraits appearing in each entrained region.

Roughly speaking about the solutions of Eq. (6.1), the fixed points and the invariant curves for a relatively small value of B are similar to the ones occurring in van der Pol's equation with a forcing term [19,20]. When B is large enough, the effect of negative damping is equivalently suppressed by the external force. In this case, the phase-portrait changes from van der Pol type into Duffing type [1,9].

In the case where the restoring force of the system is nonlinear, we have seen the nonperiodic oscillations whose successive images of the mapping do not lie on a simple closed curve but are dispersed in the phase plane. The transition from the harmonic oscillation to such nonperiodic oscillation occurring near the boundary of the harmonic

entrainment is summarized as follows;

a. When B is relatively small, a harmonic oscillation whose phase-portrait is similar to the one of van der Pol's equation (see Fig. 4.3).

b. As B and ν are increased from the previous case, the homoclinic structure of invariant curves appears in the phase plane (see Fig. 4.4).

c. If B is increased or decreased from this state and given just outside the region of the homoclinic structure (see Fig. 4.2), the homoclinic points disappear. Hence the one of the α-branch keeps on meandering around the unstable point U^1 without tending to any stable set (see Fig. 4.5).

d. The coalescence of points S^1 and D^1 occurs at the boundary of the harmonic entrainment. Then, if we increase ν or decrease B beyond this boundary, there exists solely the nonperiodic oscillation whose successive images of the mapping are given by the dispersed points in the phase plane (see Fig. 5.3).

From the above-mentioned explanation, we may conjecture that the appearance of such nonperiodic oscillations occurring near the region of the harmonic entrainment is greatly affected by the homoclinic structure of invariant curves.

We have also obtained the various types of phase-portraits in the region of subharmonic entrainment. In order to investigate the deformation of invariant curves from van der Pol type, we have emphatically pointed out the intersections caused by the α_1-branches

(or α_2-branches) and ω-branches of point D.

If the system parameters are set in the region of subharmonic entrainment and B is chosen to be a relatively small value, point U^1 is encircled by the invariant closed curve which the stable point S and the unstable point D lie (see Fig. 4.8 and Fig. 4.14). The sailent features of transitions from this phase-portrait are summarized as follows;

a. When ν is decreased, the α_1-branch of point D intersects the ω-branch of point D (see Fig. 4.9 and Fig. 4.15). Therefore, we obtain the homoclinic and heteroclinic structure of invariant curves in the phase plane. With further decreasing ν, the α_1-branch lies outside the ω-branch without intersecting the other branches.

b. When ν is increased, the α_2-branch of point D intersects the ω-branch of point D (see Fig. 4.11 and Fig. 4.19). The further increase in ν brings about the fact that the α_2-branch does not intersect the ω-branch. Hence, we obtain the phase-portrait of Duffing type for a sufficient large value of B.

We have also determined the region of the second- and third-harmonic entrainments as the examples of higher-harmonic oscillations. In the region between the harmonic entrainment and the third-harmonic entrainment, we can obtain the nonperiodic oscillations whose successive images of the mapping do not lie on a simple closed curve but are dispersed in the phase plane (see Fig. 5.7). The relationship among the nonperiodic oscillations and two types

of the above-mentioned periodic oscillations is explained as follows;

a. If we decrease the frequency ν in the region of harmonic entrainment, the higher-harmonics of the harmonic oscillation are gradually built up. A further decrease in ν results in a lot of multiplications of fixed and periodic points. Too many unstable points corresponding to the subharmonic oscillations of higher orders influence upon the movement of the successive images of the mapping, when the oscillation become to be unentrained.

b. We can see the homoclinic structure of invariant curves in the region of the third-harmonic entrainment (see Fig. 4.34). Analogous to the preceeding case of the harmonic oscillations, the complicated nonperiodic oscillation sustains after the homoclinic structure of invariant curves disappears.

As an example of subharmonic oscillations whose higher-harmonic components are dominant, we have investigated the 5/3-harmonic oscillations (see Fig. 4.30). In this case, there exist the stable points S^3 and S^1 corresponding to the 5/3-harmonic oscillations and the harmonic oscillation respectively in the phase plane. A slight modification of the system parameters results in the change from the stable points S^3 and S^1 to the unstable ones. Then, the successive images of the mapping continue to move complicatedly without tending to any point, because the α-branches of points D intersect their ω-branches repeatedly (see Fig. 5.6). Therefore we can obtain the nonperiodic oscillation whose successive images are dispersed in the phase plane (see Fig. 5.5).

ACKNOWLEDGEMENT

The auther wishes to express sincere gratitude to Dr. C. Hayashi, Professor of Kyoto University, for his constant guidance and encouragement.

In the preparation of the present monograph the auther was greatly aided by Dr. Y. Ueda, Assistant Professor of Kyoto University, and Mr. H. Kawakami, Lecturer of Tokushima University, and the members of Professor C. Hayashi's researching group, who gave him valuable suggestions.

The author is also grateful to Dr. E. Ikeno, Professor of Tokushima University, and Mr. A. Ushida, Assistant Professor of Tokushima University, for their constant encouragement.

REFERENCES

[1] C. Hayashi: "Nonlinear oscillations in physical systems," McGraw-Hill Book Company, New York (1964).

[2] M. L. Cartwright: "Forced oscillations in nearly sinusoidal systems," J. Inst. Elec. Engrs. (London), 95 (3), p. 88 (1948).

[3] H. Poincaré: "Les Méthodes nouvelles de la méchanique céleste," Gauthier-Villars, Paris (1892).

[4] G. D. Birkhoff: "Surface transformations and their dynamical applications," Acta Math., 43, p. 1 (1920).

[5] G. D. Birkhoff: "Dynamical systems," p. 189, American Mathematical Society, Providence, Rhode Island (1927).

[6] W. F. Chow: "Principles of tunnel diode circuits," p. 33, John Wiley and Sons, Inc., New York (1964).

[7] N. Levinson: "Transformation theory of non-linear differential equations of the second order," Ann. Math., 45, p. 723 (1944).

[8] J. L. Massera: "The number of subharmonic solutions of non-linear differential equations of the second order," Ann. Math., 50, p. 118 (1949).

[9] C. Hayashi, Y. Ueda and H. Kawakami: "Transformation theory as applied to the solutions of nonlinear differential equations of the second order," Int. J. Non-Linear Mechanics, 4, p. 235 (1969).

[10] N. Levinson: "On the existence of periodic solutions for second order differential equations with a forcing term," J. Math. Phys., 22, p. 41 (1943).

[11] V. V. Nemytskii and V. V. Stepanov: "Qualitative theory of differential equations," p. 353, Princeton University Press, Princeton (1960).

[12] H. Poincaré: "Sur les courbes définies par les équations différentielles," J. Math., 4-1, p. 167 (1885).

[13] A. Denjoy: "Sur les courbes définies par les équations différentielles à la surface du tore," J. Math., 11, p. 333 (1932).

[14] P. Bohl: "Über die hinsichtlich der unabhängigen und abhängigen Variabln periodische Differentialgleichung erster Ordnung," Acta Math., 40, p. 321 (1916).

[15] E. A. Coddington and N. Levinson: "Theory of ordinary differential equations," McGraw-Hill Book Company, New York (1955).

[16] G. D. Birkhoff and P. A. Smith: "Structure analysis of surface transformations," J. Math., 9-7, p. 345 (1928).

[17] G. D. Birkhoff: "On the periodic motions of dynamical systems," Acta Math., 50, p. 359 (1927).

[18] G. D. Birkhoff: "Nouvelles recherches sur les systèmes dynamiques," Mem. Pont. Acad. Sci. Novi Lyncaei, 3-1, p. 85 (1935).

[19] B. van der Pol: "Nonlinear theory of electric oscillations," Proc. IRE, 22, p. 1051 (1934).

[20] C. Hayashi, Y. Ueda, N. Akamatsu: "Analysis of forced self-oscillatory systems using mapping concepts," Papers of Technical Group on Nonlinear Problems, I. E. C. E., Japan (July 1968).

[21] C. Hayashi, Y. Ueda, N. Akamatsu and H. Itakura: "On the behavior of self-oscillatory systems with external forcing," I. E. C. E., Japan, 53-A, p. 150 (Mar. 1970).

[22] J. J. Stoker: "Nonlinear vibrations," Interscience Publishers, Inc., New York (1950).

[23] H. Bohr: "Zur Theorie der fastperiodischen Funktionen, Acta Math., 45, p. 29 (1924); 46, p. 101 (1925); 47, p. 237 (1926).

[24] E. R. van Kampen: "The topological transformations of a simple closed curve into itself," Amer. J. Math., 57, p. 142 (1935).

[25] C. Hayashi, Y. Ueda and H. Kawakami: "Periodic solutions of Duffing's equation with reference to doubly asymptotic solution," Fifth International Conference on Nonlinear Oscillations, Kiev (1969).